TIME VARIANT COMPONENT AND SYSTEM RELIABILITY ANALYSIS OF BRIDGES

A THESIS SUBMITTED TO
THE GRADUATE SCHOOL OF NATURAL AND APPLIED SCIENCES
OF
MIDDLE EAST TECHNICAL UNIVERSITY

BY

VAHID GHASEMNEJAD BERENJI

IN PARTIAL FULFILLMENT OF THE REQUIREMENTS
FOR
THE DEGREE OF MASTER OF SCIENCE
IN
ENGINEERING SCIENCES

SEPTEMBER 2015

Approval of the thesis:

TIME VARIANT COMPONENT AND SYSTEM RELIABILITY ANALYSIS OF BRIDGES

submitted by **VAHID GHASEMNEJAD BERENJI** in partial fulfillment of the requirements for the degree of **Master of Science in Engineering Sciences Department, Middle East Technical University** by,

Prof. Dr. Gülbin Dural _____
Dean, Graduate School of **Natural and Applied Sciences**

Prof. Dr. Murat Dicleli _____
Head of Department, **Engineering Sciences**

Assoc. Prof. Dr. Ferhat Akgül _____
Supervisor, **Engineering Sciences Department, METU**

Examining Committee Members:

Prof. Dr. Murat Dicleli
Engineering Sciences Department, METU _____

Assoc. Prof. Dr. Ferhat Akgül
Engineering Sciences Department, METU _____

Assoc. Prof. Dr. Senih Gürses
Engineering Sciences Department, METU _____

Assoc. Prof. Dr. Tolga Yılmaz
Engineering Sciences Department, METU _____

Assoc. Prof. Dr. Mürsel Erdal
Department of Civil Engineering Faculty Tech., Gazi Uni. _____

Date: _____

I hereby declare that all information in this document has been obtained and presented in accordance with academic rules and ethical conduct. I also declare that, as required by these rules and conduct, I have fully cited and referenced all material and results that are not original to this work.

Name, Last Name: VAHID GHASEMNEJAD BERENJI

Signature :

ABSTRACT

TIME VARIANT COMPONENT AND SYSTEM RELIABILITY ANALYSIS OF BRIDGES

Ghasemnejad Berenji, Vahid

M.S., Department of Engineering Sciences

Supervisor : Assoc. Prof. Dr. Ferhat Akgül

September 2015, 155 pages

This study aims to develop a time variant reliability algorithm for a bridge component or system capable of incorporating multiple deterioration and live load models to be selected by the user. The algorithm is developed as a shell program built over a previously developed core program (RELSYS) which is based on the First Order Reliability Method (FORM). After reviewing previous research performed on both time invariant and time variant bridge reliability, the fundamental concepts of time-variant reliability such as time to failure and failure rate are discussed and formulated. Furthermore, Load and capacity formulations start with the most simple deterministic load and deterministic capacity cases. As a first step toward time variant reliability study, load and capacity reliability problems are solved using the computer program RELSYS. Reliability problems including limit state functions containing normal and non-normal random variables as well as correlation cases are studied for both component and system analyses. Within this context, parallel, series and series-parallel systems are evaluated. Prior to developing a time-variant reliability algorithm, different time variant reliability approaches are reviewed and separately formulated. These formulations included: repetitive loading and three periods of failure, the bathtub curve, stochastic load model containing two independent Poisson processes and random strength degradation function, and the load and capacity formulation. Finally, a computer algorithm in the form of a shell script is developed for time variant reli-

ability analysis, based on five different deterioration models, two separate live load models including Nowak's and Sivakumar's models, and the RELSYS as the core program. Deterioration models or resistance degradation functions include corrosion, diffusion control, traffic spray, sulfate attack and load carrying models. Effects of these models on time variant reliability problem are observed. The developed computer program has the capability to read input data for both time variant or time invariant problems. Moreover, it provides the user with different options of defining deterioration and live load models for the problem at hand for a given time horizon along with the option of defining specific input data. This study showed that, because of highly uncertain nature of time-variant reliability, the selection of a degradation model and a live load model to be used for a given analysis may have an important effect on time variant reliability computation. Furthermore, implementation and testing of available or newly developed deterioration and load models into time-variant bridge reliability programs is an area that requires further study.

Keywords: Bridge, Reliability, Structural Reliability, System Reliability, Time Variant Analysis, Deterioration, Failure Rate, Stochastic Loads

ÖZ

KÖPRÜLERİN ZAMANA BAĞLI ELEMAN VE SİSTEM GÜVENİLİRLİĞİ ANALİZİ

Ghasemnejad Berenji, Vahid
Yüksek Lisans, Mühendislik Bilimleri Bölümü
Tez Yöneticisi : Doç. Dr. Ferhat Akgül

Eylül 2015 , 155 sayfa

Bu çalışma; kullanıcı tarafından seçilebilir çoklu yıpranma ve hareketli yük modellerini içine dahil edebilen ve köprü elemanı veya sistemi için zamanla değişken bir güvenilirlik algoritmasını geliştirmeyi hedeflemektedir. Algoritma daha önceden Birinci Dereceden Güvenilirlik Yöntemine (FORM) dayalı olarak geliştirilmiş olup, çekirdek bir program olan RELSYS'in üzerine bir kabuk program şeklinde geliştirilmiştir. Zamanla değişken olmayan ve zamana dayalı köprü güvenilirliği üzerine yapılmış olan geçmiş araştırmalar gözden geçirildikten sonra, arıza zamanı ve bozulma oranı gibi zamana dayalı güvenilirliğin temel kavramları gözden geçirilmiş ve formülize edilmiştir. Ayrıca, yük ve kapasite formülasyonları, en basit şekliyle belirleyici (rastgele olmayan) yük ve belirleyici kapsasite durumları ile başlamaktadır. Zamana dayalı güvenilirlik çalışmasının ilk adımı olarak, yük ve kapasite problemleri RELSYS programı kullanılarak çözülmüştür. Normal ve normal olmayan rastgele değişkenler içeren limit durum eşitliklerinden oluşan güvenilirlik problemleri ve korelasyon durumları çalışılmıştır. Bu kapsamda, paralel, seri ve seri-paralel sistemler değerlendirilmiştir. Her bir çözüm için iterasyon sayısı da gözlemlenmiş ve grafiklendirilmiştir. Zamana dayalı bir güvenilirlik algoritması geliştirmeden önce farklı zamana dayalı güvenilirlik yaklaşımları gözden geçirilmiş ve ayrı ayrı formülize edilmiştir. Çalışılan formülasyonlar sırasıyla: tekrar eden yükleme ve üç arıza süresi, küvet eğrisi, iki bağımsız Poisson süreci ve rastgele mukavemet yıpranması fonksiyonu içeren stokastik yük

modeli ve yük ve kapasite formülasyonudur. Sonuçta, beş farklı yıpranma modeline, Nowak'ın ve Sivakumar'ın modelleri olmak üzere iki ayrı hareketli yük modeline ve çekirdek program olarak RELSYS'e dayanan bir zamana dayalı güvenilirlik analizi için kabuk yazılım şeklinde bir bilgisayar algoritması geliştirilmiştir. Yıpranma modelleri veya mukavemet azalma fonksiyonları: korozyon, difüzyon kontrolü, trafik spreyi, sülfat atağı ve yük taşıma modellerini içermektedir. Söz konusu modellerin zamana dayalı güvenilirlik problemi üzerindeki etkileri gözlenmiştir. Geliştirilmiş olan bilgisayar programı, zamana dayalı olmayan ve zamana dayalı problemlerin her ikisi için de girdi dosyası okuma özelliğine sahiptir. Buna ilaveten, kullanıcıya eldeki problem ve verilmiş olan bir zaman süresi için farklı yıpranma ve hareketli yük modelleri için seçenekler sunmakla beraber belirli bir girdi dosyası oluşturma seçeneği de sunmaktadır. Bu çalışma, zamana dayalı güvenilirliğin yüksek derecede belirsizlik içeren yapısı sebebiyle, belirli bir analiz için kullanılacak olan yıpranma modeli ve hareketli yük modelinin seçiminin zamana dayalı güvenilirlik hesabında önemli bir etkiye sahip olabileceğini göstermiştir. Buna ilaveten, mevcut veya yeni geliştirilmiş olan yıpranma ve yük modellerinin zamana dayalı köprü güvenilirliği programlarına uygulanması ve denenmesi ileride üzerinde çalışılması gereken bir alandır.

Anahtar Kelimeler: Köprüler, Güvenilirlik, Yapısal Güvenilirlik, Sistem Güvenilirliği, Zamana Bağlı Güvenilirlik Analiz, Yıpranma, Çökme Oranı, Stokastik Yükler

To my family and people who are reading this page

ACKNOWLEDGMENTS

Firstly, I would like to express my deepest gratitude to my advisor, Assoc. Prof. Dr. Ferhat Akgül, for his contributions, supports, suggestions and endless guidance during the research for my thesis. I am truly grateful for his wise comments on my thesis.

Besides, I would like to thank the rest of my thesis committee: Prof. Dr. Murat Dicleli, Assoc. Prof. Dr. Senih Gürses, Assoc. Prof. Dr. Tolga Yılmaz and Assoc. Prof. Dr. Mürsel Erdal, who were more than generous with their precious time and for their participation and insightful comments.

Last but not the least, I would like to thank my family. My parents for their financial and emotional supports. My dear sister, Fahimeh Qasemnejad Berenji, for her generous support. I am also grateful to Elmira Pourreza for her endless love and support.

TABLE OF CONTENTS

LIST OF TABLES

TABLES

LIST OF FIGURES

FIGURES

LIST OF ABBREVIATIONS

AGREE	Advisory Group on Reliability of Electronic Equipment
ASR	Alkali-Silica Reactivity
CDF	Cumulative Distribution function
DoD	Department of Defense
FORM	First-Order Reliability Method
FRP	Fiber Reinforced Polymer
FTA	Fault Tree Analysis
MCS	Monte Carlo Simulation
MSR	Matrix-based System Reliability
MTTF	Mean Time To Failure
PDF	Probability Density Function
RC	Reinforced Concrete
SORM	Second-Order Reliability Method
WIM	Weigh-in-Motion

CHAPTER 1

INTRODUCTION

1.1 Reliability Engineering

The word ‘reliability’ was first used by the poet Samuel Coleridge in 1816 (Saleh & Marais, 2006). However, technological meaning of reliability emerged after World War I (Rausand & Hoyland, 2004). This new discipline needed several essential ingredients such as: mass production, probability and statistics. The theory of probability was established by Blaise Pascal and Pierre de Fermat in 1654, and the theory was later expanded from probability into probability and statistics by Laplace in 1812. The other ingredient was mass production (the production of goods in large quantities from a standardized part), which was popularized by Henry Ford in 1910. In 1906, the vacuum tube was invented by Lee de Forest, which had a vital role in electronic equipments during World War II. The vacuum tube played an important role in the emergence of Reliability Engineering. During the war, the failures of vacuum tubes were the main reason of equipment failures. After the war, the US Department of Defense started looking for the cause of these failures, which accelerated the birth of Reliability Engineering. Reliability Engineering is indebted to Walter Shewhart, who was the first person to apply statistical methods to quality control problems in manufacturing (Saleh & Marais, 2006). In 1952, a group was established between the US Department of Defense (DoD) and the American electronics industry, named the Advisory Group on Reliability of Electronic Equipment (AGREE), to recommend measures that would result in more reliable equipment, better education on reliability, and application of reliability programs (Coppola, 1984) . AGREE published its work after 5 years from its establishment in 1957. Most of the authors accept 1957 as the

birth date of Reliability Engineering even though the first conference on reliability was held in 1954. After that date, reliability was known as a new discipline.

1.2 Definition of Reliability

The Cambridge English Dictionary defines reliability as 'how well a machine, piece of equipment, or system works'. Reliability is a measure that involves both statistical and engineering aspects to measure whether a system's performance is successful or not. One of the accepted definitions is: 'Reliability is the probability of a device performing its function over a specified period of time and under specified operating conditions' (Rao, 2015). The definition from the early days of new discipline was 'the probability that an item will perform a required function under stated condition for a stated period of time'. Moreover, ISO 8402's definition of reliability is: 'the ability of an item to perform a required function, under given environmental and operational conditions and for a stated period of time' (Rausand & Hoyland, 2004). From all these definitions, we can conclude that reliability is a method to see if a project, system or a device is going to perform successfully in a desired period of time .

1.3 Application of Reliability to Bridge Engineering

In civil engineering, bridges are one of the most important structures due to the advantages they provide for local and national economy regarding transportation, the need to access affected regions by different types of natural disasters such as floods, hurricanes, and earthquakes, and their strategic importance for national defense. Despite the fact that the construction of bridges has the mentioned importance, engineers' work does not come to an end with the construction of a bridge, and they encounter various problems after its inauguration. In the United States, for example, most bridges were built in the 1950s and the 1960s, according to the data based on the bridges. These bridges deteriorated because of aging, increased live loads, cracking, corrosion, environmental effects, fatigue, and may other causes. As a result, they eventually needed repair, rehabilitation, or replacement.

Regarding different causes for deterioration, they can be classified into two groups: man-made and natural causes. Man-made causes include inadequate maintenance resulting in corrosion and cracking, overloads, collisions between vehicles or vessels, acts of vandalism or intended damages, and terrorist attacks such as explosion and arson. Moreover, natural hazards include winds such as hurricanes and tornadoes, snow or ice, floods, earthquakes, temperature effects, or material degradation. These problems may happen during the construction of the bridge or after its construction. This means that the engineers' work does not end after the construction of the bridge is completed, and finding methods for the prediction of future changes in bridge conditions is essential to solve such problems. After the inauguration of a bridge and crossing of the first vehicle over the bridge, the project comes to an end. However, the next step after the establishment is continuous inspection and maintenance of the structure which requires substantial budgets. Despite the fact that this process is too costly, it is not comparable to the costs in terms of lives which are unrecoverable (Estes, 1997).

To illustrate, a recent bridge failure that resulted in large number of casualties happened in Mississippi river bridge 9340 in Minneapolis, Minnesota on August 1, 2007. The bridge failed and collapsed into the river and onto the riverbanks beneath during the traffic rush hour. Inspection of the bridge could not be completed in 2007 due to construction work. This lack of inspection resulted in the death of 13 people and injury of 145 people in this accident (Figure 1.1) (Rao, 2015). Another more recent failure happened in India, where Kota Chambal Bridge collapsed and 9 civilians died and 45 people were missing on December 25, 2009. In the incident of Kutai Kartanegara bridge in Indonesia on November 26, 2011, there were serious casualties: 20 dead and 40 injured (Wikipedia, 2015). There are many other bridge failures in history that demonstrate the importance of inspection and maintenance for the bridges.

The rehabilitation and maintenance of bridges throughout their lifetimes is a strong financial commitment. For this reason, optimization of time-variant (life-cycle) costs and the application of techniques for inspection are necessary. The reliability methods can be helpful for this aim.

Figure 1.1: Failure of Mississippi bridge on I-35W in August 2007 (CBS Minnesota, 2013).

1.4 Statement of the Problem

After the construction of a bridge, engineers need to predict the probability of safety and failure of a bridge since a structure has a specific life span and stress mechanism results in its deterioration and the decline in the structure's strength or capacity. Consequently, this can cost huge expenses regarding lives and finance. This deterioration occurs through time; that is to say, it is a time variant phenomena. For this reason, for the purpose of devising a reliable prediction for the probability of safety or failure of a structure, it is necessary to determine the time variant reliability of a bridge. To this end, the factors causing deterioration in a structure should be considered to devise a proper time variant reliability method. In this thesis, some of the deterioration mechanisms and live load models are incorporated to come up with a more realistic time variant reliability analysis.

1.5 Objective and Scope of the Thesis

This thesis focuses on the concept of time variant reliability of a bridge structure. The objective of the study is to examine the previous works implemented on time invariant and time variant reliability of bridges, as well as to develop a time variant reliability algorithm based on the previous works in this field. The subjects studied to reach the main objective are five different deterioration models, two live load models, and the FORM (First-Order Reliability Method) technique in order to develop an algorithm to analyze the time variant reliability of a bridge component or a system. The scope of the thesis is the development of an algorithm to calculate time variant reliability for bridges based on different deterioration and live load models.

1.6 Research Methodology

The following approach was adopted in this study. First, relevant literature, publications and studies were reviewed in order to obtain an in-depth information on bridge reliability. Second, reliability theory is explained through introduction of main concepts and different models. Then, load and capacity time invariant reliability problems are analyzed and evaluated to obtain formulations for the reliability of the structural component. These formulations are based on the safety factor and First-Order Reliability method (FORM). Afterwards, the previous methods are examined for time variant reliability, and a computational algorithm for time variant reliability analysis is developed according to deterioration and live load models available in the literature. Finally, the information obtained from the developed algorithm is analyzed and compared.

1.7 Organization of the Thesis

Chapter 1 serves as an introduction to the reliability engineering, definition of reliability, application of reliability to bridge engineering, statement of the problem and objective and scope of the thesis.

Chapter 2 demonstrates the previous works related to time invariant and time variant reliability. First, reliability methods are introduced as well as a comparison between deterministic and stochastic models is made. Causes of degradation are briefly explained such as, general corrosion versus localized corrosion. Also, the failure-case assessment as another application related to reliability assessment is briefly described. Finally, deterioration models are reviewed.

Chapter 3 provides a brief description of the reliability theory. In this chapter, important concepts including random variables, time to failure, reliability function, and failure rate function are introduced. Then, the probability density function (PDF) and cumulative distribution function (CDF) and some other important probability distributions are used to model failure rates.

Chapter 4 presents the formulations for the reliability of a structural component. Calculation of the reliability is performed based on the First-Order Reliability Method (FORM) using the computer program RELSYS developed by Estes, A.C. and Frangopol, D.M. (1997).

Chapter 5 presents various formulations and a computer algorithm developed based on five different deterioration models, two live load models, and the FORM technique for time variant reliability.

Chapter 6 summarizes the research results and compares the outcomes obtained from the formulations and the program which was developed in Chapter 5.

CHAPTER 2

LITERATURE SURVEY

2.1 Introduction

Reliability engineering has been used in various fields of engineering. It was first used in electronic field, however, with the expansion of this discipline, it started covering other branches of engineering too. The reliability studies evolved with time. Accordingly, it is essential and important to review the papers published related to this discipline over the past several decades. In this study, papers related to bridge reliability have been reviewed. This chapter covers published works in the areas of both time variant and time invariant bridge reliability. In the following sections, relationship between reliability methods and its related models will be discussed along with the time variant reliability analysis. An outline of these relationships is illustrated in Figure 2.1. In this figure, reliability methods are classified into different applications such as, resistance and load modeling, component reliability, and forensic analysis. In forensic analysis, researchers and engineers apply failure-cause assessment study to identify and understand the causes of failure to avoid the repetition of bridge failures. This can be performed by a deterministic approach, which does not systematically take into account any information on the uncertainties involved in a structural failure. To compensate this problem, a reliability-based failure-cause assessment methodology is developed to incorporate the uncertainties involved in structural failures. This proposed methodology uses Bayesian approach based on the experimental laboratory testing data (Choi, Lee, Choi, Cho, & Mahadevan, 2006).

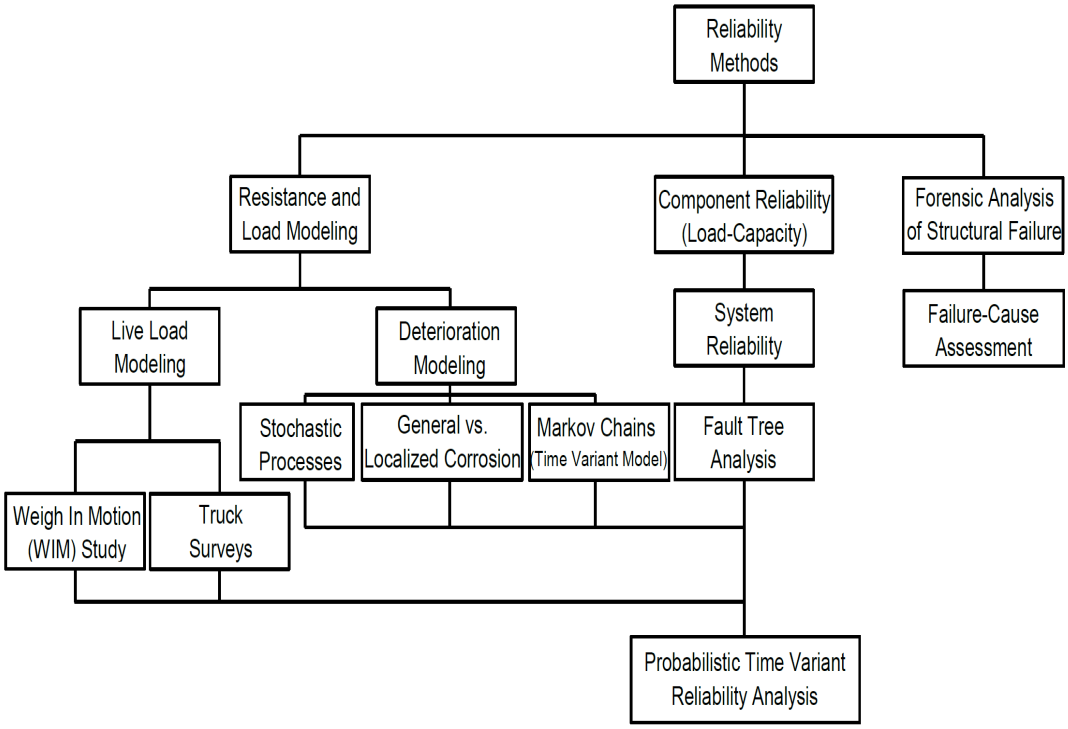

Figure 2.1: Relationship Between Structural Reliability Methods and its Related Models and the Time Variant Reliability Analysis.

2.2 Reliability Methods

In the past, several methods have been developed for reliability analysis, including First-Order Reliability Method (FORM), Second-Order Reliability Method (SORM), Out-crossing methods, Surrogate Model-based methods, Matrix-based System Reliability method (MSR) and Monte Carlo Simulation (MCS)-based methods (Kuschel & Rackwitz, 2000; Mahadevan & Dey, 1997; Melchers, 1999; Kand, Song, & Gardoni, 2008). Each method has its own advantages and disadvantages. Based on the system, structure, and the conditions, researcher should decide which method is suitable for the problem at hand. For instance, when no analytical solution exists and no general numerical procedure is available, Monte Carlo Simulation method is preferred. The disadvantages of this method, however, are slow convergence and higher computational expense, especially for small probability problems (Olsen, 2006). When there is incomplete information on the component probabilities and/or the statistical depen-

dence in a system, it will be adequate to apply the Matrix-based System Reliability method (MSR). Since it is possible to describe any general system event in a simple matrix form by this method, this method can handle the system event in a more convenient way and estimate its probability when compared to other methods. (Kand et al., 2008).

The accuracy of reliability prediction, in addition to the advantages and disadvantages of the methods and the method chosen, is remarkably influenced by the uncertainty quantification. Uncertainty can be divided in two types: model uncertainty, when approximate models are present, and data uncertainty, when insufficient or imprecise models are present (Ling, 2013).

2.3 Deterministic vs. Stochastic Models

A deterministic model is the one in which the material properties are well known, i.e. deterministic, none of them is random. Also the applied loads are also deterministic. As a result, for a given set of initial conditions, a deterministic model always preforms the same way. This is an idealized case not reflecting the reality. In real physical world, randomness always exists in materials properties and the loads.

On the other hand, a stochastic model has random properties. In a stochastic model, probability distributions, not unique values describe the variable states; e.g. the Young's modulus is a random variable with uniform distribution or normal distribution (with a given mean or standard deviation); the applied load is a random variable, e.g. wind load, earthquake (vibration of random amplitude and displacement). The collection of enough failure data for statistical analysis is hardly possible and even if enough data can be collected, the validation of underlying failure mechanism is argued to be static. Therefore, stochastic model is a more suitable model in reliability studies.

2.4 Live Load Models

One of the major factor that causes the deterioration of a bridge and influences its reliability is the live load, which refers to the amount of the applied force on the bridge by moving vehicles. The parameters that determine the live load are the truck weight, span length, axle configuration, axle loads, number of vehicles on the bridge, position of the vehicle on the bridge, girder spacing, and stiffness of structural members. Based on two different sources of live load data, which are truck surveys and Weigh-in-Motion (WIM) studies, the live load models have been developed. WIM refers to the study of measuring the weights of vehicles passing at various speeds on bridges or highways.

To formulate the bridge live load models, it is necessary to have statistical data on vehicle gross weights, axle weights and axle spacings. These data can be obtained from truck surveys and WIM studies. When there is an accurate mathematical distributions of these parameters, it is easier to obtain a formulation for live load since WIM studies have the advantage of providing a great amount of realistic data on traffic. However, WIM system was outdated in formulating the live load models in the mid 1980s because a large portion of data was not reliable. Instead, truck surveys were used to obtain the data. Afterwards, based on new and modified data, WIM has been used again instead of truck surveys in formulating live load models (Tabsh & Nowak, 1991; A. Nowak, 1993; A. Nowak & Hong, 1991).

2.5 Deterioration Models

Bridges can be categorized by their structural systems, by being fixed or moveable, by their use or function, or by the materials that are used to build them. For instance, the materials used to build bridges until the end of the 18^{th} century consisted of timber, stone, and masonry. However, the materials mostly used in modern bridges consist of concrete, steel, fiber reinforced polymers (FRP), stainless steel or combinations of these. No matter which material is used in the construction of a bridge, bridges are always exposed to environmental attacks, which cause their deterioration (Akgul, 2002). Some examples of the distress mechanisms for concrete structures

include Alkali-Silica Reactivity (ASR), sulfate attack, freeze-thaw cycling, and reinforcing corrosion. There are many others. There are many studies that have focused on modeling the structural deterioration and resistance degradation of bridges. These models are investigated by laboratory tests, statistical analysis and mathematical modeling (González, Andrade, Alonso, & Feliu, 1995; Leira & Lindgard, 2000; Papadakis, Roumeliotis, Fardis, & Vagenas, 1996; Patev, Schaaf, & James, 2000; Rendell, Jauberthie, & Grantham, 2002).

As an example, the most common type of damage that occurs on a bridge is the corrosion. The corrosion of a metal, such as steel, can be categorized into two types: general and localized corrosion. General corrosion, which is known as uniform corrosion, is the most common type of corrosion. This type of corrosion occurs when steel is exposed to water, soil or open atmosphere. It may occur in reinforced concrete also and can cause cracking, spalling or delamination of the concrete cover. However, it can be easily detected by the rust stains during an inspection. The other type of corrosion is the localized corrosion. Unlike general corrosion, it occurs at discrete spots on the metal surface, and it is difficult to detect. For instance, in a reinforced concrete member, localized corrosion produces little rust staining on the concrete which makes it difficult to detect corrosion spots during the inspection. Localized corrosion can be classified into three types: pitting, crevice and filiform corrosions. These types of corrosion result in deterioration. In the past, numerous researchers have studied the effects of corrosion on reliability of steel bridges (Kayser & Nowak, 1989; Czarneckia & Nowak, 2008) and on reinforced concrete bridges (Val & Melchers, 1997).

2.5.1 Markov Chains

Markov chains or Markov process is a method used for stochastic modeling of bridge deterioration. Parameters which result in invariable changes in the state of a system are space or time. This transition normally depends on the prior states. To model such transitions, Markov process may be used when the transition probability is only based on the current state. Furthermore, Markov chains may be used when the state space is a countable or finite set, and a discrete parameter Markov chain may be used when this change occurs only at discrete points (Ang & Tang, 1975). Moreover, regarding

the Markov model, there are two main concepts: System State and State Transition. The state of a system refers to a specific combination of system parameters at any given instant of time, and the state transition refers to the control over the changes of a state occurring within a system. The system goes from one state to another, until it reaches the failure state. Failure rates, fault coverage factors, and repair rates are the parameters that describe the state transitions. Furthermore, the Markov chain deterioration model does not consider the prior state transition but the present state transition in order to predict the future probabilistic behavior of a process (Misra, 2008).

Consider four ratings for a bridge member: A, B, C, and D, where A indicates new or nearly new condition, and D indicates a state which represents that the element must be replaced. The deterioration model is developed based on a transition matrix, which displays the probability of the structural element transitioning from one state to another state such as from A to B or from C to D. Initial distribution is multiplied by the transition matrix to produce a new state distribution for the next time period.

For modeling deterioration of bridges and infrastructure assets, Markov chains has been used extensively. It can predict the probability of a structural element continuing to remain in the same condition state (such as in A) or transition into another condition state (such as to B) considering certain environmental and initial conditions. The advantages of using Markov process are as follows. The essential parameters of a dynamic change is summarized in the basic transition matrix. It can consider time dependence and uncertainty of deterioration process and can be applied at both component and system levels. The disadvantages are as follows. It requires large amount of historical data. For instance, Zhang, Sun, and Wang (2003) used inspection records of approximately 100 bridges from VicRoads database from 1996 to 2001 to develop the transition matrices. For more a realistic modeling, data on thousands of bridges may be needed. The other disadvantage is the absence of accuracy and failure to link the data with environmental variables (Zhu, 2008).

2.5.2 Fault Tree Analysis

In a system, such as a bridge, deterioration of one component influences the deterioration of another. This interaction between the components will affect the performance of the system, which may lead to the failure of the whole system (i.e. the bridge itself). Fault tree analysis (FTA) is a schematical graphical model which illustrates the various failure paths that lead to an unacceptable outcome. Many researchers such as Sianipar and Adams (1997) and Davis-McDaniel, Chowdhury, Pang, and Dey (2013) used this method to assess the risk of a bridge collapse. Lebeau and Wadia-Fascetti (2000) used the FTA to model the deterioration of a bridge performance.

A bridge consists of three main components: deck, substructure, and superstructure. The overall performance of the bridge will be affected if any basic component of the bridge deteriorates. The top event (T) is the deterioration of bridge performance which is the undesirable outcome. It is evaluated by the union of the deck condition (A), superstructure condition (B) and substructure condition (C), where A is also the union of the joint condition (A_1) and deck material condition (A_2), B is the union of the girders condition (B_1) and bearings condition (B_2). The top event can be evaluated by a Boolean equation (i.e. in terms of unions and intersections of events). Besides the advantages of the fault tree analysis, displaying the cause-effect relationships and showing the complexity in a single model, FTA is a difficult technique for determining the probabilities of component failures (Zhu, 2008).

2.5.3 Stochastic Process

A stochastic process is the most convenient method to model the uncertainty in time-dependent deterioration. Examples in this process are the Gaussian process and the Gamma process. A Gamma process is a stochastic with independent non-negative Gamma distributed increments. A property of the Gaussian process is that a structure's resistance alternately increases and decreases. Due to the fact that resistance deteriorate with time and does not increase with time, this process is not an appropriate one in deterioration modeling if the deterioration moves in one direction. To solve this problem, the Gamma process will be a good option as the cumulative amounts of

deterioration is normally present in the inspection measurements. Additionally, the resulting modeling of inspections obtained through stochastic processes is natural and realistic. Even when there are problems with the inspections, particularly when there is a lot of uncertainty in the applied deterioration process, these imperfect inspections can be solved through the mathematical models despite the complexities. Various researches have studied bridge reliability using the stochastic process technique. Examples are van Noortwijk, van der Weide, Kallen, and Pandey (2007), Straub (2009), and Huang and Chen (2015).

2.5.4 Probabilistic Time Variant Reliability Analysis

As the age of a structure increases, the effect of corrosion on the bridge also increases, which causes the deterioration and possibly the failure of the bridge in the long term. For this reason, deterioration changes with time, which means that the reliability will also be a time variant value. Since corrosion of reinforcement is a major cause of structural deterioration, many researchers in the past studied the effects of corrosion on various types of bridges, such as reinforced concrete (RC) girder bridges (Frangopol, Lin, & Estes, 1997), RC slab bridges (Val, Stewart, & Melchers, 1998; Vu & Stewart, 2000) and prestressed concrete structures (Bin, Zhao, & Xiang, 2010).

Including RC slab bridges, Val and Melchers (1997) studied a method for reliability assessment. They considered a traffic load model, a corrosion model (both general and localized), and a nonlinear finite element structural model using the first-order reliability method and taking into account uncertainties related to material properties, geometry, loads, and corrosion parameters. As a result, the impact of these uncertainties is analyzed on the reliability. Similarly, Stewart and Rosowsky (1998) conducted a research on a marine environment based on Monte Carlo simulation to calculate the reliability of a structure.

Moreover, for steel bridges, Czarneckia and Nowak (2008) selected representative structures, formulated limit state functions, and analyzed reliability of the selected bridges. They also developed load models, and resistance models for corroded steel girders, a reliability analysis method, and time-dependent reliability profiles including deterioration due to corrosion.

Bridges consist of various components which are connected in a parallel, series or in a series-parallel fashion, and due to the presence of a discrepancy between the reliability level of individual members and the overall bridge reliability, it is important to analyze time variant system reliability of bridges also. Accordingly, many researchers investigated this field. Some examples are Enevoldsen and Sørensen (1993), A. S. Nowak and Zhou (1990), A. S. Nowak (2004), and Ghosn (2010).

Time variant reliability approaches have also been used for service life prediction of aging bridges. Since bridges are subjected to environmental attack, the resistance of a bridge element changes with time. Also, the truck loads (live loads) are not constant in time. For this reason, time variant load and resistance should be used for a more realistic reliability analysis and for the remaining service life prediction. An algorithm was developed by Enright and Frangopol (2000, 1998) for life prediction of deteriorating systems. It used importance sampling, numerical integration, fault tree analysis and an adaptive algorithm to evaluate the reliability of a bridge. This approach was first proposed for nuclear power plants by Ellingwood and Mori (1993).

The advantages of probabilistic time variant reliability analysis are the possibility of including time and uncertainty, achieving reliable computational outcomes with practical meanings, being applicable for any types of structure, and being applicable in reliability based design and management. However, the disadvantages of this analysis are the presences of difficulties in computations, the demand for powerful softwares, and the requirement of real statistical data on probability distributions of various uncertain parameters based on laboratory tests or statistics (Zhu, 2008).

2.6 Summary

In this chapter, a literature review of the reliability of bridges is presented in the areas of both time invariant and time variant bridge reliability. Moreover, there was a discussion over the relationship between reliability methods and its related models, and the time variant reliability analysis. To review the research conducted on the reliability of bridges in the past, this chapter introduced some of the different types of reliability methods and resistance and load modeling methods. Reliability

is a vast field of study extending into many different fields of engineering and science. Structural reliability is a more focused area of study including the reliability of bridge structures. Probabilistic methods form the foundations of reliability methods discussed in this chapter. In the following chapter, reliability theory will be explained in a general context introducing the fundamental concepts such as time to failure and failure rate.

CHAPTER 3

RELIABILITY THEORY

3.1 Introduction

Reliability is defined as the probability that a component or a system will perform properly under a given set of operating conditions for a stated time interval. In this definition, it is necessary to have criteria for failure to know at what point the system is no longer functioning properly. Moreover, operating conditions consist of loading to which the system is subjected as well as environmental conditions. In this chapter, the focus will be on the reliability and the failure rate to develop modeling failure rate through probability distributions. Firstly, there is a brief overview of what important concepts, including random variables, time to failure, reliability function, and failure rate function, in reliability theory are. Secondly, in order to develop modeling failure rates, the probability density functions (PDF) and cumulative distribution functions (CDF) of some of the important probability distributions are provided. Then, these concepts will be used to obtain the failure rates and reliabilities for time to failure of each probability distribution. Consequently, there will be a comparison between different distributions for time to failure, and there will be a discussion of what their pros and cons are. Based on this comparison, conclusions will be made about which distribution type is preferred for which case.

3.2 Random Variables

There is a strong association between probability and some special variables whose values can only be assessed using statistical data obtained from laboratory experiments or field data. Random variable is any variable whose value is selected randomly. For instance, in testing the compressive strength of concrete cubes, several specimens can be used. The test results of these specimens will not be the same; therefore, the outcome of the result is considered as a random variable because the testing is performed on a random specimen and the experiment is also a random experiment. There are two sorts of random variables named as discrete and continuous random variables. When the variables are integers, or more precisely a countable subset of real numbers, they are called discrete random variables. When the range consists of continuous values over an interval of real numbers, they are called as continuous random variables. By random variable, it is implied that each number of the sampled population should have an equal chance of being selected (Mishra, 2006).

3.3 Time to Failure

Time to failure of a component or a system refers to the elapsed time from the beginning of the component's or system's operation until its failure for the first time. The range of the elapsed time can vary from 0 to infinity as the exact time of failure is not known; therefore, the time to failure can be any value in this range. However, there are specific lifetimes that are known to be within certain time periods. A light bulb's or a concrete bridge girder's lifetimes are very different and each has its own limits. For instance, it is possible that a bridge fails in the first year or 80 years from the inauguration of the bridge. As a result, the time to failure is assumed to be a continuous random variable.

3.4 Reliability Function

The reliability function, or the survivor function, is the probability related to the survival of a component or a system. It is also related to the specified time period $(0, t]$

at which the component or the system does not fail. In this specified time period $(0, t]$, t is the time at which the component or system is still operating. The reliability function is mathematically defined as follows:

$$R(t) = 1 - F(t) = 1 - \int_0^t f(u)du = \int_t^\infty f(u)du \tag{3.1}$$

where $F(t)$ is the probability of failure within the time interval $(0, t]$ and $f(u)$ is the probability density function of time to failure. As the Eq. 3.1 indicates, the range of reliability function is between 0 and 1.

3.5 Failure Rate Function

The failure rate function, or hazard rate function, is the probability that a component or a system will fail within a specified time period $(t, t + \Delta t]$ by knowing the fact that the component or the system is functioning at time t. This probability can be defined as:

$$\begin{aligned} Pr(t < T \leq t + \Delta t | T > t) &= \frac{Pr(t < T \leq t + \Delta t)}{Pr(T > t)} \\ &= \frac{F(t + \Delta t) - F(t)}{R(t)} \end{aligned} \tag{3.2}$$

To obtain the failure rate function $\lambda(t)$, we take the limit of Eq. 3.2 as $\Delta t \to 0$ after dividing it by Δt which yields as:

$$\begin{aligned} \lambda(t) &= \lim_{\Delta t \to 0} \frac{Pr(t < T \leq t + \Delta t | T > t)}{\Delta t} \\ &= \lim_{\Delta t \to 0} \frac{F(t + \Delta t) - F(t)}{\Delta t} \frac{1}{R(t)} = \frac{f(t)}{R(t)} \end{aligned} \tag{3.3}$$

where $f(t)$ is the probability density function and $R(t)$ is the reliability function of time to failure.

3.6 Probability Distributions

The concept of mathematical variables and functions of variables can be used to represent qualitative values that can not be predicted precisely. Variables with their associated uncertainty can be quantified by probabilistic models and distributions. There are several types of probability distributions for describing various types of discrete and continuous random variables. In the following sections, modeling of failure rate using some of the probability distributions for time to failure have been introduced.

3.6.1 Modeling Failure Rate Using Normally Distributed Time to Failure

The most commonly used probability distribution in statistics is the normal distribution. Many natural phenomena can be approximated by normal distribution. The probability density function (PDF) of normal distribution with time to failure t is defined as follows:

$$f(t) = \frac{1}{\sigma\sqrt{2\pi}} e^{-\frac{(t-\mu)^2}{2\sigma^2}} \tag{3.4}$$

where μ is the mean value, which is also known as MTTF (Mean Time To Failure), σ is the standard deviation and σ^2 is the variance of the normally distributed time to failure t. Probability density function of normal distribution for the assumed values of $\mu = 2.0$ and $\sigma = 0.2$ is shown in Figure 3.1.

Cumulative distribution function (CDF) of the normal distribution is defined as:

$$F(t) = \int_{-\infty}^{t} \frac{1}{\sigma\sqrt{2\pi}} e^{-\frac{(t'-\mu)^2}{2\sigma^2}} dt' \tag{3.5}$$

or

$$F(t) = \phi(\frac{t-\mu}{\sigma}) \tag{3.6}$$

The reliability for normal distribution is:

$$R(t) = 1 - \phi(\frac{t-\mu}{\sigma}) \tag{3.7}$$

Failure rate for normal distribution is:

$$\begin{aligned}\lambda(t) &= \frac{f(t)}{R(t)} \\ &= \frac{1}{\sigma\sqrt{2\pi}[1-\phi(\frac{t-\mu}{\sigma})]} e^{-\frac{(t-\mu)^2}{2\sigma^2}}\end{aligned} \tag{3.8}$$

The cumulative distribution function, the failure rate and reliability for normal distribution are shown in Figures 3.2, 3.3 and 3.4 respectively.

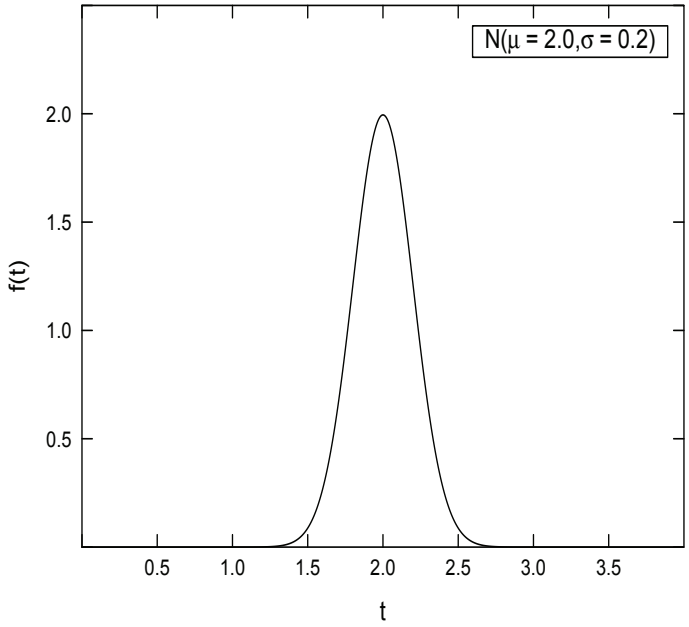

Figure 3.1: Probability Density Function of Time to Failure Having Normal Distribution.

3.6.2 Modeling Failure Rate Using Lognormally Distributed Time to Failure

If time to failure (t) has a large uncertainty, the use of normal distribution is not appropriate because of the tail of the distribution continuing in the negative region. Lognormal distribution is generally used to describe fatigue and other phenomena caused by aging and wear. Random variable t is log-normally distributed if log(t) has normal distribution. The probability density function (PDF) of time to failure t having lognormal distribution is defined as:

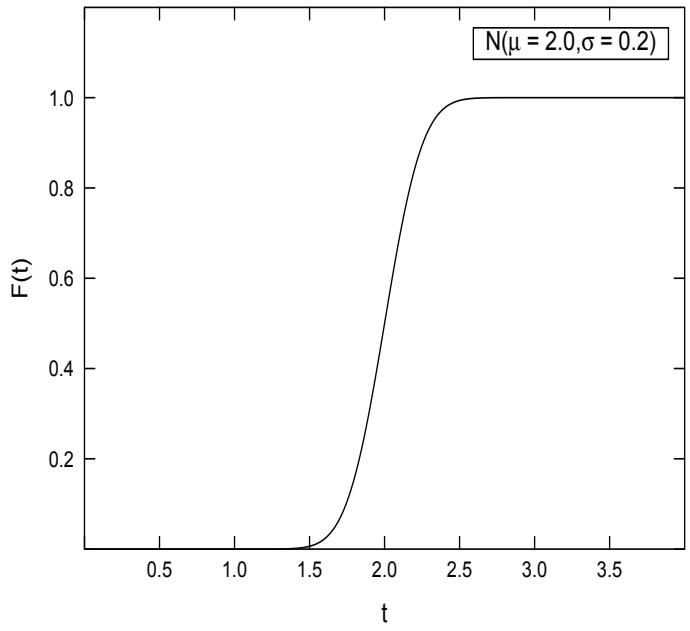

Figure 3.2: Cumulative Distribution Function of Time to Failure Having Normal Distribution.

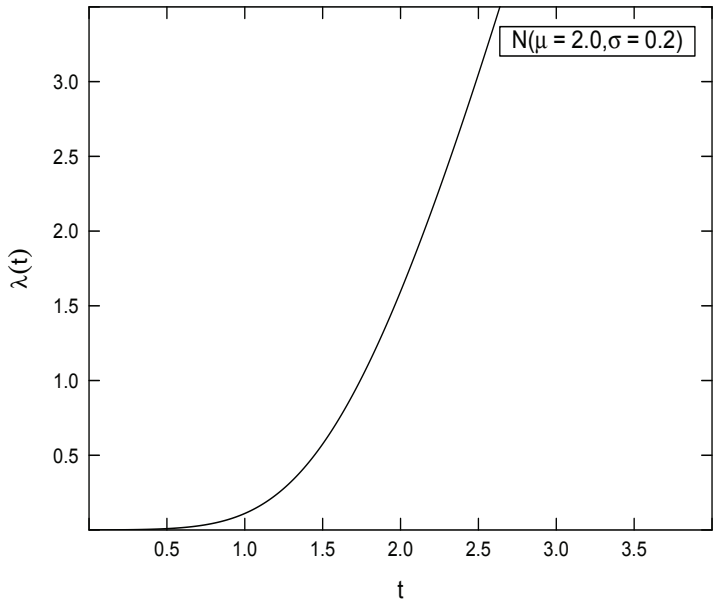

Figure 3.3: Time Dependent Failure Rate $\lambda(t)$ for the Normally Distributed Time to Failure t.

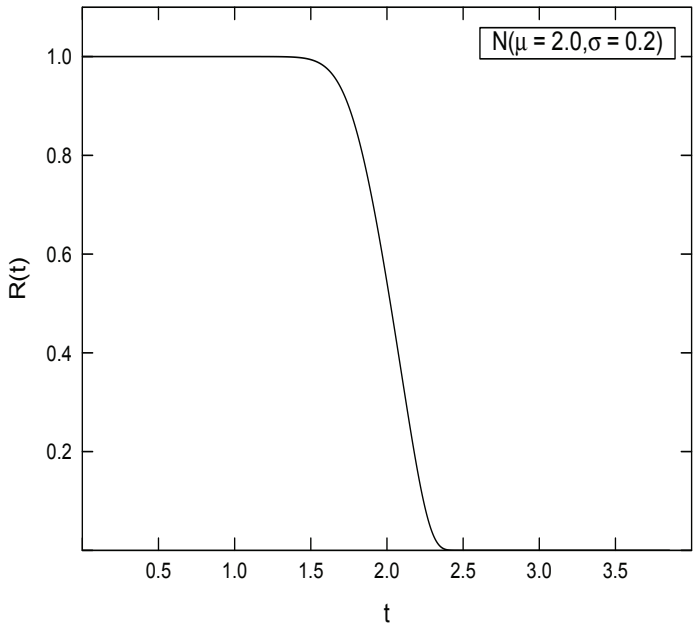

Figure 3.4: Reliability for Time to Failure Having Normal Distribution.

$$f(t) = \frac{1}{t\sigma\sqrt{2\pi}} e^{-\frac{(\ln t - \mu)^2}{2\sigma^2}} \tag{3.9}$$

Cumulative distribution function (CDF) of the lognormal distribution is:

$$F(t) = \phi(\frac{\ln t - \mu}{\sigma}) \tag{3.10}$$

The reliability for lognormal distribution is:

$$R(t) = 1 - \phi(\frac{\ln t - \mu}{\sigma}) \tag{3.11}$$

Failure rate for lognormal distribution is:

$$\begin{aligned} \lambda(t) &= \frac{f(t)}{R(t)} \\ &= \frac{1}{t\sigma\sqrt{2\pi}[1 - \phi(\frac{\ln t - \mu}{\sigma})]} e^{-\frac{(\ln t - \mu)^2}{2\sigma^2}} \end{aligned} \tag{3.12}$$

Figures 3.5, 3.6, 3.7 and 3.8 show the PDF, CDF, failure rate and reliability of lognormal distribution, respectively. In these figures lognormal distribution is plotted for the assumed values of $\mu = 1.0$ and $\sigma = 0.1$, 0.5, and 1.0.

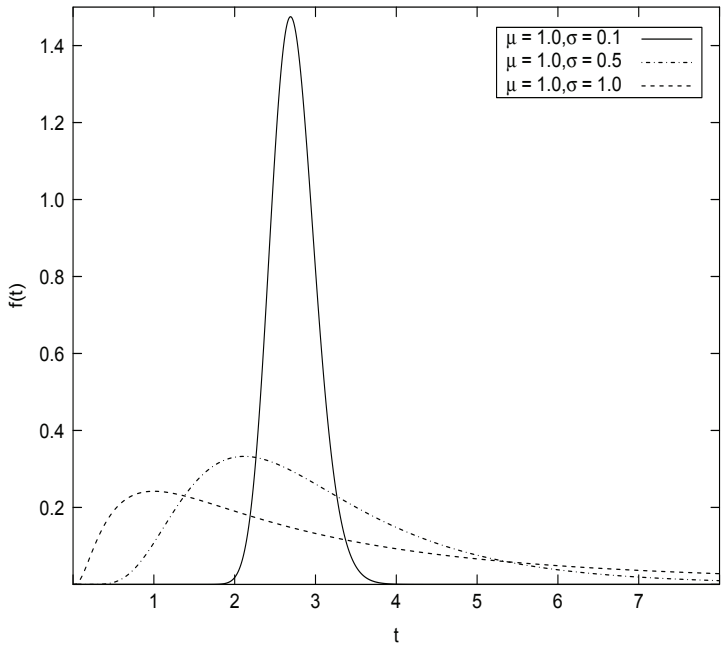

Figure 3.5: Probability Density Function of Time to Failure Having Lognormal Distribution.

3.6.3 Modeling Failure Rate Using Exponentially Distributed Time to Failure

Exponential Distribution describes the time between events in a Poisson process, i.e. a process in which events occur continuously and independently at a constant average rate. Constant failure rate model for continuously operating system leads to an exponential distribution, i.e. $\lambda(t) = \lambda$. Probability density function (PDF) of exponential distribution with time to failure t is:

$$f(t) = \lambda e^{-\lambda t} \tag{3.13}$$

Cumulative distribution function (CDF) of the exponential distribution is:

$$F(t) = 1 - e^{-\lambda t} \tag{3.14}$$

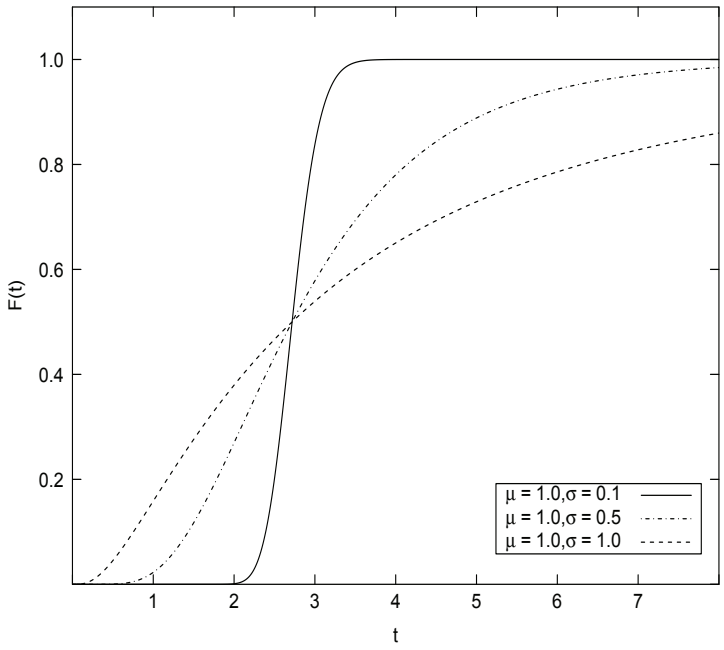

Figure 3.6: Cumulative Distribution Function of Time to Failure Having Lognormal Distribution.

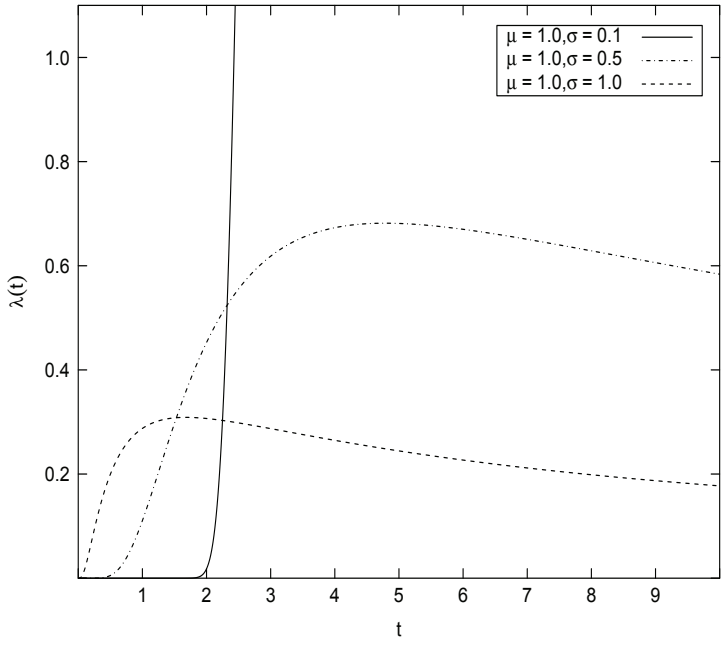

Figure 3.7: Time Dependent Failure Rate $\lambda(t)$ with Lognormally Distributed Time to Failure t.

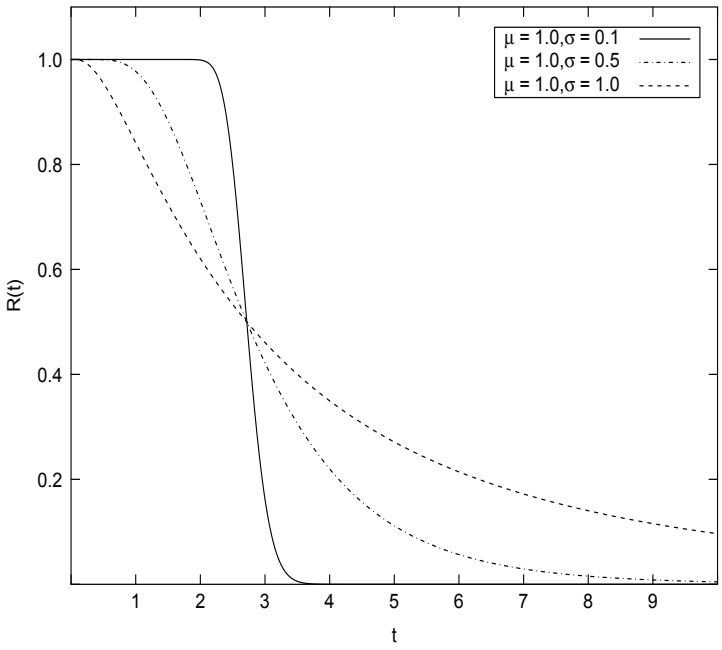

Figure 3.8: Reliability for Time to Failure Having Lognormal Distribution.

and the reliability based on exponentially distributed time to failure becomes:

$$R(t) = e^{-\lambda t} \tag{3.15}$$

Figures 3.9, 3.10 and 3.11 show the graphs of PDF, CDF and reliability for the exponentially distributed time to failure t, respectively. For four separate values of the parameter λ, (i.e. 1, 2, 3, and 4).

3.6.4 Modeling Failure Rate Using Weibull Distributed Time to Failure

The most commonly used distribution in reliability engineering is Weibull distribution. The reason for this is that a variety of failure rate types can be modeled using Weibull distribution such as:

- Constant failure rate
- Wearing failure rate
- Wear-out failure rate

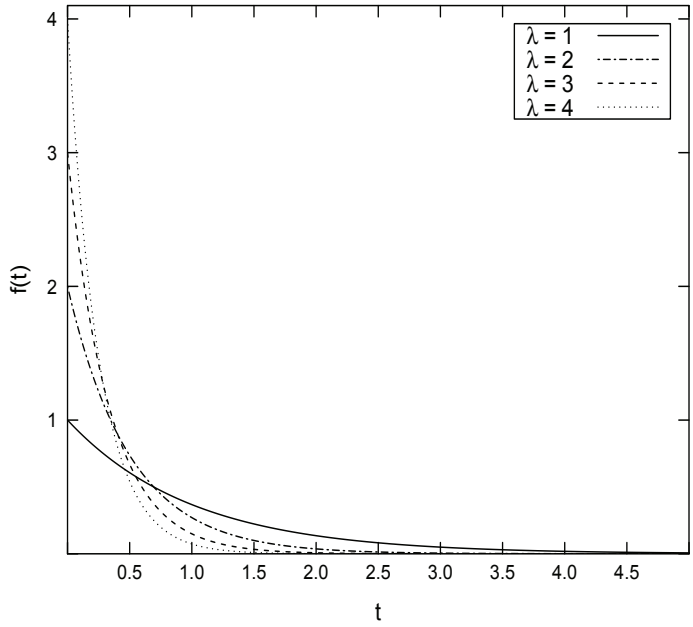

Figure 3.9: Probability Density Function of Time to Failure Having Exponential Distribution.

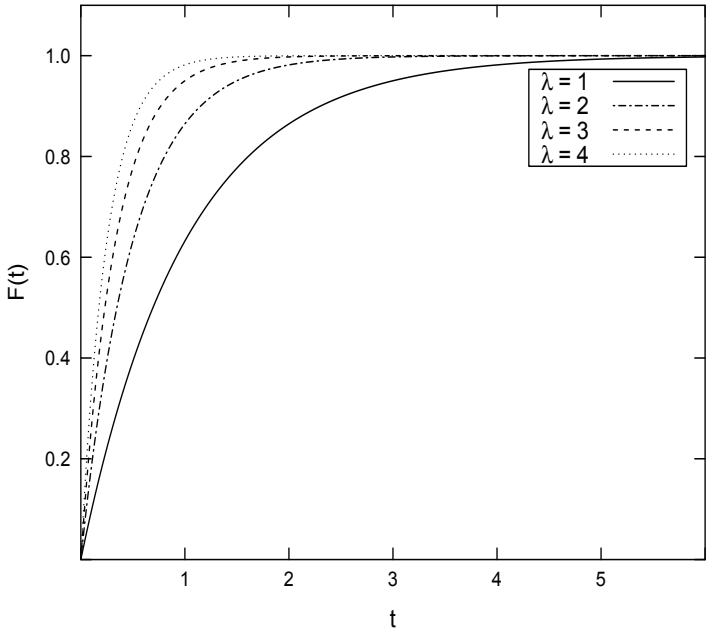

Figure 3.10: Cumulative Distribution Function of Time to Failure Having Exponential Distribution.

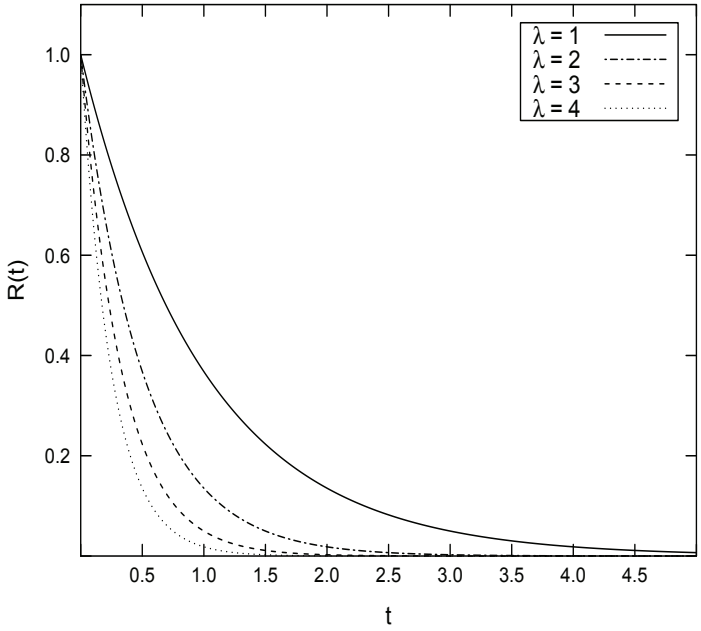

Figure 3.11: Reliability for Time to Failure Having Exponential Distribution.

Probability density function of time to failure t having Weilbull distribution is given as:

$$f(t) = \frac{m}{\theta}(\frac{t}{\theta})^{m-1}e^{-(\frac{t}{\theta})^m} \tag{3.16}$$

Cumulative distribution function (CDF) of the Weibull distribution is:

$$F(t) = 1 - e^{-(\frac{t}{\theta})^m} \tag{3.17}$$

The reliability for Weibull distribution is:

$$R(t) = e^{-(\frac{t}{\theta})^m} \tag{3.18}$$

and the failure rate for Weilbull distribution is:

$$\begin{aligned}\lambda(t) &= \frac{f(t)}{R(t)} \\ &= \frac{m}{\theta}(\frac{t}{\theta})^{m-1}\end{aligned} \tag{3.19}$$

where θ is the scale parameter and m is the shape parameters of the Weibull distribution defining the steepness and shape of the distribution curve.

Figures 3.12, 3.13, 3.14 and 3.15 are related to PDF, CDF, failure rate and reliability of Weibull distributed time to failure t, respectively, for $\theta = 1$ and for four separate values of $m = 0.5, 1, 2, 4$.

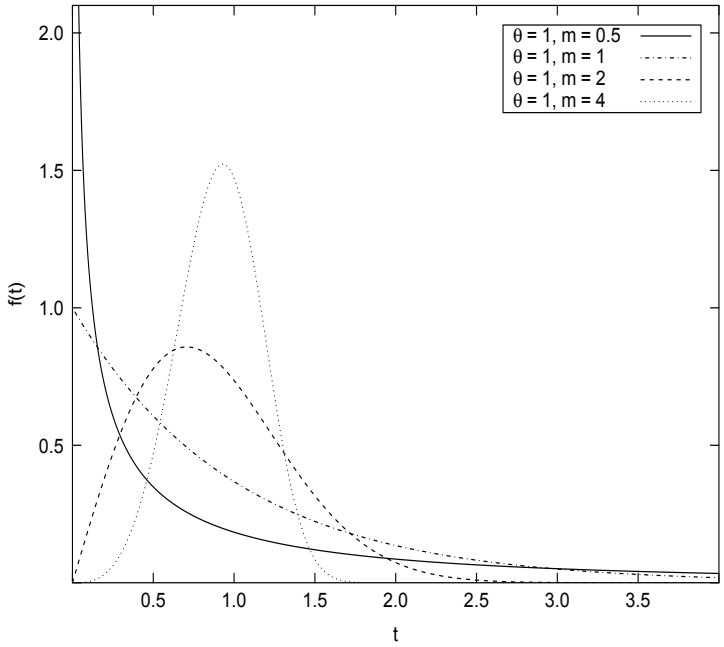

Figure 3.12: Probability Density Function of Time to Failure Having Weibull Distribution.

3.7 Summary

To model the failure rate, four different probability distributions are used. Each of these four probability distributions were used in order to obtain the failure rates and reliabilities for time to failure for each probability distribution. The probability distributions used were normal, lognormal, exponential and Weibull. The first distribution

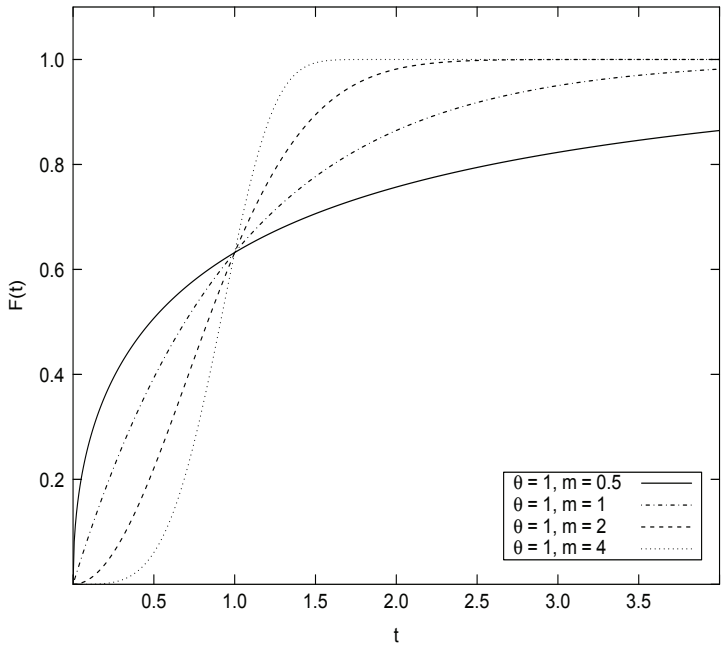

Figure 3.13: Cumulative Distribution Function of Time to Failure Having Weibull Distribution.

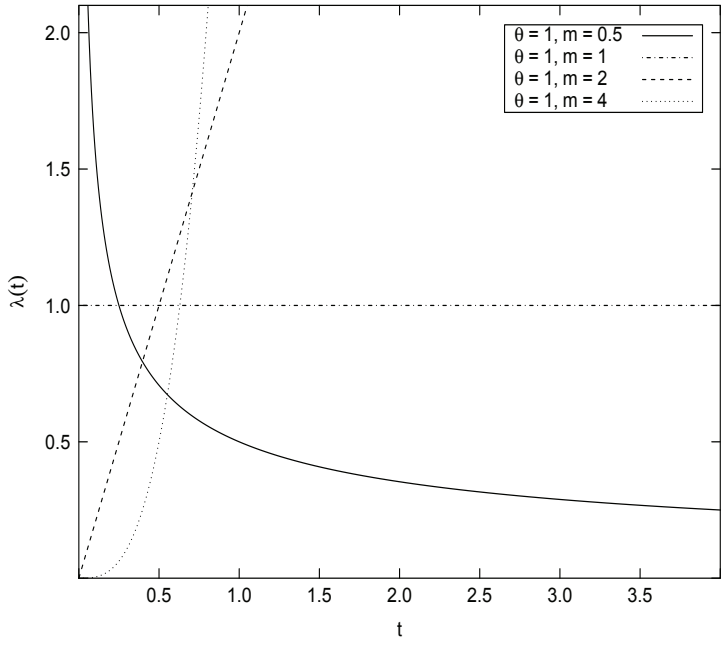

Figure 3.14: Time Dependent Failure Rate $\lambda(t)$ with Weibull Distributed Time to Failure t.

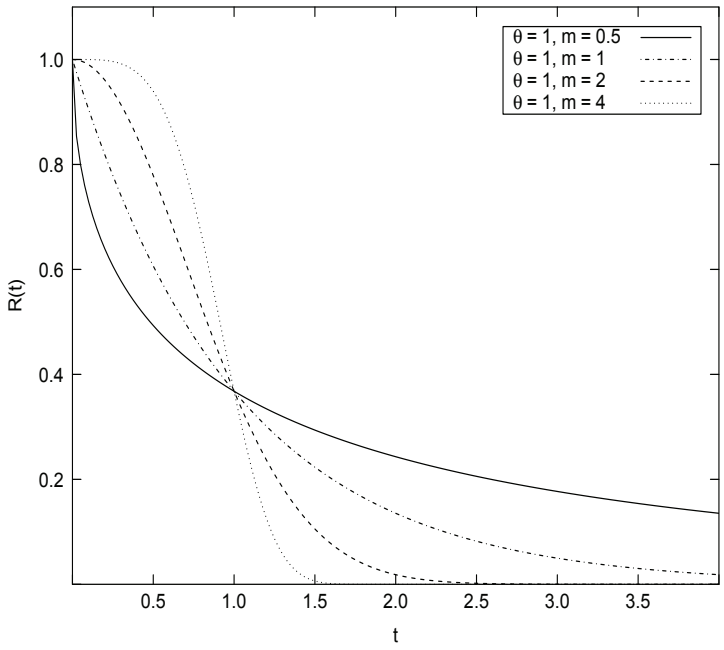

Figure 3.15: Reliability for Time to Failure Having Weibull Distribution.

type, normal distribution, is generally used to model the aging failure. This distribution is the most commonly used probability distribution in statistics and it is used to model natural phenomena in engineering and science. However, in reliability studies, its usage is limited to the situations with a reasonably well-defined wear-out time. For instance, this distribution can be used to model aging failure of a cutting edge in a machine tool. Despite the large range of its applications, normal distribution is not always appropriate because it extends from zero to infinity. This is a disadvantage due to the fact that most of the variables in reliability have their values only in the positive range.

The second distribution studied was lognormal distribution. Similar to normal distribution, it is also frequently used to model aging failure. Unlike normal distribution, it is a more versatile distribution because of its range of shapes. As a result, it can be more appropriate to deal with reliability data, such as populations with wear-out features. Moreover, it does not have the disadvantage of the normal distribution because the tail of distribution is always in the positive region. This distribution is often applied to the cases such as repair times of a maintained system, count of switch operations, and vehicle mileage per year in order to model usage data.

In contrast to normal and lognormal distributions, exponential distribution is generally used to model random failure. Constant failure rate model for the continuously operating systems leads to an exponential distribution, which describes the situation in which there is a constant hazard rate. Finally, Weibull distribution can model early, random, and aging failures. It can be used to describe the phenomena for which some threshold time must elapse before there can be failure. Since this distribution has the advantage of adjusting the distribution parameters in reliability studies and fits many situations of life-like distributions, it is the most popular statistical distribution for reliability engineering. Considering the characteristics of all four distributions, it can be concluded that the most appropriate probability distribution to develop the best modeling failure rate depends on the situation and the problem at hand.

CHAPTER 4

ANALYSIS AND EVALUATION OF LOAD AND CAPACITY RELIABILITY PROBLEMS

4.1 Introduction

The objective of a reliability study for a given structure or a bridge component is to ensure that the structure is safe to use and remains safe for a given period of time. An important stage begins after its construction because its exposure to different environmental attacks or distress mechanisms results in the structural component's deterioration. To define the safety of a structural component, structural engineers, in its most simple form, use deterministic load (or stress) and deterministic capacity (or strength) to define the reliability and the so-called safety factor. In this chapter, the concept of safety factor will be used to develop formulations for the reliability of a structural component. Based on these formulations, load and capacity will be considered as random variables, and two different distribution types, normal and lognormal distributed load and capacity, will be used. In addition, calculation of the reliability will be performed using the First-Order Reliability Method (FORM) and RELSYS, a computer program developed by Estes, A.C. and Frangopol, D.M. (1997), in order to verify the results of various examples presented RELSYS manual and also Ang and Tang (1975).

4.2 Formulation of Load and Capacity Reliability

In structural engineering, deterministic load (or stress) and deterministic capacity (or strength) are used to define the safety of a structural component. In engineering, factor of safety (F.S) and safety margin concepts are traditionally used to define the relationship between load and capacity. Safety factor is defined as the ratio between the capacity and the load ($v = \frac{c}{l}$), while safety margin is defined as the difference between capacity and load ($m = c - l$). If a structure's safety factor is less than one, or safety margin is less than zero, this means that the structure or system will fail. This failure can be formulated as shown in Eq. 4.1, which shows the probability of the load exceeding the capacity when load and capacity are random variables. On the contrary, if a structure's safety factor is more than one, or safety margin is more than zero, the structure or system will not fail and will be safe. This safety condition can be formulated as shown in Eq. 4.2, which shows the probability of safety, also known as reliability, where load and capacity are random variables. Since reliability is also a probability, Eq. 4.2 gives the fundamental relationship between reliability and the probability of failure.

$$p_f = P(l \geq c) \tag{4.1}$$

$$r = 1 - p_f = P(l < c) \tag{4.2}$$

Probability density functions of random load and random capacity are shown in Figures 4.1 and 4.2. Formulas of PDF and CDF of l and c are shown in Eqs. 4.3 through 4.6.

$$f_l(l) = P(l \leq L \leq l + dl) \tag{4.3}$$

$$F_l(l) = \int_0^l f_l(l')dl' \tag{4.4}$$

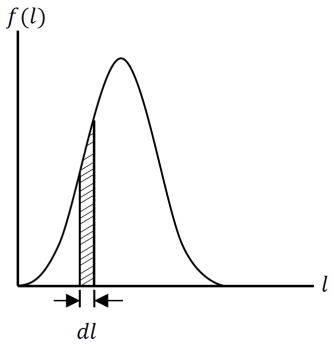

Figure 4.1: Probability Density Function of the Load.

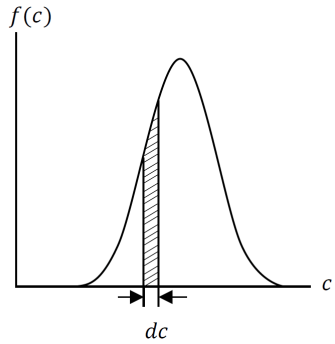

Figure 4.2: Probability Density Function of the Capacity.

$$f_c(c) = P(c \leq C \leq c + dc) \tag{4.5}$$

$$F_c(c) = \int_0^c f_c(c')dc' \tag{4.6}$$

Let us now consider two extreme cases for the randomness of the load and capacity. When the capacity c is fixed and the load l is variable, PDF of the load and the fixed capacity are displayed as shown in Figure 4.3. As the figure shows, the area at the left side of the fixed capacity is the reliability (shaded region). This can be formulated as shown in Eq. 4.7. As c goes to infinity, reliability becomes equal to 1, and when c goes to zero, reliability becomes equal to 0.

$$r = P(l < c) = r(c) = \int_0^c f_l(l)dl \tag{4.7}$$

However, on the contrary, when the load l is fixed and the capacity c is variable, PDF

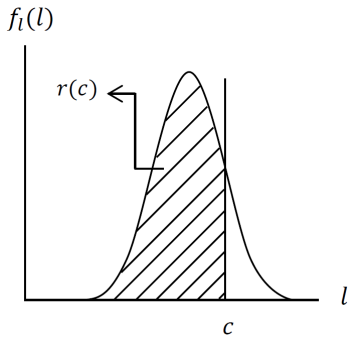

Figure 4.3: Probability Density Function of the Load When the Capacity is Fixed.

of the capacity and the fixed load are displayed in Figure 4.4. As the figure shows in this case, the area at the right side of the fixed load is the reliability (shaded region). This can be formulated as shown in Eq. 4.8. As l goes to infinity, reliability becomes 0, and when l goes to zero, reliability becomes 1.

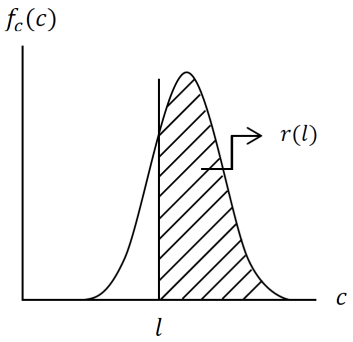

Figure 4.4: Probability Density Function of the Capacity When the Load is Fixed.

$$r = P(c > l) = r(l) = \int_l^{\infty} f_c(c)dc = 1 - \int_0^l f_c(c)dc \tag{4.8}$$

Now, let us consider the most general case when both the capacity and the load are random variables. For this case, PDFs of the capacity and the load are displayed in Figure 4.5. In this case, since the expected value of a random function $g(x)$ is

$$E\left[g(x)\right] = \int_0^{\infty} g(x) f_x(x)dx \tag{4.9}$$

by using the expected value $E[*]$ concept, reliability can be formulated as follow:

$$r = E[r(c)] = \int_0^{\infty} r(c) f_c(c) dc \tag{4.10}$$

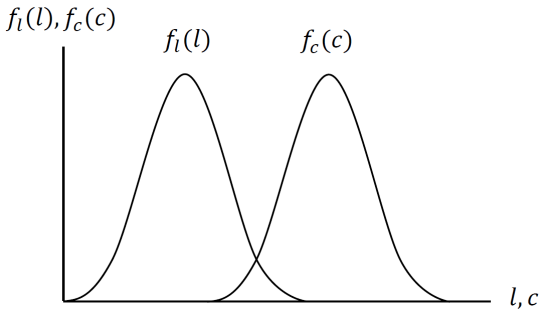

Figure 4.5: Probability Density Functions of the Load and the Capacity When Both are Random Variables.

When the capacity exceeds the load, the reliability can be obtained by substituting Eq. 4.7 into Eq. 4.10, as follows:

$$r = \int_0^{\infty} \left[\int_0^{c} f_l(l) dl \right] f_c(c)\, dc \tag{4.11}$$

where $f_l(l)$ is the PDF of the load and $f_c(c)$ is the PDF of the capacity.

When the load is known and the capacity is uncertain, the reliability becomes:

$$r(l) = \int_l^{\infty} f_c(c)\, dc = 1 - \int_0^{l} f_c(c)\, dc \tag{4.12}$$

In case both the capacity and the load are uncertain, reliability is written as:

$$r = \int_0^{\infty} f_l(l) r(l)\, dl = \int_0^{\infty} f_l(l) \left[\int_l^{\infty} f_c(c)\, dc \right] dl \tag{4.13}$$

which is defined as the convolution integral.

4.3 Reliability and Safety Factors

Alternatively, reliability can also be expressed in terms of the so-called safety factor (v) and uncertainty in l and c. In this case, safety factor needs to be defined in relation

to the independent PDFs of load and capacity.

Central safety factor is defined as:

$$v = \frac{\overline{c}}{\overline{l}} \tag{4.14}$$

where $\overline{c} = \int_{-\infty}^{\infty} c\ f_c(c)\ dc$ and $\overline{l} = \int_{-\infty}^{\infty} l\ f_l(l)\ dl$ are the mean values of c and l respectively.

Safety factor can also be written in terms of the modes of the load and the capacity as:

$$v = \frac{c_0}{l_0} \tag{4.15}$$

where c_0 and l_0 are the most probable values of capacity and load distributions respectively.

4.3.1 Normally Distributed Load and Capacity

If we consider load and capacity as normally distributed, their PDFs are defined as follows:

$$f_l(l) = \frac{1}{\sqrt{2\pi}\sigma_l} e^{-\frac{1}{2}\frac{(l-\bar{l})^2}{\sigma_l^2}} \tag{4.16}$$

$$f_c(c) = \frac{1}{\sqrt{2\pi}\sigma_c} e^{-\frac{1}{2}\frac{(c-\overline{c})^2}{\sigma_c^2}} \tag{4.17}$$

Substituting Eqs. 4.16 and 4.17 into Eq. 4.11, the reliability for normally distributed load and capacity can be written as:

$$r = \int_{-\infty}^{\infty} \frac{1}{\sqrt{2\pi}\sigma_c} e^{-\frac{1}{2}\frac{(c-\overline{c})^2}{\sigma_c^2}} \left[\int_{-\infty}^{c} \frac{1}{\sqrt{2\pi}\sigma_l} e^{-\frac{1}{2}\frac{(l-\bar{l})^2}{\sigma_l^2}}\ dl \right] dc \tag{4.18}$$

By using the transformation of variables, we can simplify Eq. 4.18 using a single exponential term. In order to achieve this, the reduced variates must be used. Space of reduced variates are shown in Figure 4.6 and the transformation of variables are performed as follows:

$$x = \frac{c - \overline{c}}{\sigma_c} \rightarrow c = \sigma_c x + \overline{c} \tag{4.19}$$

and

$$y = \frac{l - \overline{l}}{\sigma_l} \rightarrow l = \sigma_l y + \overline{l} \tag{4.20}$$

Taking the derivatives of Eqs. 4.19 and 4.20 with respect to x and y, respectively, we obtain:

$$\frac{dc}{dx} = \sigma_c \rightarrow dc = \sigma_c \, dx \tag{4.21}$$

$$\frac{dl}{dy} = \sigma_l \rightarrow dl = \sigma_l \, dy \tag{4.22}$$

By applying these transformation of variables to Eq. 4.18, we obtain the following formula for reliability:

$$r = \frac{1}{(\sqrt{2\pi})^2 \sigma_c \sigma_l} \int_{-\infty}^{\infty} \left[\int_{-\infty}^{\frac{\sigma_c x + \overline{c} - \overline{l}}{\sigma_l}} e^{\left[-\frac{1}{2} \left\{ \frac{(c-\overline{c})^2}{\sigma_c^2} + \frac{(l-\overline{l})^2}{\sigma_l^2} \right\} \right]} \sigma_l dy \right] \sigma_c dx \tag{4.23}$$

Then, by rotating the axes by θ (i.e. by transformation of coordinates) as shown in Figure 4.7, we can write reliability (r) as a single standardized normal function:

$$x' = x \cos\theta + y \sin\theta \tag{4.24}$$

$$y' = -x \sin\theta + y \cos\theta \tag{4.25}$$

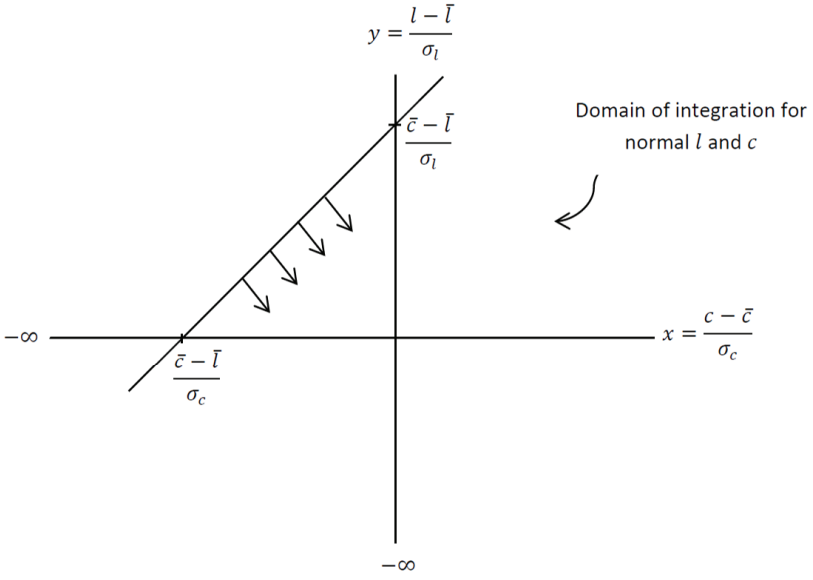

Figure 4.6: Space of Reduced Variates x and y.

Also,

$$x^2 + y^2 = x'^2 + y'^2 \tag{4.26}$$

and

$$dxdy = dx'dy' \tag{4.27}$$

As Figure 4.8 demonstrates, β, being the distance from the failure line to the origin, is a measure of reliability. Reliability in the rotated axes can be written as follows:

$$r = \frac{1}{2\pi} \int_{-\infty}^{\infty} \left[\int_{-\infty}^{\beta} e^{\left[-\frac{1}{2}\left(x'^2 + y'^2\right)\right]} dy' \right] dx' \tag{4.28}$$

By using the Pythagorean theorem, the value of beta can be calculated from:

$$\beta = \sqrt{x^2 + y^2} \tag{4.29}$$

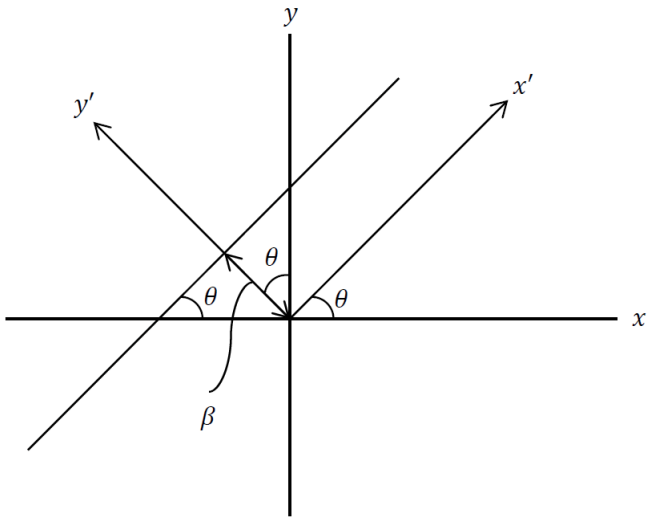

Figure 4.7: Rotation of the x and y axes by the degree θ.

By using trigonometric functions of sine and cosine, the values of x, y and β are as follows:

$$x = \beta \sin\theta \tag{4.30}$$

$$y = \beta \cos\theta \tag{4.31}$$

$$\beta = r\cos\theta \rightarrow \cos\theta = \frac{\beta}{r} \tag{4.32}$$

$$\beta = n\sin\theta \rightarrow \sin\theta = \frac{\beta}{n} \tag{4.33}$$

We substitute the values of cosine and sine based on β, which were obtained in the previous steps, into x and y. Eqs. 4.30 and 4.31:

$$x = \beta.\frac{\beta}{n} = \frac{\beta^2}{n} \tag{4.34}$$

$$y = \beta.\frac{\beta}{r} = \frac{\beta^2}{r} \tag{4.35}$$

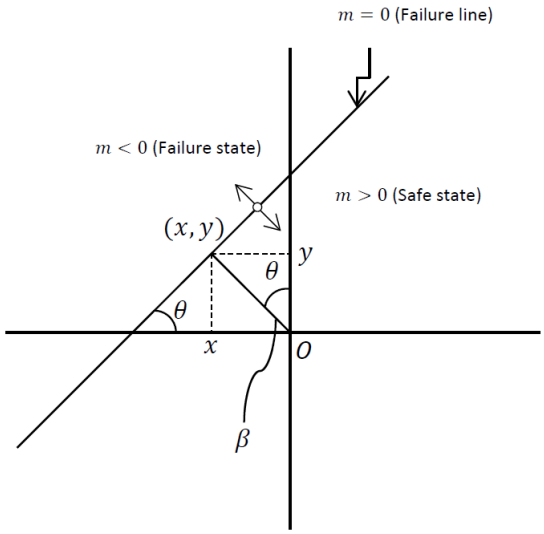

Figure 4.8: Reliability Index in a Space of Reduced Variates x and y.

After the substitution of new x and y into β based on the Pythagorean theorem (Eq. 4.29) and after some simplifications, Eq. 4.38 is obtained as follows:

$$\beta = \sqrt{\frac{\beta^4}{n^2} + \frac{\beta^4}{r^2}} \tag{4.36}$$

$$\beta = \beta^2 \sqrt{\frac{1}{\left(\frac{\bar{c}-\bar{l}}{\sigma_c}\right)^2} + \frac{1}{\left(\frac{\bar{c}-\bar{l}}{\sigma_l}\right)^2}} \rightarrow \frac{1}{\beta} = \sqrt{\frac{\sigma_c^2 + \sigma_l^2}{\left(\bar{c} - \bar{l}\right)^2}} \tag{4.37}$$

$$\beta = \frac{\bar{c} - \bar{l}}{\sqrt{\sigma_c^2 + \sigma_l^2}} \tag{4.38}$$

where β is the safety index (reliability index).

Since we know that $\frac{1}{\sqrt{2\pi}} \int_{-\infty}^{\infty} e^{-\frac{1}{2}x'^2} dx' = \Phi(\infty) = 1$, then $r = \frac{1}{\sqrt{2\pi}} \int_{-\infty}^{\beta} e^{-\frac{1}{2}y'^2} dy' = \Phi(\beta)$, i.e:

$$r = \Phi(\beta) \tag{4.39}$$

Eq. 4.39 is a fundamental relationship between reliability and the reliability index, which is valid for normally distributed load and capacity only.

For more illustration, for the assumed values of $\mu_c = 4$, $\mu_l = 3$, $\sigma_c = 1$ and $\sigma_l = 2$ by using Eqs. 4.19 and 4.20, space of reduced variates x and y is plotted in Figure 4.9. As Figure 4.9 indicates line $x - 2y + 1 = 0$ is the failure line (i.e. limit state equation). By substituting point A in the state equation, we obtain the value of 0.8 which is a positive value. Therefore, m (safety margin) is greater than zero and A is in the safe state. On the other hand, by substituting point B in the state equation, we obtain the value of -1 which is a negative value. Therefore, m is less than zero and B is in the failure state.

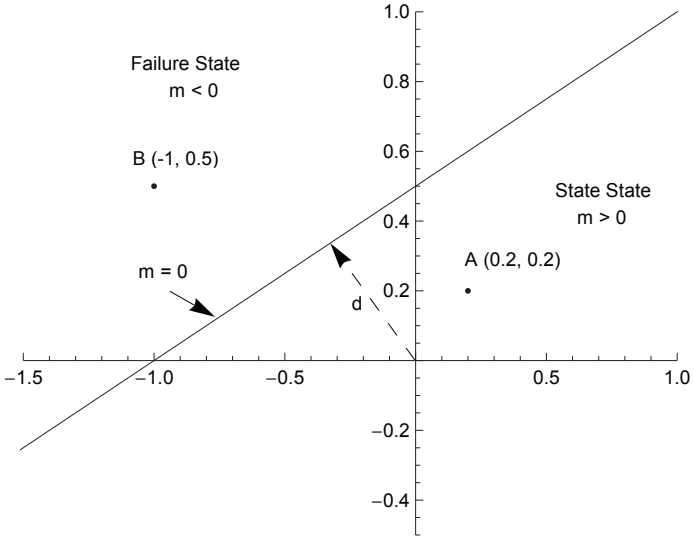

Figure 4.9: Reliability Index in a Space of Reduced Variates x and y for the Assumed Values.

The minimum distance from the origin to the limit state function is the reliability index. By using the Eq. 4.38, reliability index can be obtain as follows:

$$\beta = \frac{\overline{c} - \overline{l}}{\sqrt{\sigma_c^2 + \sigma_l^2}} = \frac{4 - 3}{\sqrt{1^2 + 2^2}} = \frac{\sqrt{5}}{5}$$

4.3.2 Lognormally Distributed Load and Capacity

When uncertainties about load and capacity are relatively large, l and c can be represented by lognormal distribution. In this case, the PDFs of load and capacity are:

$$f_l(l) = \frac{1}{\sqrt{2\pi}\omega_l\, l} e^{\left[-\frac{1}{2\omega_l^2}\ln(\frac{l}{l_0})^2\right]} \tag{4.41}$$

$$f_c(c) = \frac{1}{\sqrt{2\pi}\omega_c\, c} e^{\left[-\frac{1}{2\omega_c^2}\ln(\frac{c}{c_0})^2\right]} \tag{4.42}$$

Substituting Eqs. 4.41 and 4.42 into Eq. 4.11, reliability becomes:

$$r = \int_0^\infty \frac{1}{\sqrt{2\pi}\omega_c\, c} e^{\left[-\frac{1}{2\omega_c^2}\ln(\frac{c}{c_0})^2\right]} \left[\int_0^c \frac{1}{\sqrt{2\pi}\omega_l\, l} e^{\left[-\frac{1}{2\omega_l^2}\ln(\frac{l}{l_0})^2\right]} dl\right] dc \tag{4.43}$$

Substituting $y = \frac{1}{\omega_l}\ln\left(\frac{l}{l_0}\right)$ and $x = \frac{1}{\omega_c}\ln\left(\frac{c}{c_0}\right)$ and observing the following conditions:

When c is from $0 \to \infty$, x will be from $x = \frac{1}{\omega_c}\ln(0) = -\infty$ to $x = \frac{1}{\omega_c}\ln(\infty) = \infty$.

When l is from $0 \to c$, y will be from $y = \frac{1}{\omega_l}\ln(0) = -\infty$ to $y = \frac{1}{\omega_l}\ln\left(\frac{c}{l_0}\right)$.

where $x\omega_c = \ln\left(\frac{c}{c_0}\right) = \ln c - \ln c_0 \to x\omega_c + \ln c_0 = \ln c$

A new y is obtained as follow:

$$y = \frac{1}{\omega_l}(\ln c - \ln l_0) = \frac{1}{\omega_l}(x\omega_c + \ln c_0 - \ln l_0) = \frac{1}{\omega_l}\left[\omega_c x + \ln\left(\frac{c_0}{l_0}\right)\right] \tag{4.44}$$

also converting dc and dl to dx and dy, respectively, we obtain:

$$\ln c = x\omega_c + \ln c_0 \to \frac{d}{dx}\ln c = \omega_c \to \frac{1}{c}\frac{dc}{dx} = \omega_c \to dc = \omega_c.c.dx \tag{4.45}$$

$$\ln l = y\omega_l + \ln l_0 \to \frac{d}{dy}\ln l = \omega_l \to \frac{1}{l}\frac{dl}{dy} = \omega_l \to dl = \omega_l.l.dy \tag{4.46}$$

And finally, by substituting Eqs. 4.44, 4.45 and 4.46 into Eq. 4.43, reliability for lognoramally distributed load and capacity can be written as:

$$r = \frac{1}{2\pi} \int_{-\infty}^{\infty} \left[\int_{-\infty}^{\left\{ \frac{1}{\omega_l} \left[\omega_c x + \ln\left(\frac{c_0}{l_0}\right) \right] \right\}} e^{\left[-\frac{1}{2}\left(x^2+y^2\right) \right]} dy \right] dx \tag{4.47}$$

Therefore, using Eq. 4.47, reliability index for lognormally distributed load and capacity can be written as:

$$\beta = \frac{\ln\left(\frac{c_0}{l_0}\right)}{\sqrt{\omega_c^2 + \omega_l^2}} \tag{4.48}$$

4.4 First-Order Reliability Method

In order to calculate the probability of safety or failure, knowledge on distributions or joint distributions of the load and capacity is required. However, it is not always possible to obtain this knowledge practically since there is no sufficient statistical data available for these random variables. Even when the data is available, it is normally only adequate to calculate the first and second moments of these random variables (i.e. mean value and standard deviation). As a result, it would be more useful to limit the implementation of reliability concepts to a formulation on the basis of the first and second moments of the random variables only. When the formulation of the mean and variance is limited to first order terms, the method is called as the First Order Reliability Method (FORM). Alternatively, these variables can also be limited to a second moment formulation or (SORM). (Ang & Tang, 1975).

Resistance and load have a vital role to estimate the probability of failure in structural engineering. The difference between the resistance R and the load Q is known as state function $g(x) = R - Q$, where $x = (x_1, x_2, ..x_n)$ is a vector representing the design variables of the system. When R and Q are equal ($R = Q$), state function is in limiting state which is called as the limit state function i.e. $g(x) = R - Q = 0$. When the load is greater than the resistance, the event of failure occurs. On the contrary, when resistance is greater than load, the system is in the safe state.

To calculate the reliability, the volume integral of $f_x(x)$ over the safe region $g(x) > 0$ needs to be evaluated. With the second-moment approach (SORM), the reliability

index β may be evaluated using a function of the mean values and standard deviations of the design variables. To do this, the reliability index should be written in terms of the limit state function; a process which is performed by using the mathematical concept of reduced space as shown in Figure 4.10. Let

$$X_i' = \frac{X_i - \mu_x}{\sigma_{xi}}; \quad i = 1, 2, ..., n \tag{4.49}$$

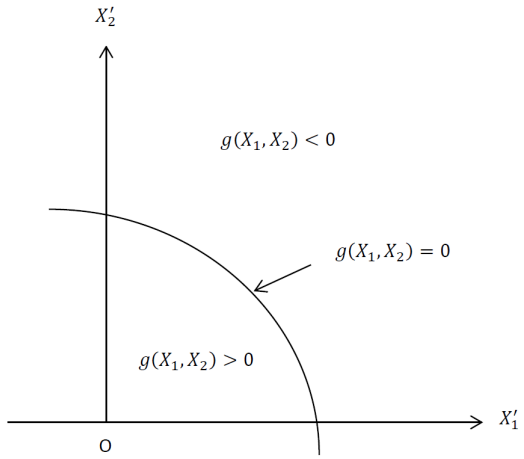

Figure 4.10: Definition of Safe and Failure States in the Space of the Reduced Variates.

Figure 4.10 shows a nonlinear limit state function $g(X_1, X_2) = 0$ (also called as the failure surface). When limit-state function moves closer to the origin, it causes the reduction of the safe region i.e. $g(X_1, X_2) > 0$. On the contrary, when limit-state function moves further away from the origin, it increases the safe region.

The most probable failure point is on the failure surface $g(X) = 0$ with a minimum distance from a point $X' = (X_1', X_2', ..., X_n')$ to the origin. Therefore, this minimum distance may be employed as a measure of reliability, and it is

$$D = \sqrt{X_1'^2 + ... + X_n'^2} = \left(X'^t X'\right)^{1/2} \tag{4.50}$$

For the purpose of determining the minimum distance of the point on the failure surface to the origin, it is essential to minimize function D when it is subjected to the

constraint $g(X) = 0$. To solve the optimization problem, the method of Lagrange's multiplier may be used. Let

$$L = D + \lambda g(x) \tag{4.51}$$

At optimum, the following conditions must be satisfied:

$$\frac{\partial L}{\partial X_i} = 0 \quad i = 1, 2, ..., n \tag{4.52}$$

$$\frac{\partial L}{\partial \lambda} = 0 \tag{4.53}$$

Writing Eq. 4.51 in scalar notation, we have

$$L = \sqrt{X_1'^2 + ... + X_n'^2} + \lambda g(X_1, ..., X_n) \tag{4.54}$$

where, from Eq. 4.49, $X_i = \sigma_{Xi} X_i' + \mu_{Xi}$.

By minimizing the function L and subjecting it to $g(X) = 0$, the following set of equations is obtained:

$$\frac{\partial L}{\partial X_i'} = \frac{X_i'}{\sqrt{X_1'^2 + ... + X_n'^2}} + \lambda \frac{\partial g}{\partial X_i'} = 0; \quad i = 1, 2, ..., n \tag{4.55}$$

and

$$\frac{\partial L}{\partial \lambda} = g(X_1, ..., X_n) = 0 \tag{4.56}$$

To obtain the solution of the Eqs. 4.55 and 4.56, which is the most probable failure point, the following gradient vector is introduced:

$$\mathbf{G} = \left(\frac{\partial g}{\partial X_1'}, \frac{\partial g}{\partial X_2'}, ..., \frac{\partial g}{\partial X_n'} \right) \tag{4.57}$$

Eq. 4.55 can be written by substituting Eqs. 4.50 and 4.57 into Eq. 4.55 as follows:

$$\frac{X^{'}}{D} + \lambda \mathbf{G} = 0 \tag{4.58}$$

from which

$$X^{'} = -\lambda D \mathbf{G} \tag{4.59}$$

Therefore,

$$D = \left[\left(\lambda D \mathbf{G}^{t} \right) \left(\lambda D \mathbf{G} \right) \right]^{1/2} = \lambda D \left(\mathbf{G}^{t} \mathbf{G} \right)^{1/2} \tag{4.60}$$

thus,

$$\lambda = \left(\mathbf{G}^{t} \mathbf{G} \right)^{-1/2} \tag{4.61}$$

Substituting Eq. 4.61 into Eq. 4.59 yields

$$X^{'} = \frac{-\mathbf{G} D}{\left(\mathbf{G}^{t} \mathbf{G} \right)^{1/2}} \tag{4.62}$$

thus,

$$D = \frac{-\mathbf{G}^{t} X^{'}}{\left(\mathbf{G}^{t} \mathbf{G} \right)^{1/2}} \tag{4.63}$$

By substituting Eq. 4.62 into Eq. 4.56, a single equation can be obtained, an equation whose solution is the minimum distance $d_{min} = \beta$, so

$$\beta = \frac{-G^{*t} X^{'*}}{\left(G^{*t} G^{*} \right)^{1/2}} \tag{4.64}$$

where G^{*} is the gradient vector at the most probable failure point $(x_1^{'*}, x_2^{'*}, ..., x_n^{'*})$. Eq. 4.64can also be written in scalar form as follows:

$$\beta = \frac{-\sum_i x_i'^* \left(\frac{\partial g}{\partial X_i'}\right)_*}{\sqrt{\sum_i \left(\frac{\partial g}{\partial X_i'}\right)_*^2}} \tag{4.65}$$

in which the derivatives $\left(\frac{\partial g}{\partial X_i'}\right)_*$ are evaluated at $(x_1'^*, x_2'^*, ..., x_n'^*)$

By substituting Eq. 4.65 into 4.62, the most probable point on the failure surface is as follows:

$$X'^* = \frac{-\mathbf{G}^*\beta}{(\mathbf{G}^{*t}\mathbf{G}^*)^{1/2}} \tag{4.66}$$

Eqs. 4.64 and 4.66 can be interpreted according to first-order approximation by expanding the performance function $g(X)$ in a Taylor series as follows:

$$\begin{aligned} g(X_1, X_2, ..., X_n) = g(x_1^*, x_2^*, ..., x_n^*) + \sum_{i=1}^{n}(X_i - x_i^*)\left(\frac{\partial g}{\partial X_i}\right)_* \\ + \frac{\sum_{j=1}^{n}\sum_{i=1}^{n}(X_i - x_i^*)(X_j - x_j^*)}{\left(\frac{\partial^2 g}{\partial X_i \partial X_j}\right)_*} + ... \end{aligned} \tag{4.67}$$

and by knowing $g(x_1^*, x_2^*, ..., x_n^*) = 0$ on the failure surface, Eq. 4.67 becomes as follows:

$$\begin{aligned} g(X_1, X_2, ..., X_n) = \sum_{i=1}^{n}(X_i - x_i^*)\left(\frac{\partial g}{\partial X_i}\right)_* \\ + \frac{\sum_{j=1}^{n}\sum_{i=1}^{n}(X_i - x_i^*)(X_j - x_j^*)}{\left(\frac{\partial^2 g}{\partial X_i \partial X_j}\right)_*} + ... \end{aligned} \tag{4.68}$$

By knowing

$$X_i - x^* = \left(\sigma_{Xi}X_i' + \mu_{Xi}\right) - \left(\sigma_{Xi}x_i'^* + \mu_{Xi}\right) = \sigma_{Xi}\left(X_i' - x_i'^*\right) \tag{4.69}$$

and also

$$\frac{\partial g}{\partial X_i} = \frac{\partial g}{\partial X_i'}\left(\frac{dX_i'}{dX_i}\right) = \frac{1}{\sigma_{Xi}}\left(\frac{\partial g}{\partial X_i'}\right) \tag{4.70}$$

Eq. 4.68 becomes:

$$g(X_1, X_2, ..., X_n) = \sum_{i=1}^{n}(X_i' - x_i'^*)\left(\frac{\partial g}{\partial X_i'}\right)_* + ... \tag{4.71}$$

When the series is truncated at the first-order term, the mean value of the function $g(X)$ becomes:

$$\mu_g \simeq -\sum_{i=1}^{n} x_i'^*\left(\frac{\partial g}{\partial X_i'}\right)_* \tag{4.72}$$

However, for uncorrelated variates , the corresponding first-order approximation of the variance is

$$\sigma_g^2 \simeq -\sum_{i=1}^{n}\sigma_{X_i'}^2\left(\frac{\partial g}{\partial X_i'}\right)_*^2 = \sum_{i=1}^{n}\left(\frac{\partial g}{\partial X_i'}\right)_*^2 \tag{4.73}$$

From Eqs. 4.72 and 4.73, the following ratio can be written as:

$$\frac{\mu_g}{\sigma_g} = \frac{-\sum_{i=1}^{n} x_i'^*\left(\frac{\partial g}{\partial X_i'}\right)_*}{\sqrt{\sum_{i=1}^{n}\left(\frac{\partial g}{\partial X_i'}\right)_*^2}} \tag{4.74}$$

Comparing Eq. 4.74 with Eq. 4.65, the reliability index can be written as:

$$\beta = \frac{\mu_g}{\sigma_g} \tag{4.75}$$

Moreover, the linear performance function can be used as the basis for an approximation to nonlinear performance function. If a linear performance function can be written as follows:

$$g(X) = a_0 + \sum_i a_i X_i \tag{4.76}$$

where both a_0 and a_i are constants, the limit state equation is

$$a_0 + \sum_i a_i X_i = 0 \tag{4.77}$$

In terms of the reduced variates, the limit state equation is as follows:

$$a_0 + \sum_i a_i(\sigma_{X_i} X_i^{'} + \mu_{X_i}) = 0 \tag{4.78}$$

Eq. 4.78 can be written in three dimensions as follows:

$$a_0 + a_1(\sigma_{X_1} X_1^{'} + \mu_{X_1}) + a_2(\sigma_{X_2} X_2^{'} + \mu_{X_2}) + a_3(\sigma_{X_3} X_3^{'} + \mu_{X_3}) = 0 \tag{4.79}$$

Eq. 4.79 is a plane surface in the $x_1^{'}, x_2^{'}, x_3^{'}$ space. This plane surface is shown in Figure 4.11.

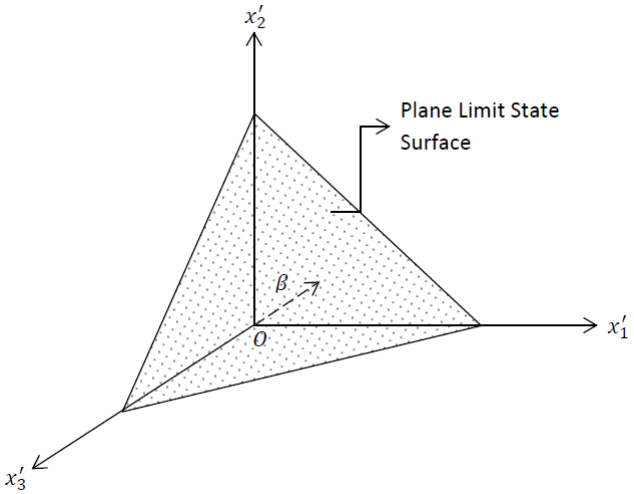

Figure 4.11: Linear limit state surface in $x_1^{'}, x_2^{'}, x_3^{'}$ space.

The distance of the failure plane to the origin of the reduced variates $X^{'}$ is

$$\beta = \frac{a_0 + \sum_i a_i \mu_{X_i}}{\sqrt{\sum_i (a_i \sigma_{X_i})^2}} \tag{4.80}$$

For uncorrelated normal variates, the reliability is a function of the distance of the

failure surface to the origin of the reduced variates. By definition of probability of safety:

$$P_s = P\left(g(X) > 0\right) \tag{4.81}$$

Therefore, reliability becomes:

$$\begin{aligned} r &= P\left(a_0 + \sum_i a_i X_i > 0\right) \\ &= 1 - \Phi\left[\frac{-(a_0 + \sum a_i \mu_{X_i})}{\sqrt{\sum (a_i \sigma_{X_i})^2}}\right] \\ &= \Phi\left[\frac{(a_0 + \sum a_i \mu_{X_i})}{\sqrt{\sum (a_i \sigma_{X_i})^2}}\right] \end{aligned} \tag{4.82}$$

In other words, the reliability is

$$r = \Phi(\beta) \tag{4.83}$$

for the general case of n independent random variables.

When the limit state equation is linear, and all random variables are normal and independent, FORM can be useful if an exact value of the probability of failure is desired. However, when the limit state equation is nonlinear and in the presence of non-normal variables, the outcome will be an approximation, and there will be convergence issues (Lopez, Miguel, Belo, & Cursi, 2014).

4.5 Evaluation of Probability of Failure and Reliability Index for a Structural Component or System

Computer programs are available that can compute the reliability of individual structural components and the reliability of any structural system that can be modeled as a series-parallel combination of those components.

First-Order Reliability Method (FORM) is an approach that can be used to compute the reliability index β and the probability of failure for any individual component. All distribution types must first be converted to equivalent normal distributions. Then the inputs based on limit state equation and random variable parameters must be provided. Examples below are solved using the FORM technique. Most of the problem definitions presented in this section are taken from the manual of computer program RELSYS (Estes, A.C. and Frangopol, D.M., 1997). They are solved here to verify the results presented in the manual. After these verifications, additional examples are solved to be able to obtain further exercises and cases for the FORM technique.

4.5.1 Uncorrelated Normal Random Variables (With Two Variates)

The following limit state equation is given:

$$g(\mathbf{X}) = 2X_1^2 - 2X_2 \tag{4.84}$$

Random variables X_1 and X_2 are normally distributed and uncorrelated as and their descriptor values are shown in Table 4.1. Plots of probability distributions for the given μ's and σ's of random variables X_1 and X_2 are shown in Figure 4.12. The reliability index β is obtained after eleven iterations. The reliability index is calculated as 1.2317, the probability of failure is 0.10903, and the probability of safety is 0.89097. Figure 4.13 shows the convergence of the reliability index as the number of iterations increased.

Table 4.1: Random Variables of the Limit State Equation With Two Uncorrelated Normal Variates.

Random Variable	Mean Value	Standard Deviation	Distribution Type
X_1	2.0	0.2	Normal
X_2	3.0	0.3	Normal

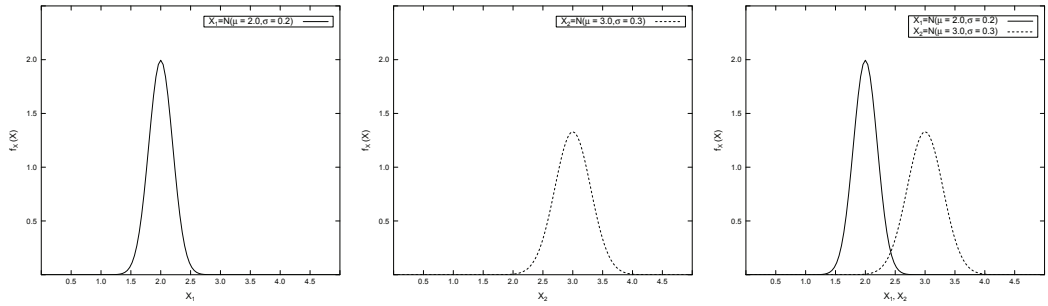

Figure 4.12: Probability Distributions of the Random Variables of Limit State Equation With Two Uncorrelated Normal Variates.

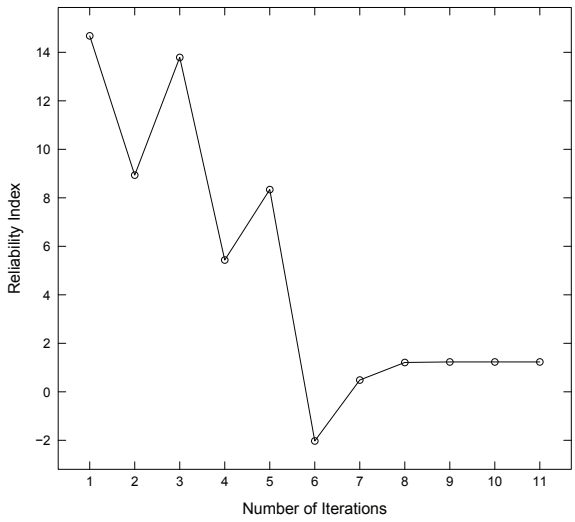

Figure 4.13: Convergence of Iterations of the Limit State Equation With Two Uncorrelated Normal Variates.

4.5.2 Uncorrelated Normal Random Variables (With Three Variates)

The following limit state equation contains three random variables,

$$g(\mathbf{X}) = X_1 X_2 - X_3 \tag{4.85}$$

Random variables X_1, X_2 and X_3 are normally distributed and uncorrelated and their main descriptors are shown in Table 4.2.

Plots of probability distributions for the given μ's and σ's of random variables X_1,

Table 4.2: Random Variables of the Limit State Equation With Three Uncorrelated Normal Variates.

Random Variable	Mean Value	Standard Deviation	Distribution Type
X_1	40	5.0	Normal
X_2	50	2.5	Normal
X_3	1000	200.0	Normal

X_2 and X_3 are shown in Figure 4.14. The reliability index β is obtained after four iterations. The reliability index is calculated as 3.0491, the probability of failure is 0.001478, and the probability of safety is 0.99885. Figure 4.15 shows the convergence of the reliability index as the number of iterations increased.

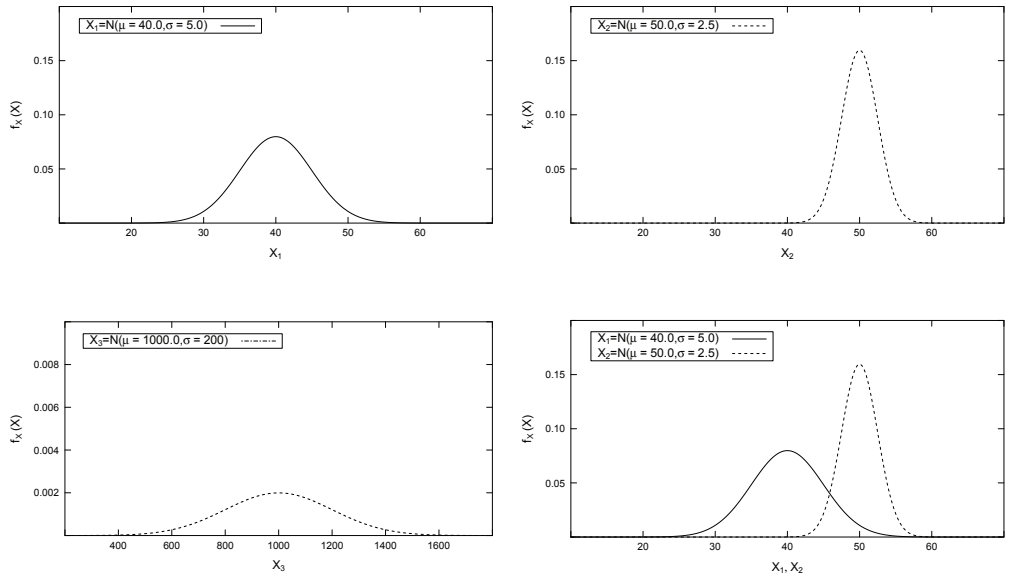

Figure 4.14: Probability Distributions of the Random Variables of Limit State Equation With Three Uncorrelated Normal Variates.

4.5.3 Correlated Normal Random Variables (With Three Variates)

The same limit state equation used in the problem of uncorrelated normals (Section 4.5.2) is solved here again for correlated normal random variables using the descriptor values given in Table 4.3. It is assumed that the random variables X_1 and X_2 are partially correlated with $\rho_{X_1,X_2} = 0.40$.

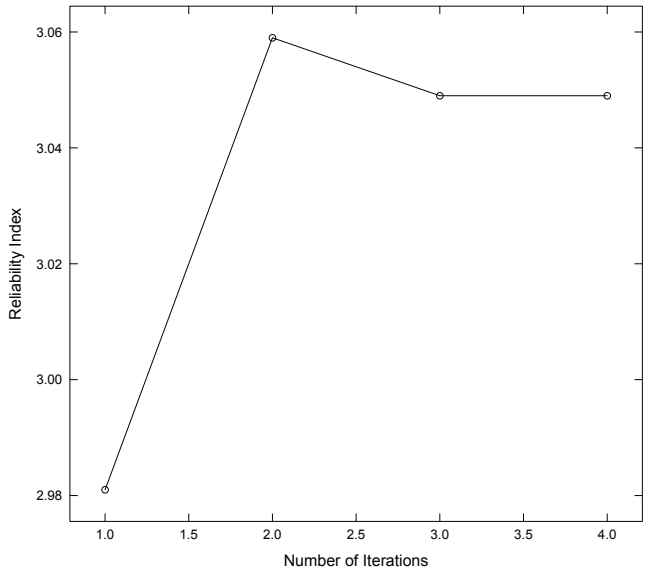

Figure 4.15: Convergence of Iterations of the Limit State Equation With Three Uncorrelated Normal Variates.

Table 4.3: Random Variables of the Limit State Equation With Two Correlated Normal Variates.

Random Variable	Mean Value	Standard Deviation	Distribution Type	Correlation
X_1	40	5.0	Normal	$\rho_{X_1,X_2} = 0.40$
X_2	50	2.5	Normal	
X_3	1000	200.0	Normal	

The reliability index β is obtained after four iterations. The reliability index is calculated as 2.8629, the probability of failure is 0.0020992, and the probability of safety is 0.99790. Figure 4.16 shows the convergence of the reliability index as the number of iterations increased.

4.5.4 Uncorrelated Non-Normal Random Variables Having Lognormal and Type-I Largest Value Distributions

The same limit state equation used in the problem of uncorrelated normals (Section 4.5.2) is solved here again for uncorrelated non-normal random variables using the descriptor values given in Table 4.4.

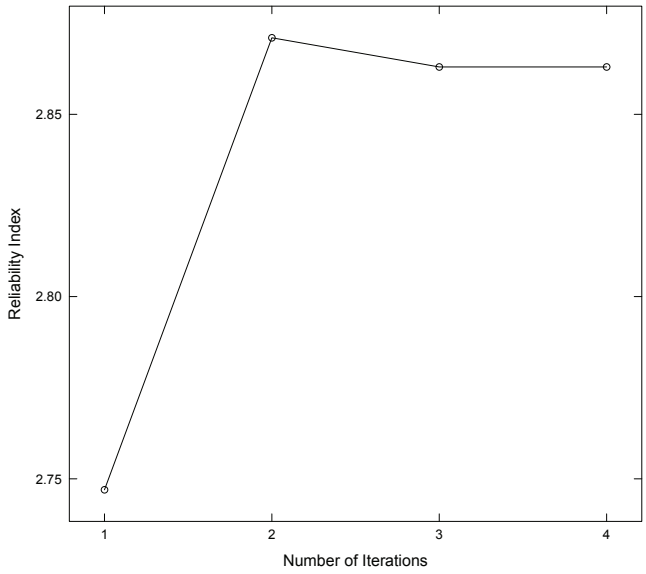

Figure 4.16: Convergence of Iterations of the Limit State Equation With Two Correlated Normal Variates.

Table 4.4: Random Variables of the Limit State Equation With Three Uncorrelated Non-Normal Variates.

Random Variable	Mean Value	Standard Deviation	Distribution Type
X_1	40	5.0	Lognormal
X_2	50	2.5	Lognormal
X_3	1000	200.0	Type-I Large

Plots of probability distributions for random variables X_1, X_2 and X_3, and the convergence of the reliability index are shown in Figures 4.17 and 4.18 respectively. The reliability index β is obtained after seven iterations. The reliability index is calculated as 2.7376, the probability of failure is 0.0030949, and the probability of safety is 0.99691.

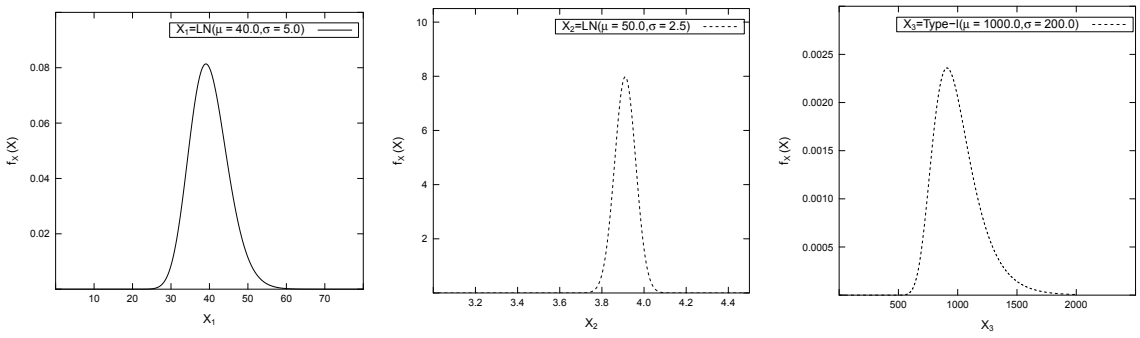

Figure 4.17: Probability Distributions of the Random Variables of Limit State Equation With Three Uncorrelated Non-Normal Variates.

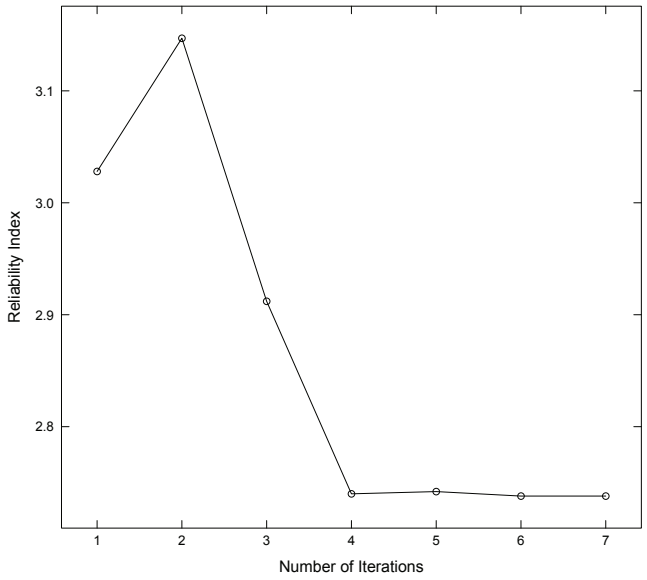

Figure 4.18: Convergence of Iterations of the Limit State Equation With Three Uncorrelated Non-Normal Variates.

4.5.5 Correlated Non-Normal Random Variables Having Lognormal and Type-I Largest Value Distributions

The same limit state equation used in the problem of uncorrelated normals (Section 4.5.2) is solved here again for correlated non-normal random variables using the descriptor values given in Table 4.5.

Table 4.5: Random Variables of the Limit State Equation With Two Correlated Non-Normal Variates.

Random Variable	Mean Value	Standard Deviation	Distribution Type	Correlation
X_1	40	5.0	Lognormal	$\rho_{X_1,X_2} = 0.40$
X_2	50	2.5	Lognormal	
X_3	1000	200.	Type-I Large	

The reliability index β is obtained after seven iterations. The reliability index is calculated as 2.6598, the probability of failure is 0.0039094, and the probability of safety is 0.99609. Figure 4.19 shows the convergence of the reliability index as the number of iterations increased.

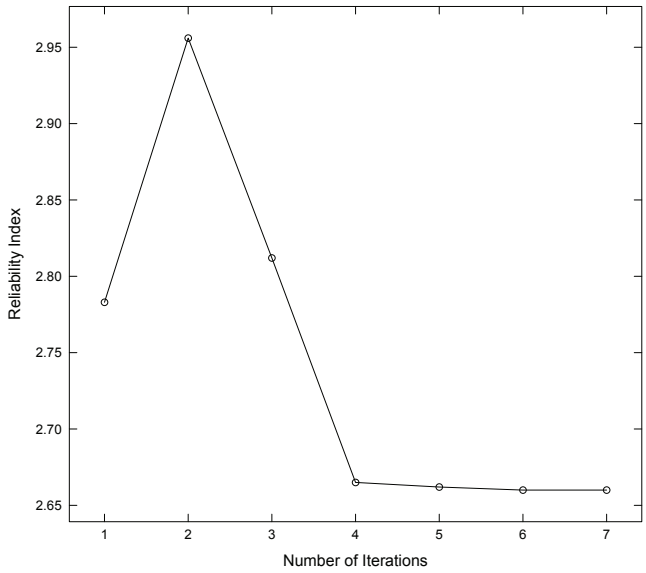

Figure 4.19: Convergence of Iterations of the Limit State Equation With Two Correlated Non-Normal Variates.

4.5.6 Uncorrelated Non-Normal Random Variables (With Six Variates)

The following limit state equation contains six random variables,

$$g(\mathbf{X}) = X_1 X_2 X_3 X_4^{\frac{3}{2}} - X_5 X_6 \tag{4.86}$$

It is assumed that the random variables are uncorrelated normal and non-normal variates as shown in Table 4.6.

Table 4.6: Random Variables of the Limit State Equation With Normal and Non-Normal Uncorrelated Non-Normal Variates.

Random Variables	Mean Value	Standard Deviation	Distribution Type
X_1	1.00	0.20	Normal
X_2	3.85	0.27	Normal
X_3	93.40	5.60	Normal
X_4	12.00	0.72	Normal
X_5	0.70	0.98×10^{-1}	Normal
X_6	9146.00	3201.00	Type-I Large

Plots of probability distributions for random variables X_1 through X_6, and the convergence of the reliability index are shown in Figures 4.20 and 4.21 respectively. The reliability index β is obtained after eleven iterations. The reliability index is calculated as 2.2306, the probability of failure is 0.012854, and the probability of safety is 0.987150.

4.5.7 Series System Including Three Failure Components (A Chain With Three Links)

Consider the following series system shown in Figure 4.22 comprised of three failure components as described by limit state equations $g(1)$, $g(2)$, and $g(3)$.

$$g(1) = 2X_1^2 - 2X_2 \tag{4.87}$$

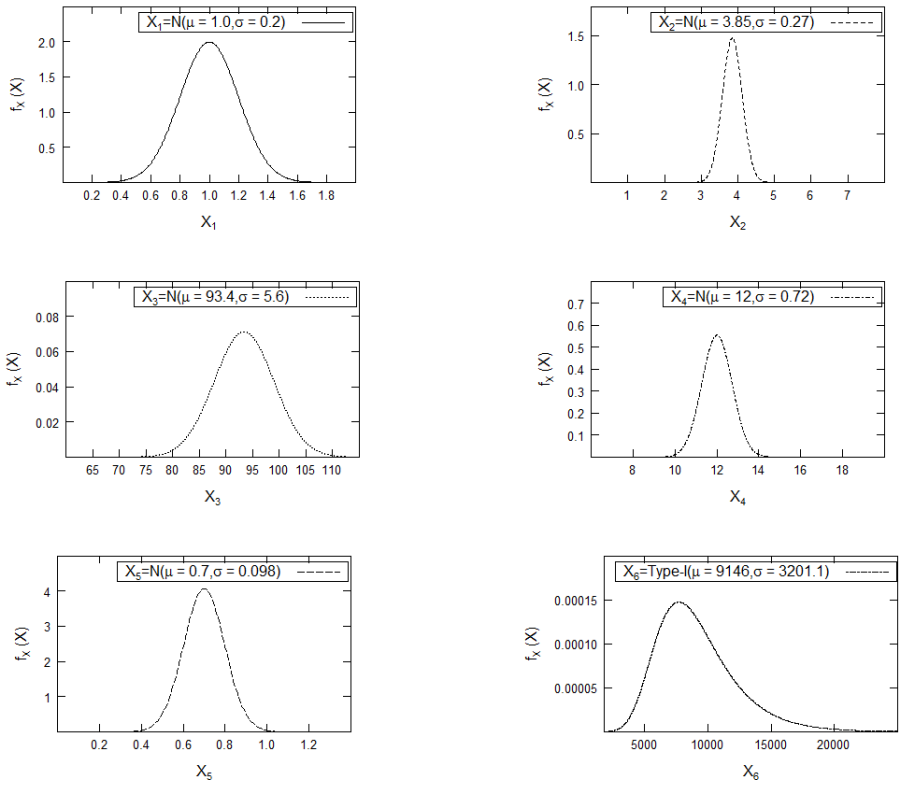

Figure 4.20: Probability Distributions of the Random Variables of Limit State Equation With Normal and Non-Normal Uncorrelated Variates.

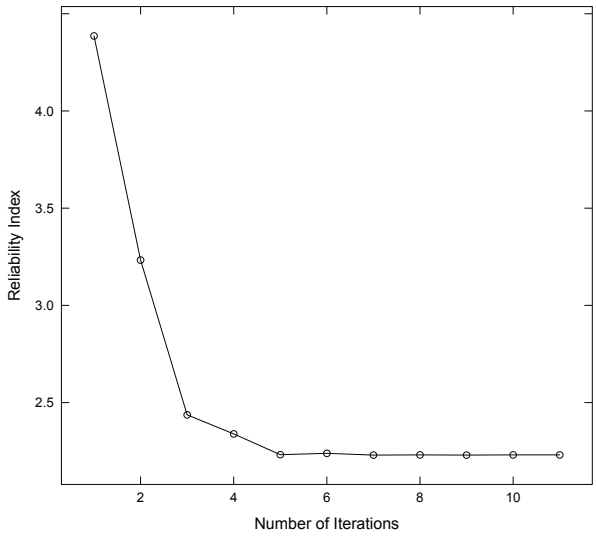

Figure 4.21: Convergence of Iterations of the Limit State Equation With Normal and Non-Normal Uncorrelated Variates.

$$g(2) = X_1 - X_3 \tag{4.88}$$

$$g(3) = 1.5X_1 + 0.5X_3^2 - X_2 \tag{4.89}$$

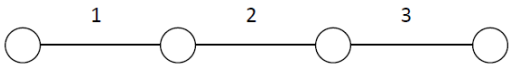

Figure 4.22: Chain With Three Links.

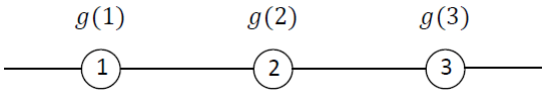

Figure 4.23: Failure Modes of the Series System.

It is assumed that the random variables are uncorrelated normal variates as shown in Table 4.7.

Table 4.7: Random Variables of the Limit State Equations With Three Uncorrelated Normal Variates for a Series System (A Chain with three links).

Random Variable	Mean Value	Standard Deviation	Distribution Type
X_1	2.0	0.2	Normal
X_2	3.0	0.3	Normal
X_3	1.0	0.1	Normal

Plots of probability distributions for random variables X_1, X_2, and X_3, and the convergence of the reliability index are shown in Figures 4.24 and 4.25 respectively. The reliability index, the probability of failure, and the probability of failure are calculated for the components, and the results are shown in Table 4.8. The reliability index obtained after system reliability analysis is calculated as 1.0267, the probability of failure is 0.15228, and the probability of safety is 0.84772.

4.5.8 Series System (Failure Modes of a Simply Supported Beam)

A simply supported beam is subjected to a uniformly distributed load as shown in Figure 4.26. The performance functions for failure in bending, shear, and the combined

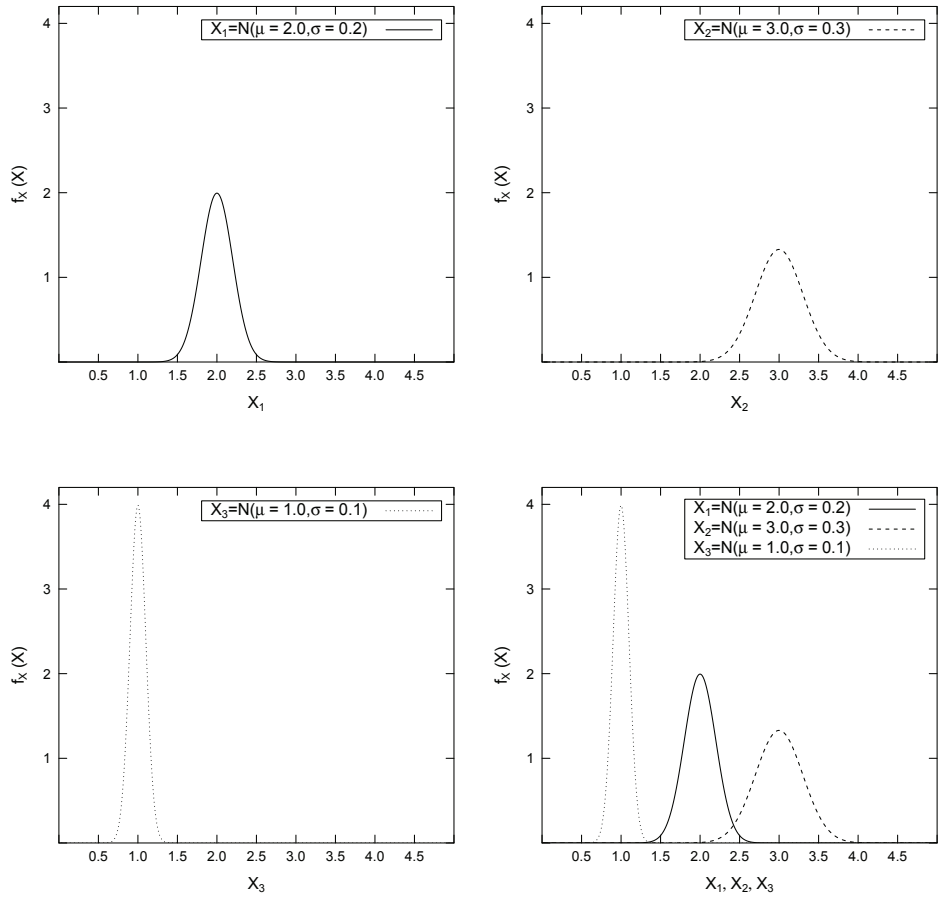

Figure 4.24: Probability Distributions of the Random Variables of Limit State Equations With Three Uncorrelated Normal Variates for a Series System (Chain With Three Links).

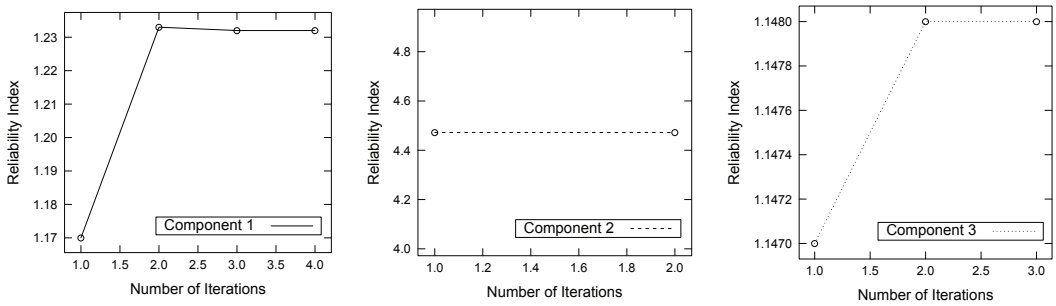

Figure 4.25: Convergence of Iterations of the Limit State Equations With Three Uncorrelated Normal Variates for a Series System (Chain With Three Links).

Table 4.8: Results for the Components of the Series System (Chain With Three Links).

Component	Number of Iterations	Reliability Index	Probability of Failure	Probability of Safety
1	4	1.2317	0.10903	0.89097
2	2	4.4721	0.38756×10^{-5}	1.00000
3	3	1.1479	0.12551	0.87449

failure modes are as follows:

$$g_1(\mathbf{X}) = M_0 - \frac{1}{8}wL^2 \tag{4.90}$$

$$g_2(\mathbf{X}) = V_0 - \frac{1}{2}wL \tag{4.91}$$

$$g_3(\mathbf{X}) = 1 - \left(\frac{wL^2}{8M_0} + \frac{wM_0}{2V_0^2}\right) \tag{4.92}$$

where L=20.

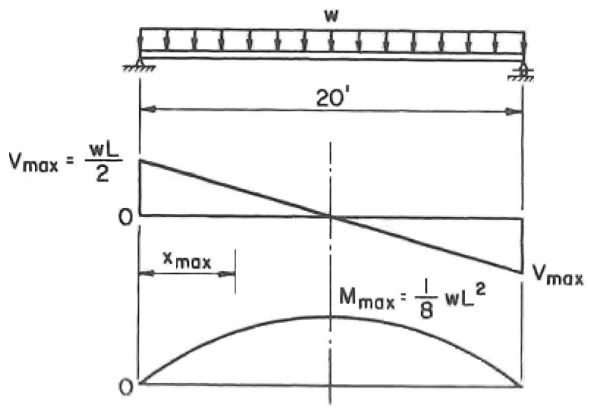

Figure 4.26: Simply Supported Beam.

Random variables X_1, X_2, and X_3 are assumed to be normally distributed and uncorrelated as shown in Table 4.9. Plots of probability distributions for random variables X_1, X_2, and X_3, and the convergence of the reliability index are shown in Figures 4.27 and 4.28 respectively. The reliability index, the probability of failure, and the probability of safety are calculated for the components as shown in Table 4.10. The

reliability index obtained after system reliability analysis is calculated as 1.5733, the probability of failure is 0.057868, and the probability of safety is 0.942132.

Table 4.9: Random Variables of the Limit State Equations With Three Uncorrelated Normal Variates for a Series System (Simply Supported Beam).

Random Variable	Symbol	Mean Value	Standard Deviation	Distribution Type
M_0	X_1	470	47	Normal
V_0	X_2	159	23.85	Normal
w	X_3	6	1.5	Normal

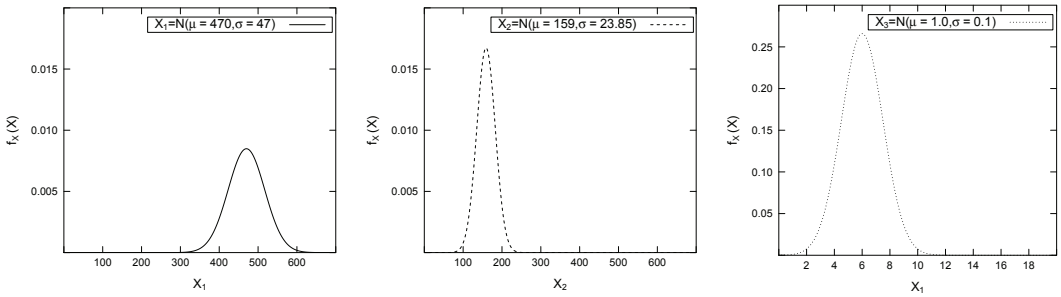

Figure 4.27: Probability Distributions of the Random Variables of Limit State Equations With Three Uncorrelated Normal Variates for a Series System (Simply Supported Beam).

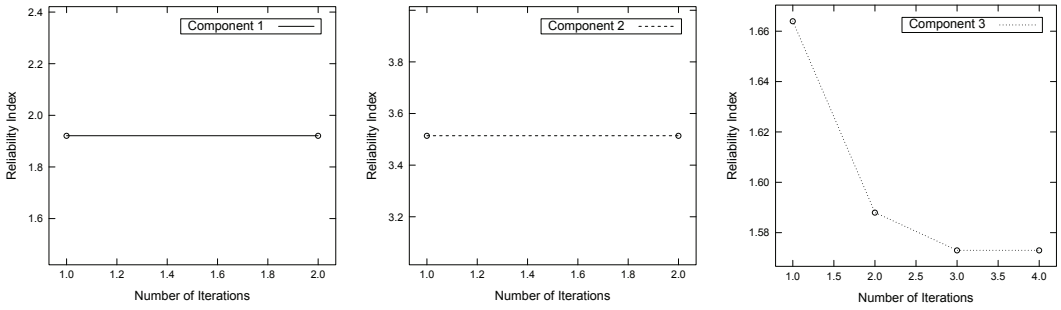

Figure 4.28: Convergence of Iterations of the Limit State Equations With Three Uncorrelated Normal Variates for a Series System (Simply Supported Beam).

Table 4.10: Results for the Components of the Series System (Simply Supported Beam).

Component	Number of Iterations	Reliability Index	Probability of Failure	Probability of Safety
1	2	1.9207	0.027385	0.97261
2	2	3.5138	0.22094 $\times 10^{-3}$	0.99978
3	4	1.5730	0.057858	0.94214

4.5.9 Parallel System

An m-bar parallel system as shown in Figure 4.29 is comprised of m-failure components as described by the limit state equations $g(1)$ through $g(m)$. For a four-bar parallel system (i.e. m=4), the limit state equations $g(1)$, $g(2)$, $g(3)$, and $g(4)$ are defined as follows:

$$g(1) = R_1 - 0.25P \tag{4.93}$$

$$g(2) = R_2 - 0.25P \tag{4.94}$$

$$g(3) = R_3 - 0.25P \tag{4.95}$$

$$g(4) = R_4 - 0.25P \tag{4.96}$$

All four bars are the same; therefore, the load P is distributed equally to four bars. The correlation between the bar resistances R_i and R_j is assumed as $\rho_{Ri,Rj} = 0.50$. Also, it is assumed that there is no correlation between the bar resistances and the load. Random variables X_1 through X_5 representing the bar resistances R_1 through R_2 are normally distributed as shown in Table 4.11. Plots of probability distributions for random variables X_1 through X_5, and the convergence of the component reliability indices are shown in Figures 4.30 and 4.31 respectively. The reliability index, the probability of failure and the probability of failure is calculated for the components as shown in Table 4.12. The reliability index obtained after system reliability analysis

is calculated as 2.0106, the system probability of failure is 0.022183, and the system probability of safety is 0.977817.

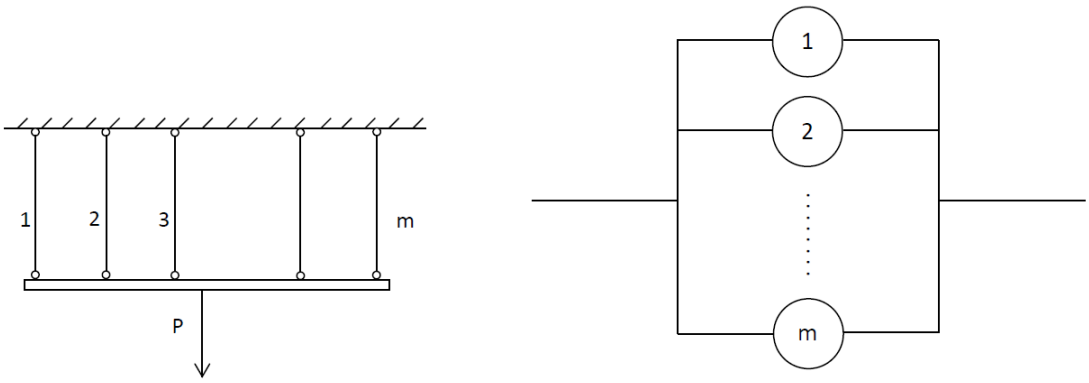

Figure 4.29: Physical View and the Failure Mode Representation of a Parallel System Made up of m-Bars.

Table 4.11: Random Variables of the Limit State Equations With Four Correlated Normal Variates for the Parallel System.

Random Variable	Symbol	Mean Value	Standard Deviation	Distribution Type
R_1	X_1	0.375	0.0375	Normal
R_2	X_2	0.375	0.0375	Normal
R_3	X_3	0.375	0.0375	Normal
R_4	X_4	0.375	0.0375	Normal
P	X_5	1.25	0.125	Normal

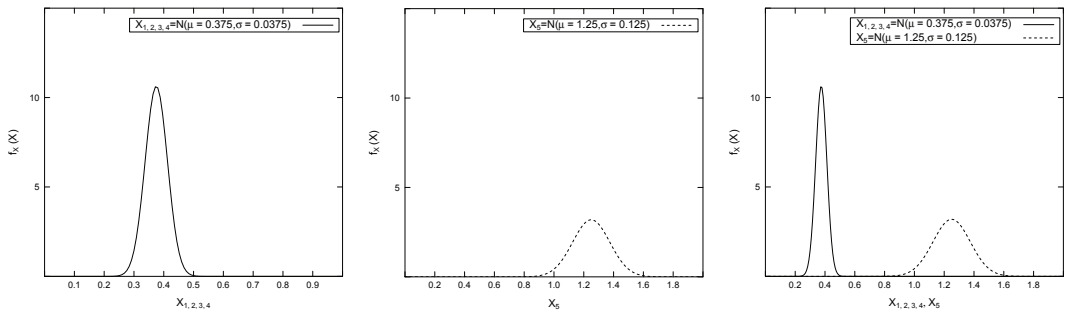

Figure 4.30: Probability Distributions of the Random Variables of Limit State Equations With Four Correlated Normal Variates for the Parallel System.

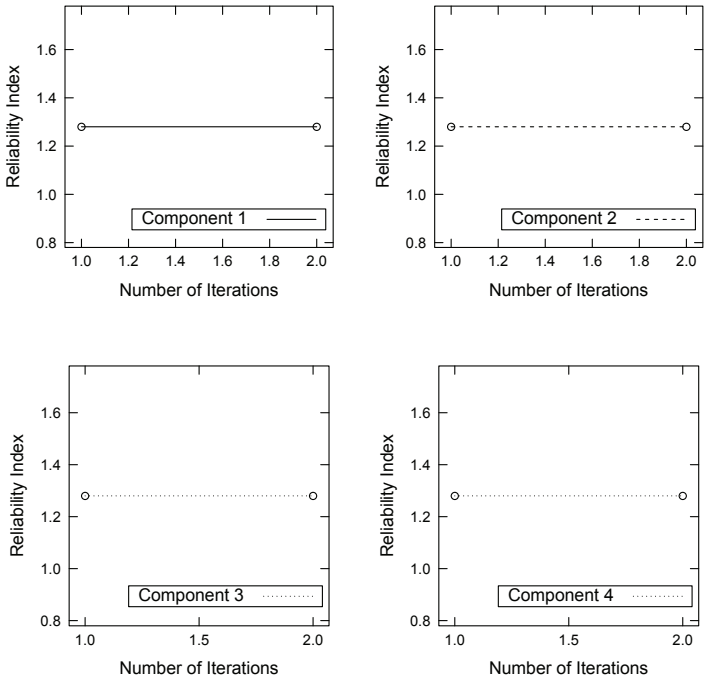

Figure 4.31: Convergence of Iterations of the Limit State Equations With Four Correlated Normal Variates for the Parallel System.

Table 4.12: Results for the Components of the Parallel System.

Component	Number of Iterations	The Reliability Index	The Probability of Failure	The Probability of Safety
1	2	1.2804	0.10021	0.89979
2	2	1.2804	0.10021	0.89979
3	2	1.2804	0.10021	0.89979
4	2	1.2804	0.10021	0.89979

4.5.10 Series-Parallel System

Th following series-parallel system (Figure 4.32) is comprised of three failure components as described by the limit state equations $g(1)$, $g(2)$, and $g(3)$ below.

$$g(1) = 2X_1^2 - 2X_2 \tag{4.97}$$

$$g(2) = X_1 - X_3 \tag{4.98}$$

$$g(3) = 1.5X_1 + 0.5X_3^2 - X_2 \tag{4.99}$$

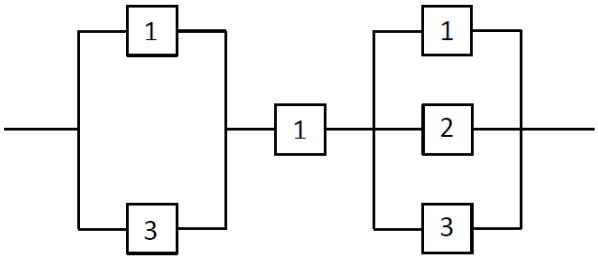

Figure 4.32: A Series-Parallel System.

The system is reduced to an equivalent single component as shown in Figure 4.33. Random variables X_1, X_2 and X_3 are normally distributed and uncorrelated and their descriptor values are shown in Table 4.13.

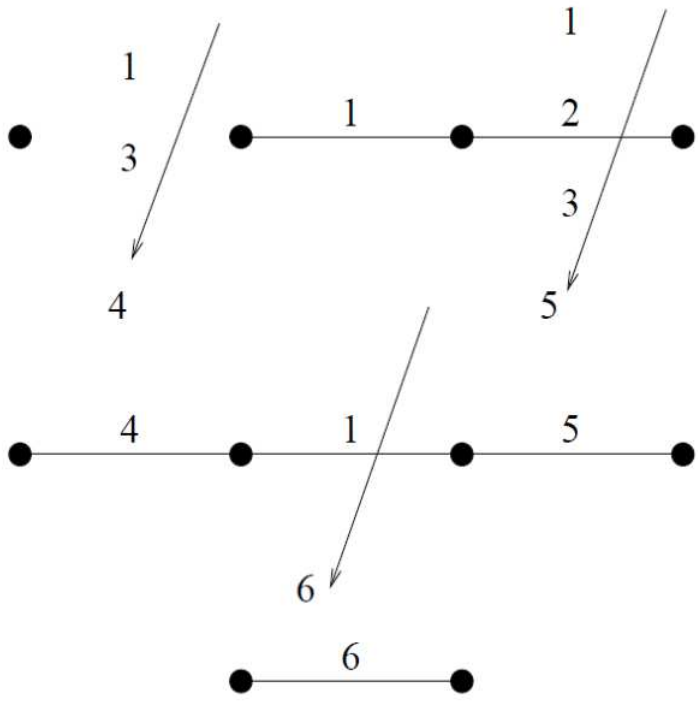

Figure 4.33: Reduction of the Series-Parallel System to an Equivalent Single Component.

Figure 4.34 shows the convergence of the reliability index as the number of iterations increased for three components. Reliability index, probability of failure and probability of safety are calculated for the three components and are listed Table 4.14. The

Table 4.13: Random Variables of the Limit State Equations With Three Uncorrelated Normal Variates for the Series-Parallel System.

Random Variable	Mean Value	Standard Deviation	Distribution Type
X_1	2.0	0.2	Normal
X_2	3.0	0.3	Normal
X_3	1.0	0.1	Normal

reliability index obtained after system reliability analysis is calculated as 1.2119, the probability of failure is 0.11281, and the probability of safety is 0.88719.

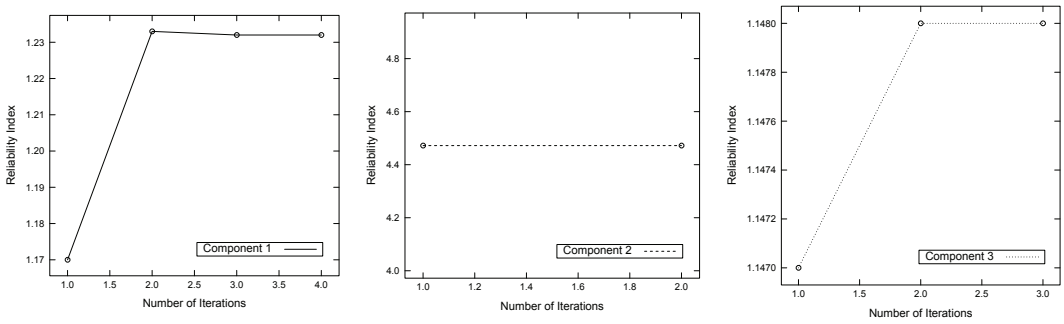

Figure 4.34: Convergence of Iterations of the Limit State Equations With Three Uncorrelated Normal Variates for the Series-Parallel System.

Table 4.14: Results for the Components of the Series-Parallel System.

Component	Number of Iterations	Reliability Index	Probability of Failure	Probability of Safety
1	4	1.2317	0.10903	0.89097
2	2	4.4721	0.38756×10^{-5}	$0.1 \times 10^{+1}$
3	3	1.1479	0.12551	0.87449

4.5.11 Series-Parallel System (Three Bars Connected in Parallel)

Figure 4.35 shows a parallel system made up of three bars. For this problem, conditional failures of the bars will be considered. For instance, if bar 1 fails first, bar 2 may fail next. This event will be denoted by Bar 2|1. After the failures of the first two bars, bar 3 may fail, which causes the failure of the system. This event will be defined as Bar3|1,2 i.e failure of bar 3 given that bars 1 and 2 have already failed. All other possible sequences of the failures of three bars can be listed in a similar

way. The resulting failure model for the system will consist of series occurrences of 6 possible scenarios where each scenario contains parallel occurrences of 3 possible failure sequences of the three bars as shown in Figure 4.36. Based on these events, limit state equations can be written. The equation that describes the failure of bar 1 is $g(1)$ where DF_1 is a distribution factor that describes how much of the load is taken by Bar 1. The limit state equations are as follows:

$$g(1) = R_1 - DF_1(P) \tag{4.100}$$

$$g(2) = R_2 - DF_2(P) \tag{4.101}$$

$$g(3) = R_3 - DF_3(P) \tag{4.102}$$

$$g(4) = R_2 - DF_4(P - \eta_1 R_1) \tag{4.103}$$

$$g(5) = R_3 - DF_5(P - \eta_1 R_1) \tag{4.104}$$

$$g(6) = R_1 - DF_6(P - \eta_2 R_2) \tag{4.105}$$

$$g(7) = R_3 - DF_7(P - \eta_2 R_2) \tag{4.106}$$

$$g(8) = R_1 - DF_8(P - \eta_3 R_3) \tag{4.107}$$

$$g(9) = R_2 - DF_9(P - \eta_3 R_3) \tag{4.108}$$

$$g(10) = R_3 - DF_{10}(P - \eta_1 R_1 - \eta_2 R_2) \tag{4.109}$$

$$g(11) = R_2 - DF_{11}(P - \eta_1 R_1 - \eta_3 R_3) \tag{4.110}$$

$$g(12) = R_1 - DF_{12}(P - \eta_3 R_3 - \eta_2 R_2) \tag{4.111}$$

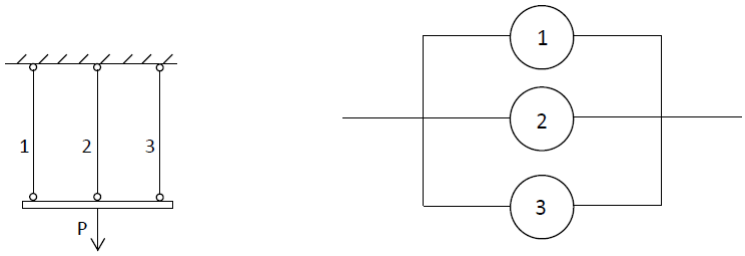

Figure 4.35: Physical View and the Failure Mode Representation of a Parallel System Made up of Three-Bars

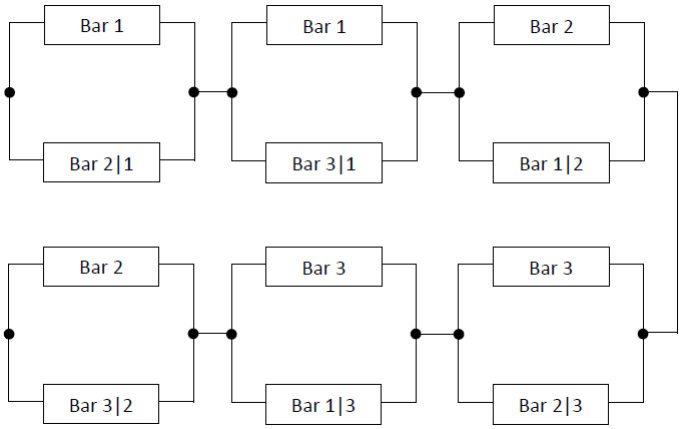

Figure 4.36: Three Bar Parallel System Modeled as a Series-Parallel System.

Similarly, equation $g(4)$ describes the failure of bar 2 given that bar 1 has already failed (Bar 2|1), and equation $g(10)$ describes the failure of bar 3 after both bars 1 and 2 have failed (Bar3|1,2). In these equations, η is the ductility factor which is the percentage of the elastic load that a bar is able to carry after failure. Random variables R_1, R_2, R_3 and P are normally distributed as shown in Table 4.15.

Plots of probability distributions for random variables R_1, R_2, R_3 and P, and the convergence of the reliability index for twelve components are shown in Figures 4.37 and 4.38 respectively. The reliability index, the probability of failure, and the probability

of safety are calculated for the failure paths as shown in Table 4.16. The reliability index based on system reliability analysis is calculated as 2.6894, the probability of failure of the system is 0.0035833, and the probability of safety of the system is 0.9964167.

Table 4.15: Random Variables of the Limit State Equations With Four Uncorrelated Normal Variates for the Three-Bar Series-Parallel System.

Random Variable	Mean Value	Standard Deviation	Distribution Type
R_1	0.5	0.05	Normal
R_2	0.5	0.05	Normal
R_3	0.5	0.05	Normal
P	1.0	0.10	Normal

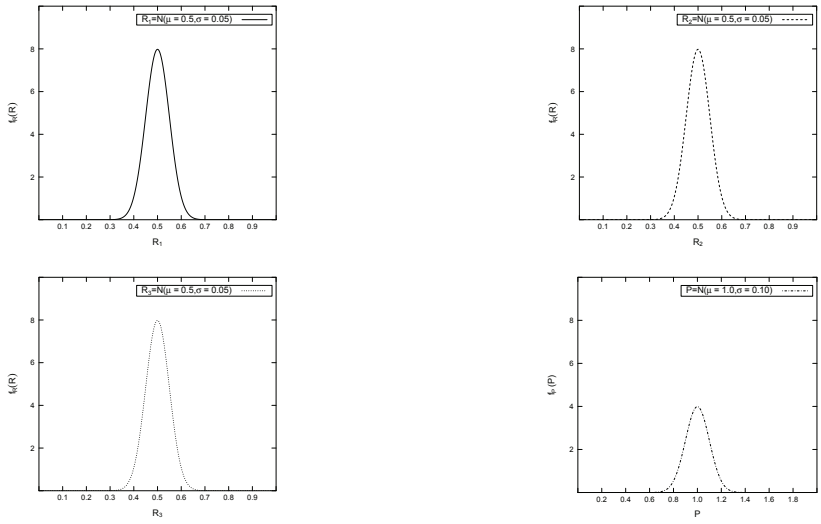

Figure 4.37: Probability Distributions of the Four Uncorrelated Normal Variates for the Three-Bar Series-Parallel System.

4.5.12 Series-Parallel System (Three-Bar Indeterminate Truss With Hinged Supports)

The system failure event for the three-bar indeterminate truss, as shown in Figure 4.39, is modeled as a series-parallel system where all possible failure paths are considered (Figure 4.40). The limit equations below define portions of these failure paths.

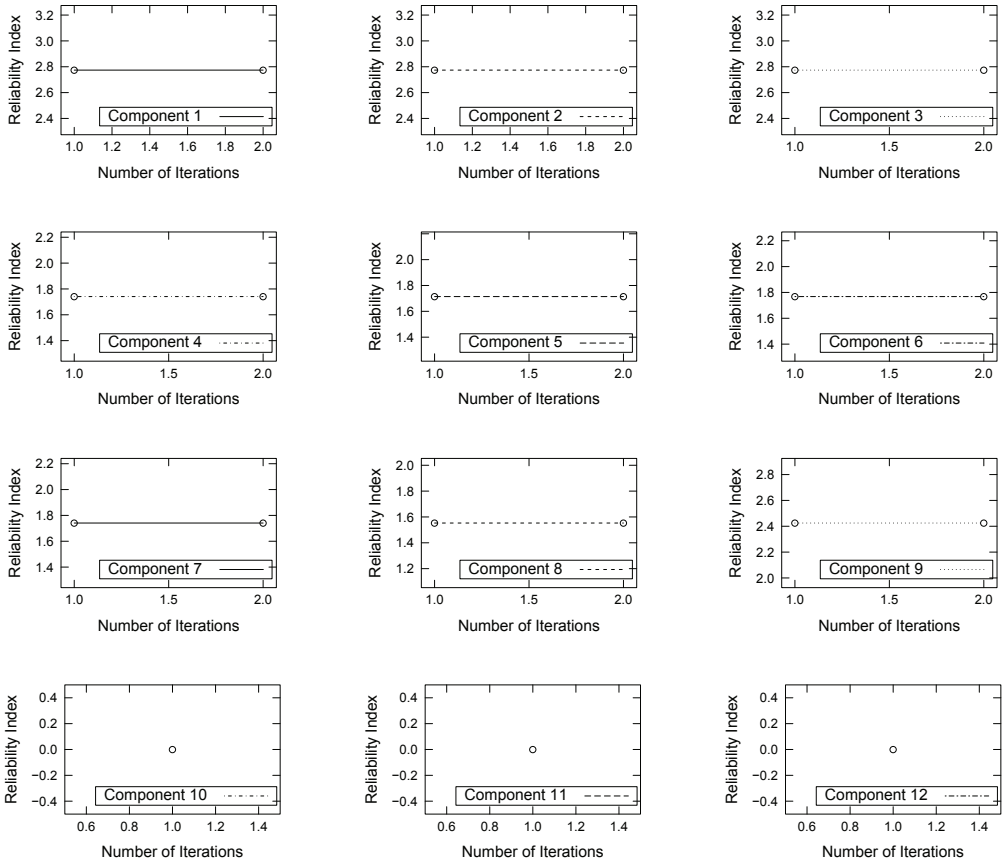

Figure 4.38: Convergence of Iterations of the Limit State Equations With Four Uncorrelated Normal Variates for the Three-Bar Series-Parallel System.

Table 4.16: Results for the Three-Bar Series-Parallel System.

Failure Event	Number of Iterations	Reliability Index	Probability of Failure	Probability of Safety
1	2	2.7736	0.27723×10^{-2}	0.99723
2	2	2.7736	0.27723×10^{-2}	0.99723
3	2	2.7736	0.27723×10^{-2}	0.99723
4	2	1.7408	0.40861×10^{-1}	0.95914
5	2	1.7142	0.43246×10^{-1}	0.95675
6	2	1.7678	0.38550×10^{-1}	0.96145
7	2	1.7408	0.40861×10^{-1}	0.95914
8	2	1.5535	0.60153×10^{-1}	0.93985
9	2	2.4254	0.76467×10^{-2}	0.99235
10	1	0.1×10^{-30}	0.5	0.5
11	1	0.1×10^{-30}	0.5	0.5
12	1	0.1×10^{-30}	0.5	0.5

$$g(1) = \sigma_1 \left(2.0A_1A_3 + \sqrt{2}\left(A_1A_2 + A_3A_2\right)\right) - \sqrt{2}PA_1\left(\cos\theta + \sin\theta\right) - 2.0PA_2\cos\theta \tag{4.112}$$

$$g(2) = \sigma_2 \left(2.0A_1A_2 + \sqrt{2}\left(A_1A_2 + A_3A_2\right)\right) - \sqrt{2}P\left(\left(A_1 - A_3\right)\cos\theta + \left(A_1 + A_3\right)\sin\theta\right) \tag{4.113}$$

$$g(3) = \sigma_3 \left(\sqrt{2}A_1A_3 + A_1A_2 + A_3A_2\right) + P\left(A_3\sin\theta - A_3\cos\theta - \sqrt{2}A_2\cos\theta\right) \tag{4.114}$$

$$g(4) = \sigma_2A_2 - P\left(\sin\theta + \cos\theta\right) + \sqrt{2}\eta\sigma_1A_1 \tag{4.115}$$

$$g(5) = \sigma_3A_3 - P\sqrt{2}\cos\theta + \eta\sigma_1A_1 \tag{4.116}$$

$$g(6) = \sigma_1A_1 - \sqrt{2}/2\left(P\left(\sin\theta + \cos\theta\right) + \eta\sigma_2A_2\right) \tag{4.117}$$

$$g(7) = \sigma_3A_3 - \sqrt{2}/2\left(P\left(\cos\theta - \sin\theta\right) + \eta\sigma_2A_2\right) \tag{4.118}$$

$$g(8) = \sigma_1A_1 - \sqrt{2}P\cos\theta + \eta\sigma_3A_3 \tag{4.119}$$

$$g(9) = \sigma_2A_2 - P\left(\sin\theta - \cos\theta\right) - \sqrt{2}\eta\sigma_3A_3 \tag{4.120}$$

The following assumptions are made. The correlation between the yield stresses of the bars σ_i and σ_j is assumed as $\rho_{\sigma i,\sigma j} = 0.30$. There is no correlation between the bar yield stresses and the load P. A_1, A_2, and A_3 are the cross-sectional areas of the three bars and η is the ductility factor. Random variables $R1$, $R2$, $R3$ and P are normally distributed as shown in Table 4.17.

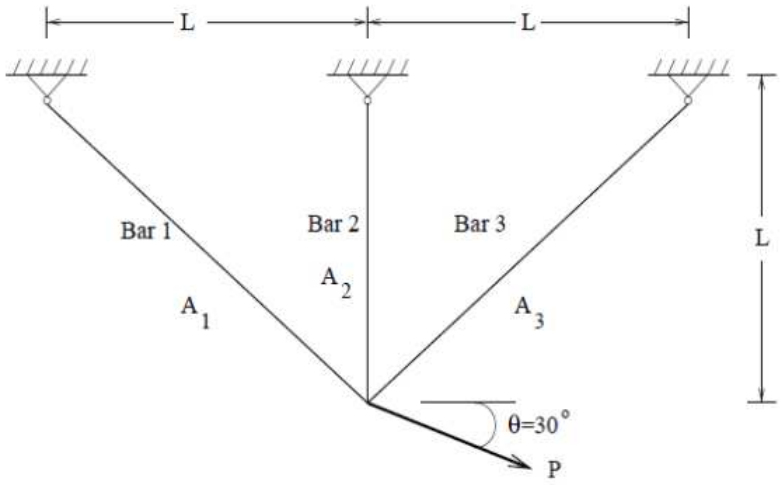

Figure 4.39: Three-Bar Indeterminate Truss.

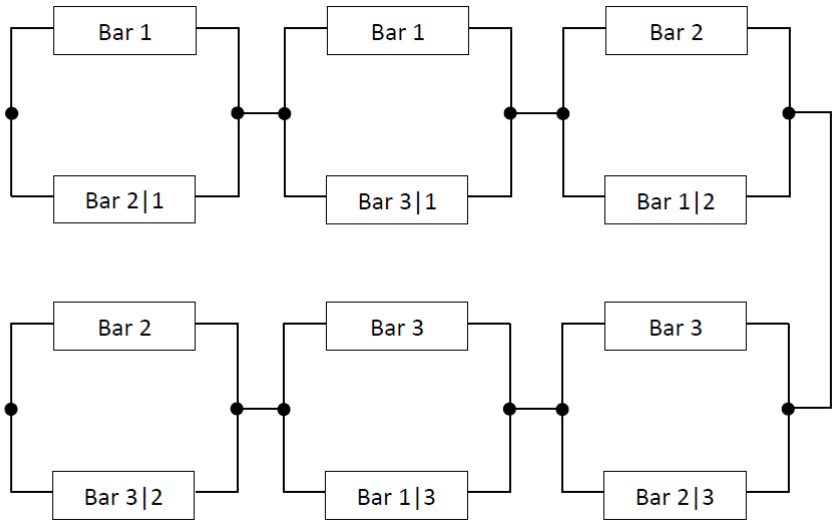

Figure 4.40: System Failure Model for the Three-Bar Indeterminate Truss.

Table 4.17: Random Variables of the Limit State Equations With Three Correlated Normal Variates for the Series-Parallel System of the Three-Bar Indeterminate Truss.

Random Variable	Mean Value	Standard Deviation	Distribution Type
R_1	15.0	1.5	Normal
R_2	15.0	1.5	Normal
R_3	10.0	1.5	Normal
P	20.0	4.0	Normal

Plots of probability distributions for the random variables $R1$, $R2$, $R3$ and P, and the convergence of the reliability index for the nine failure events are shown in Figures

4.41 and 4.42 respectively. The reliability index, the probability of failure, and the probability of safety for each failure component are calculated as shown in Table 4.18. The reliability index for the whole system after system reliability analysis is calculated as 3.4115, the probability of failure of the truss is 0.00032321, and the probability of safety of the truss is obtained as 0.99967679.

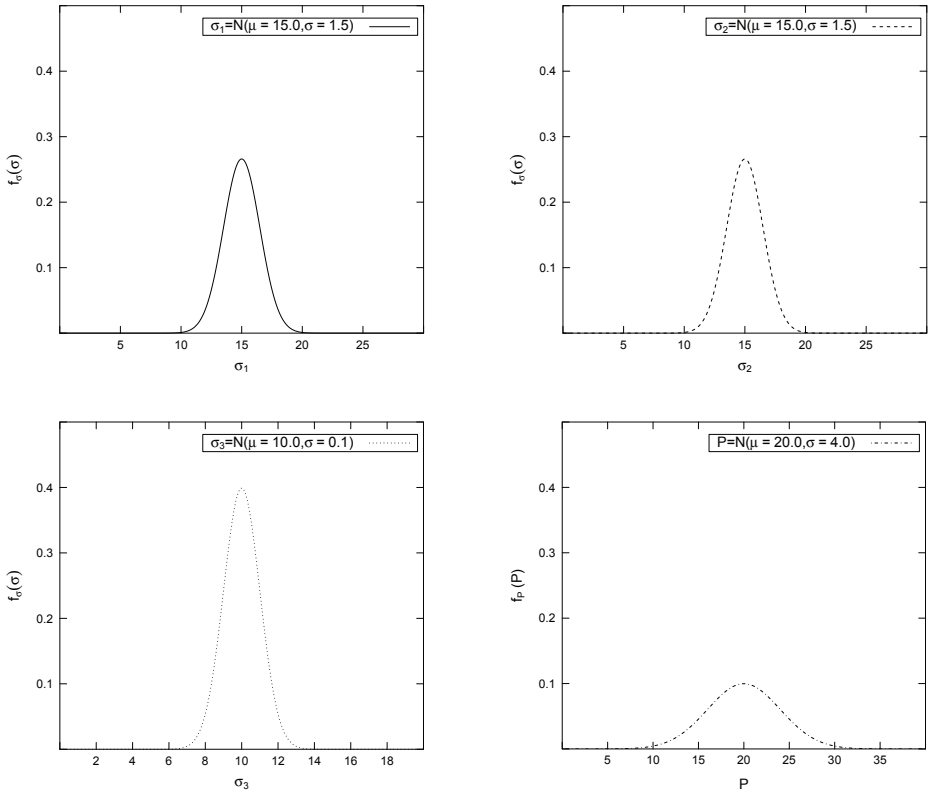

Figure 4.41: Probability Distributions of the Limit State Equations With Three Correlated Normal Variates for the Series-Parallel System for the Three-Bar Indeterminate Truss.

4.6 Summary

In this chapter, to analyze and evaluate load and capacity reliability problems, First-Order Reliability Method (FORM) implemented in the program RELSYS is used. Some of the problems from the manual of RELSYS and some additional problems from Ang and Tang (1975) are solved by using the program in order to verify that the results obtained are the same as the results presented in the manual and the book.

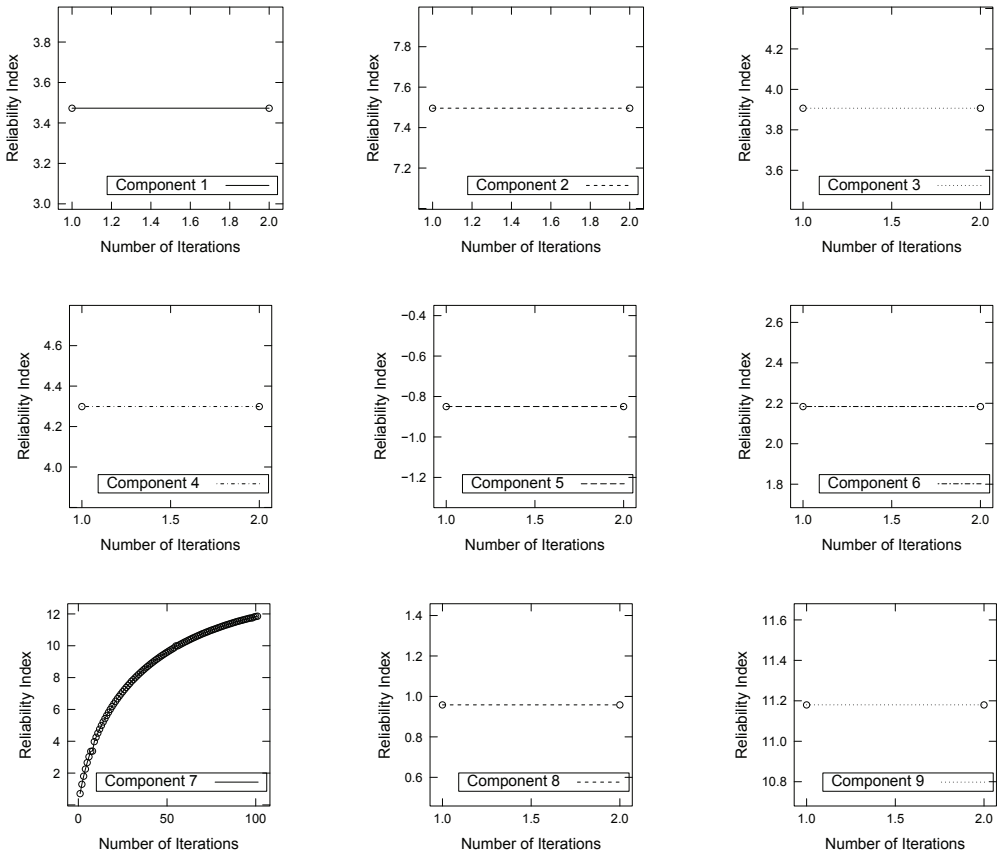

Figure 4.42: Convergence of Iterations of the Limit State Equations With Three Uncorrelated Normal Variates for the Series-Parallel System for the Three-Bar Indeterminate Truss.

Table 4.18: Results for the Series-Parallel System for the Three-Bar Indeterminate Truss.

Failure Event	Number of Iterations	Reliability Index	Probability of Failure	Probability of Safety
1	2	3.4735	0.25692×10^{-3}	0.99974
2	2	7.4960	0.33159×10^{-13}	1.00000
3	2	3.9073	0.46691×10^{-4}	0.99995
4	2	0.42985	0.33365	0.66635
5	2	-0.84945	0.80219	0.19781
6	2	2.1836	0.14495×10^{-1}	0.98550
7	101	11.865	0.92723×10^{-32}	1.00000
8	2	0.95832	0.16895	0.83105
9	2	11.180	0.26268×10^{-28}	1.00000

The procedures consisted of component and a system analyses. In the component analysis, there were both uncorrelated and correlated random variables. The uncorrelated random variables were classified into normal and non-normal distributions in terms of the same limit state equation, mean value, and standard deviation of random variables. Comparing the results, it is observed that the values of reliability for normal distributions are greater than that of non-normal distributions. Similarly, the correlated random variables are also categorized as normal and non-normal. For the correlated cases also, the values of reliability for normal distributions are observed to be greater than that of non-normal distributions. Another comparison is made between correlated and uncorrelated random variables cases, in which reliability of both uncorrelated random normal and non-normal variables are observed to be greater than that of both correlated random normal and non-normal variables.

In addition to component analyses, system analyses were also performed which were classified as series, parallel, and series-parallel system. In system problems, the number of failure components to be considered depends on the given problem. Accordingly, the reliability for each component is calculated separately and the system is eventually reduced to an equivalent single component. The new single component is used by the program to calculate the reliability of the system.

Considering all of the components and systems problems studied, two more example problems were analyzed and the obtained results indicated that a parallel system can be modeled as a series-parallel system by considering all possible failure paths. To summarize, the analyses and evaluations presented in this chapter were performed to verify the results of the program RELSYS and, based on this knowledge, to write a new algorithm, which can be used for time variant reliability analyses to be presented in the next chapter.

CHAPTER 5

DEVELOPMENT OF A COMPUTATIONAL ALGORITHM FOR TIME VARIANT RELIABILITY ANALYSIS

5.1 Introduction

A bridge structure is subjected to direct exposure of different stress mechanisms after it is built. Examples of these stress mechanisms, which cause the deterioration of the resistance of bridge component, consist of environmental attacks, such as Alkali-Silica Reactivity (ASR), sulfate attack, freeze-thaw cycling, and reinforcing corrosion among many others. Not only does the resistance of a bridge component vary with time, but also the live load varies with time because of variation in the number of vehicles and their weights on a bridge. For these reasons, the reliability becomes also a time variant value due to the variations in resistance and live load. Therefore, in order to analyze reliability, it is necessary to implement these factors into the analyses in the most realistic sense.

In order to achieve this goal, time variant reliability formulations will be obtained at the beginning of chapters. These formulations will based on different methods such as: repetitive loading,three periods of failure, bathtub curve, stochastic load model (two independent Poisson load processes), random strength degradation function, and load and capacity. Afterwards, time variant reliability will be calculated for each formulation.

In the next section, the importance of deterioration and different deterioration models in literature are discussed. To be able to calculate the time variant reliability of a

component and/or a system by using the FORM technique (i.e. RELSYS program), A FORTRAN 95 program is developed in this chapter. The verification of the FORM technique such that a new algorithm can be developed as a shell program was already achieved in Chapter 4. Moreover, various deterioration and live load models will be defined in the newly developed program. Six separate examples will be solved using the developed program and the results will be evaluated.

5.2 Time Variant Reliability Formulation

In load-capacity inference theory presented in Chapter 4, time was not considered at all. The applied load was considered as the maximum load over the lifetime of the component or system. In reality, however, for a given deteriorating structural component, subjected to increasing live load, such as a bridge structure, as time passes, probability density distribution of the load $f_l(l)$ shifts to the right and the PDF of the resistance $f_c(c)$ should take weakening with age into account as Figure 5.1 indicates and $f_c(c)$ distribution shifts to the left. Therefore, in reality, these two effects result in a decrease in reliability of the component as the time progresses. If desired, time in Figure 5.1 can be shown as the third dimension which can reveal the approaching locations of both PDFs with respect to each other at each progressing time increment.

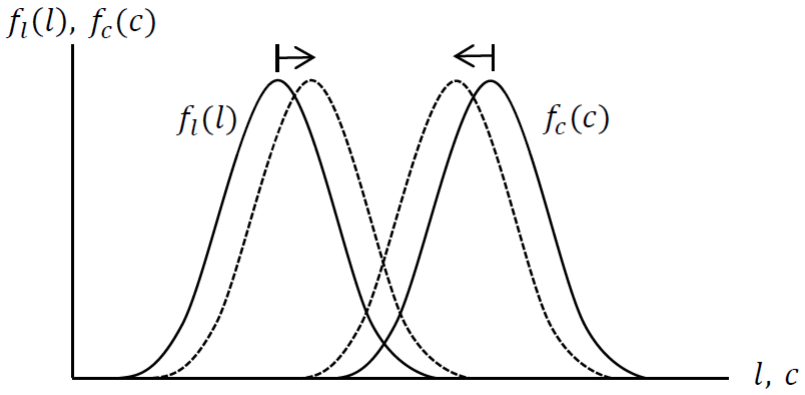

Figure 5.1: Shifting of the Probability Density Functions of the Load and the Capacity With Time.

For a system subjected to repetitive loading, magnitude of each load is defined by the random variable l described by the probability density $f_l(l)$, and the capacity $c(t)$ is known at time t, as shown in Figure 5.2. Therefore, based on this figure, the probability, which represents the event that the load occurring at time t will cause system failure, can be written as:

$$P' = \int_{c(t)}^{\infty} f_l(l)\, dl \tag{5.1}$$

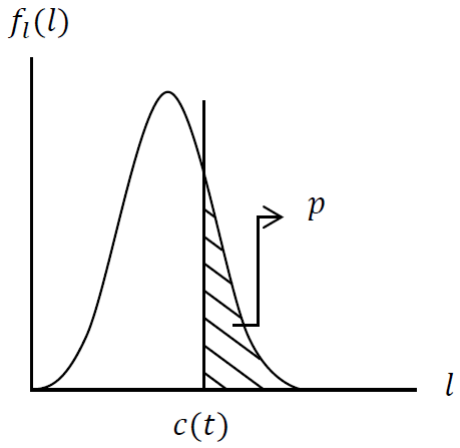

Figure 5.2: Probability Density Function of the Load When the Capacity is Time Variant.

Repetitive loading, however, may be occurring at equal (Figure 5.3) or random time intervals (Figure 5.4).

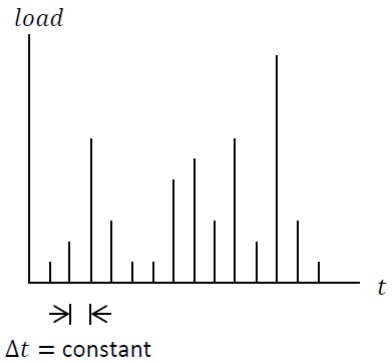

Figure 5.3: Repetitive Loading at Equal Time Intervals.

The model that will be formulated below will be based on random intervals as shown

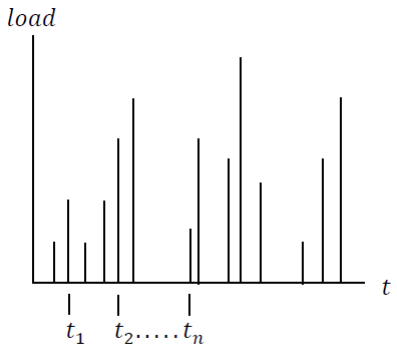

Figure 5.4: Repetitive Loading at Random Time Intervals.

in Figure 5.4. The random times at which the load occurs can be modeled as follows. During a small time increment Δt, probability of the load occurrence is $\gamma \Delta t$, where γ is the number of the load occurrences per unit time, and Δt is so small that $\gamma \Delta << 1$. Then, the probability of the load occurring at any time becomes independent of time with frequency γ. Now, using Eq. 5.1 and the definition above, the following probability can be formulated:

P(A load that is large enough to cause failure will be occurring between times t and $t + \Delta t$) = $P'.\gamma.\Delta t$

$$P = \gamma \int_{c(t)}^{\infty} f_l(l)\, dl \Delta t \tag{5.2}$$

Since the reliability is the probability that the system has survived until time t, then:

P(Failure during Δt) = P(System survived till time $t \cap$ Failure load occurs during Δt) = $R(t).P.\gamma.\Delta t$

Therefore,
$R(t + \Delta t)$ = P(System survived till time $t \cap$ No failure occurred during Δt)
or

$$R(t + \Delta t) = R(t)\,[1 - P] \tag{5.3}$$

Substituting Eq. 5.2 into Eq. 5.3, we obtain:

$$R(t+\Delta t) = \left[1 - \gamma \int_{c(t)}^{\infty} f_l(l)\ dl.\Delta t\right] R(t) \tag{5.4}$$

Performing mathematical manipulation on Eq. 5.4 results in the following steps:

$$R(t+\Delta t) = R(t) - \gamma \int_{c(t)}^{\infty} f_l(l)\ dl.\ \Delta t\ .\ R(t) \tag{5.5}$$

$$\frac{R(t+\Delta t) - R(t)}{\Delta t} = -\gamma \int_{c(t)}^{\infty} f_l(l)\ dl\ .\ R(t) \tag{5.6}$$

Taking the limit of Eq. 5.6 yields:

$$\lim_{\Delta t \to 0} \frac{R(t+\Delta t) - R(t)}{\Delta t} = -\gamma \int_{c(t)}^{\infty} f_l(l)\ dl\ .\ R(t) \tag{5.7}$$

$$\frac{d}{dt}R(t) = -\gamma \int_{c(t)}^{\infty} f_l(l)\ dl\ .\ R(t) \tag{5.8}$$

Dividing both sides of the above equation by $-R(t)$, Eq. 5.10, that is time variant failure rate $\lambda(t)$ (also called as hazard rate or mortality rate) in terms of the load distribution is obtained.

$$-\frac{1}{R(t)}\frac{d}{dt}R(t) = \gamma \int_{c(t)}^{\infty} f_l(l)\ dl \tag{5.9}$$

$$\lambda(t) = \gamma \int_{c(t)}^{\infty} f_l(l)\ dl \tag{5.10}$$

Since the capacity and the load are time variant, Eq. 5.10 is the most general formula for time variant failure rate in terms of the load distribution.

If the capacity of the system is time independent (i.e. $c(t) = c_0$), then, time t also disappears from the failure rate model in Eq. 5.10 and failure rate becomes constant:

$$\lambda(t) = \gamma \int_{c_0}^{\infty} f_l(l)\ dl \tag{5.11}$$

If $\lambda(t) = \lambda$, the time variant reliability becomes $R(t) = e^{-\lambda t}$, which is the common exponential distribution, which was first presented in Eq. ref3.15ch3 in Chapter 3.

Eq. 5.11 yielded the time-variant failure rate in terms of the load distribution $f_l(l)$ for a fixed capacity $c(t) = c_0$ case.

However, aging is closely associated with capacity deterioration, and it is present if the capacity decreases with time. Capacity deterioration in time can be formulated as:

$$c(t) = c_0 - g(t) \tag{5.12}$$

where c_0 is initial capacity at $t = 0$, and $g(t)$ is a monotonically increasing function of time with $g(0) = 0$. If $c(t)$ decreases as time elapses, $\lambda(t)$ will become larger because the lower limit $c(t)$ of the integral in Eq. 5.10 will move to zero. Despite that, the rate at which $\lambda(t)$ increases will depend on the load distribution $f_l(l)$ also. Once $\lambda(t)$ is known, the reliability can be obtained. From Eqs. 5.9 and 5.10 the following can be written:

$$\lambda(t) = -\frac{1}{R(t)}\frac{d}{dt}R(t) \tag{5.13}$$

$$\lambda(t)dt = -\frac{dR(t)}{R(t)} \tag{5.14}$$

Integrating between 0 and t:

$$\begin{aligned} \int_0^t \lambda(t')dt' &= -\int_0^t \frac{1}{R(t)}dR(t) \\ &= -\left[\ln R(t)\right]_0^t \\ &= -\left[\ln R(t)\right] \\ &= -\ln R(t) \end{aligned} \tag{5.15}$$

Using this equation, reliability can be written in terms of the failure rate as:

$$R(t) = e^{-\int_0^t \lambda(t')\ dt'} \tag{5.16}$$

Substituting Eq. 5.10 into Eq. 5.16 in terms of t' yields:

$$R(t) = e^{\left[-\int_0^t \left(\gamma \int_{c(t)}^{\infty} f_l(l)\ dl\right) dt'\right]} \tag{5.17}$$

$$R(t) = e^{\left[-\int_0^t dt' \gamma \int_{c(t)}^{\infty} f_l(l)\ dl\right]} \tag{5.18}$$

Since $c(t') = c_0 - g(t')$, this reliability can be calculated for a given c_0 as:

$$R(t|c_0) = e^{\left[-\int_0^t dt' \gamma \int_{c(t)}^{\infty} f_l(l)\ dl\right]} \tag{5.19}$$

5.3 Variable Capacity

Because of variability in the manufacturing or construction process, we now consider the situation where some components of a system have different initial capacities. We model this variable by letting c_0 become a random variable, which is described by the PDF. Considering a collection of such components, each with its own capacity, system reliability can be written as an average over c_0.

$$R(t) = \int_0^{\infty} f_c(c_0) R(t|c_0)\ dc_0 \tag{5.20}$$

Substituting Eq. 5.19 into the equation above yields:

$$R(t) = \int_0^{\infty} dc_0 f_c(c_0)\ e^{\left[-\int_0^t dt' \gamma \int_{c(t')}^{\infty} f_l(l)\ dl\right]} \tag{5.21}$$

which is the reliability formula for variable capacity case.

5.4 Time Variant Reliability Formulation Based on Repetitive Loading and Three Periods of Failure

Now, we consider the case where the system is subjected to a repetitive loading. Repetitive loading may occur at either equal or random time intervals. Figure 5.5 is a model based on random time intervals, in which there is no variability in load. In Figure 5.6, there is also no loading variability and no capacity variability, but there is capacity deterioration, and it crosses the load value at year 100. If capacity deterioration $c(t)$ crosses the load distribution within a given time, the time it crosses the mean load is called as the time to failure t_f. For instance, in Figure 5.7 capacity deterioration crosses the load distribution at year 51. Therefore, year 51 is the time to failure t_f. System does not fail before time t_f, but it fails at the first loading, thereafter, causing the rapid exponential decay in reliability. Figures 5.8 and 5.9 show the time variant failure rate and the reliability for this case.

Figure 5.10 shows a case where there is no capacity variability, capacity is constant ($c(t) = c_0$) but loading variability exists. Figures 5.11 and 5.12 show the failure rate and reliability of this case respectively.

5.5 Reliability Bathtub Curve

Bathtub curve has been used in reliability to show the three basic periods of failures of a system that originates with birth (construction) and vanishes with death (collapse) as shown in Figure 5.13. These periods are infant mortality (Early Failure) followed by a constant failure rate (Useful Life, Poisson Failure, Normal Life Failure) and concluding with the so-called wear-out failure (End of Life Failure or Aging Failure). The bathtub curve is inspired by the human life cycle and rate of death.

Due to the risks of birth and fragility of life during the period of infancy, there is a high rate of death in this early period of life. The rate of death decrease to a steady state level until we age, and our bodies start to wear-out. As medical science has tried to extend our lives in the last century, it is the responsibility of engineering sciences to increase the life of engineering products, systems or structures. It is important to

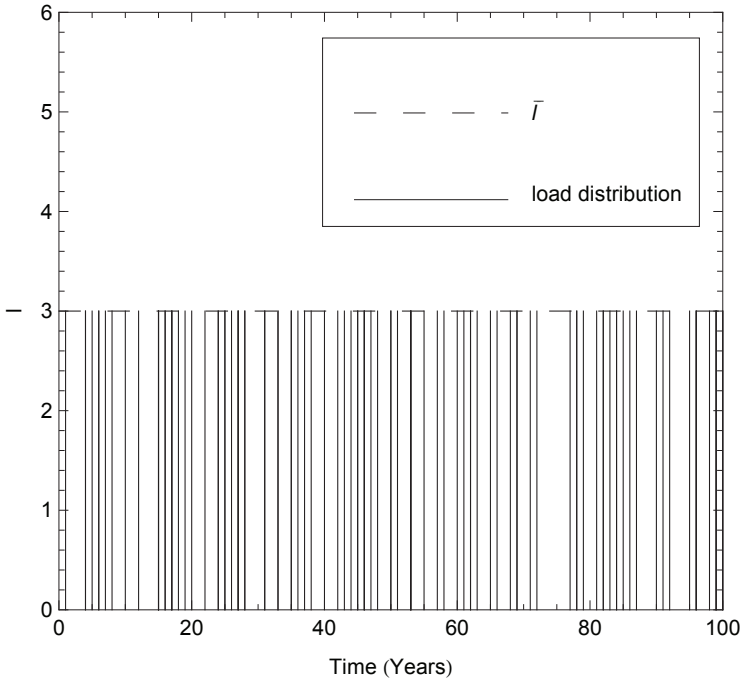

Figure 5.5: Repetitive Loading at Random Time Intervals, When There is No Loading Variability.

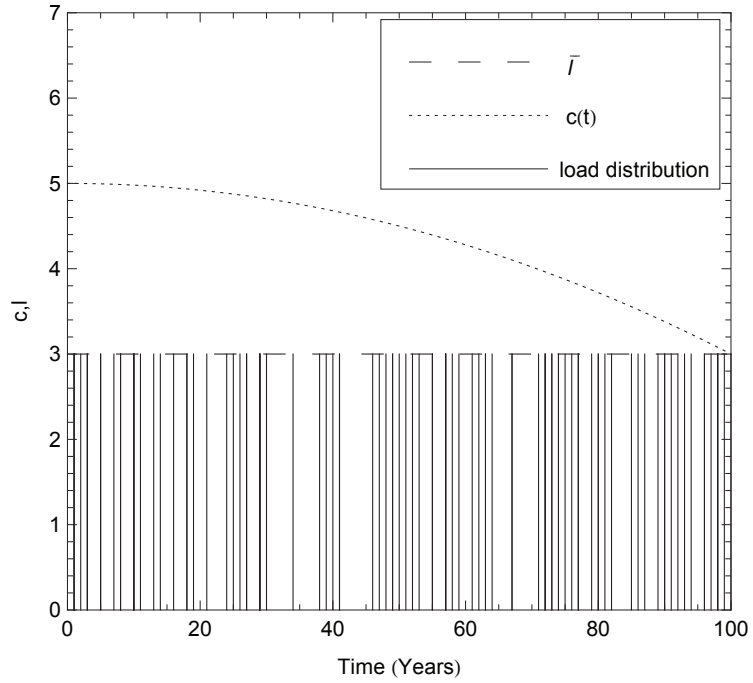

Figure 5.6: Repetitive Loading at Random Time Intervals, When There is No Loading and Capacity Variability, in the Presence of Capacity Deterioration ($t_f = 100$).

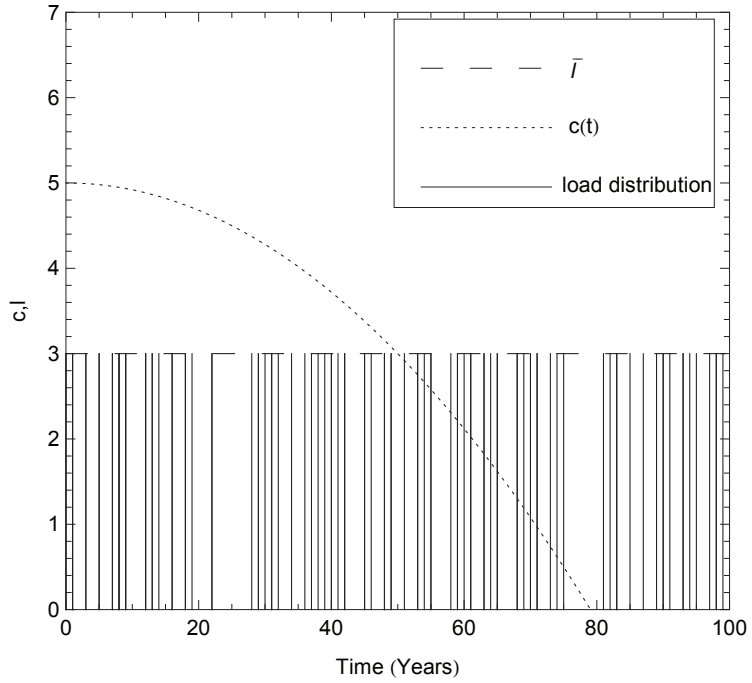

Figure 5.7: Repetitive Loading at Random Time Intervals, When There is No Loading and Capacity Variability, in the Presence of Capacity Deterioration ($t_f = 51$).

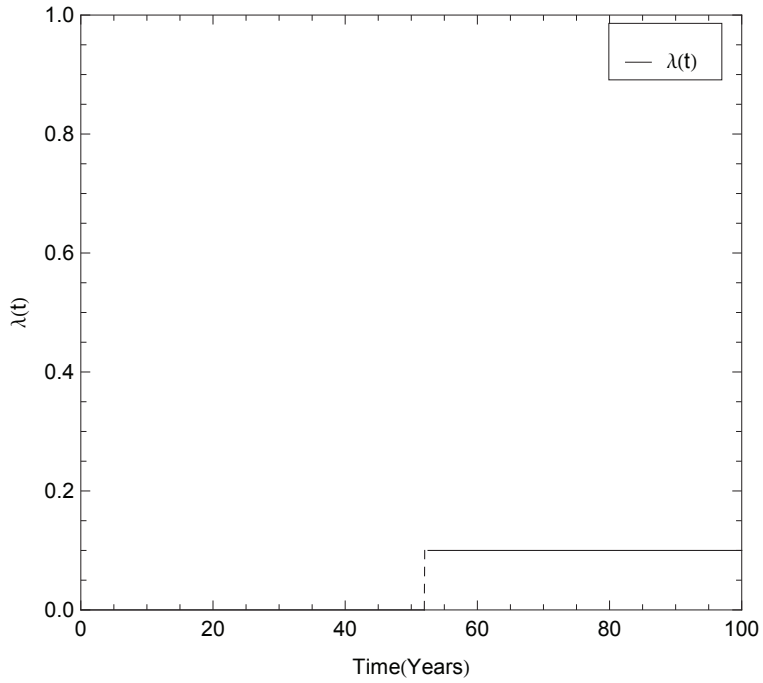

Figure 5.8: Failure Rate, When There is No Loading and Capacity Variability, in the Presence of Capacity Deterioration ($t_f = 51$).

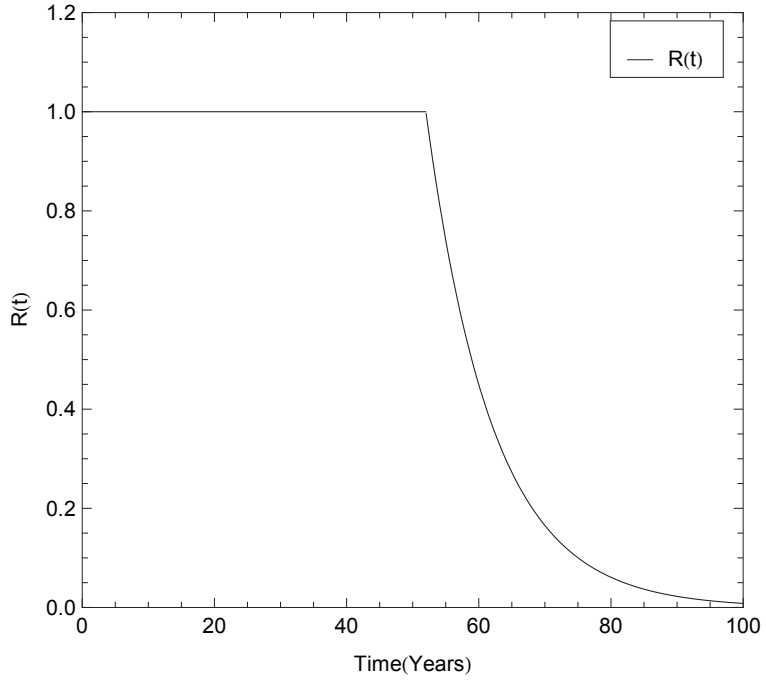

Figure 5.9: Reliability, When There is no Loading and Capacity Variability, in the Presence of Capacity Deterioration ($t_f = 51$).

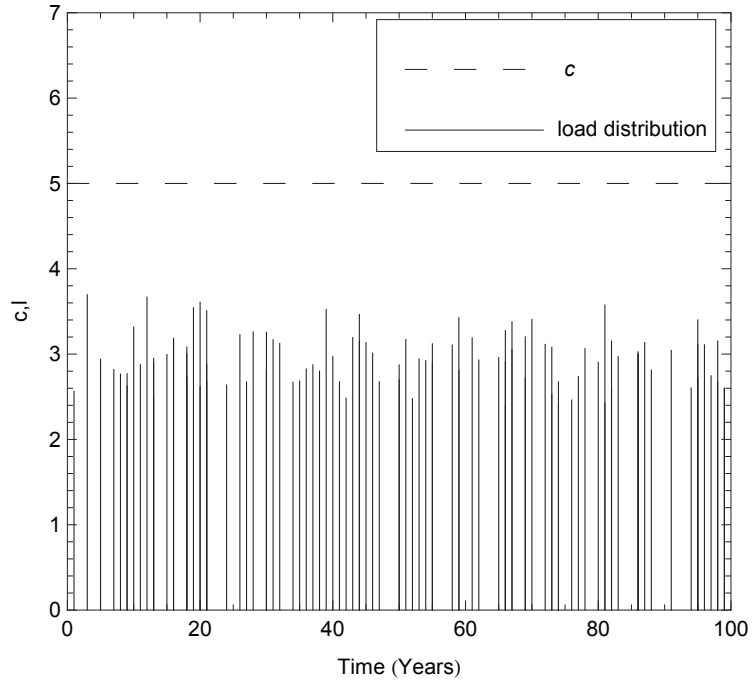

Figure 5.10: Repetitive Loading at Random Time Intervals, When There is no Capacity Variability, in the Presence of Constant Capacity and Loading Variability.

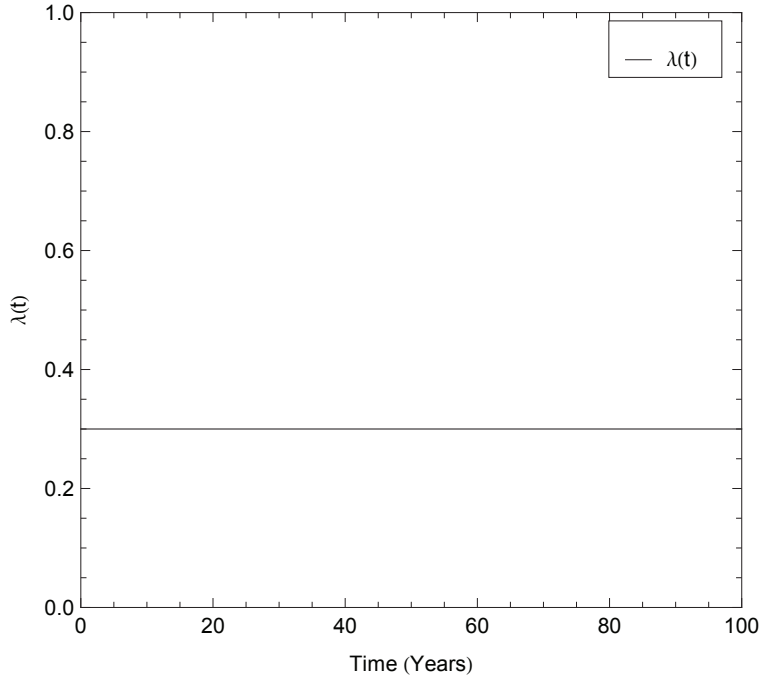

Figure 5.11: Failure Rate, When There is no Capacity Variability, in the Presence of Constant Capacity and Loading Variability.

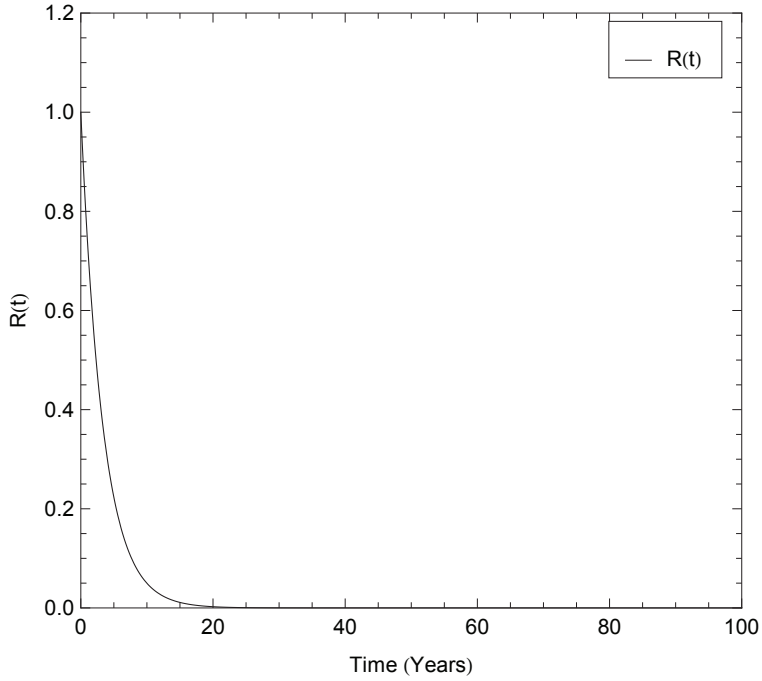

Figure 5.12: Reliability, When There is no Capacity Variability, in the Presence of Constant Capacity and Loading Variability.

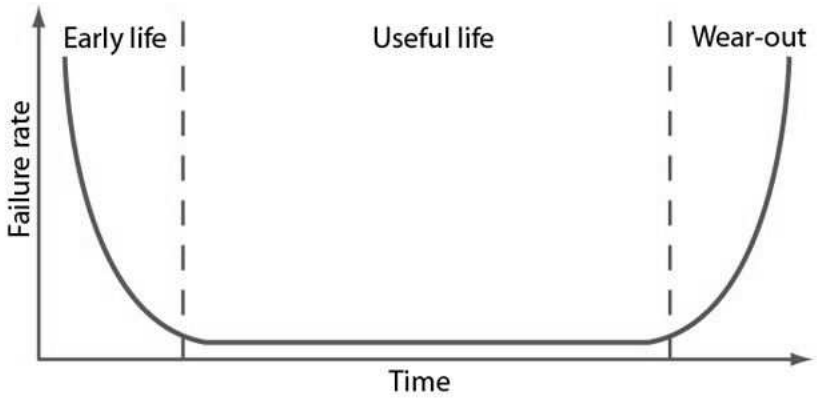

Figure 5.13: Bathtub Curve (Conor Quinn, 2010).

notice that the bathtub curve does not depict the failure rate of a single component but describes the relative failure rate of an entire system over time. For products, for instance, some individual units will fail early, which is called infant mortality failures. Failures during infant mortality are mostly caused by material defects, design blunders, or error in assembly. Some of the remaining units will fail during the following extended period, typically called as the normal life. Failures during normal life are normally considered to be a random case of "stress exceeding the strength". Finally, other remaining units will last until the wear-out period (Dennis J. Wilkins, 2002).

Infant mortality is the period over which the failure rate of a product is declining and this period may last for years. Although this period is a time when the failure rate is dropping, it is an undesirable time because a significant number of failures take place in a short period. In theory, the failures during normal life occur at random but with a relatively constant rate when measured over an extended period of time. It is our intention to have a long constant failure rate with a low bottom in this zone of the bathtub curve. In fact, until the wear-out mode takes place, the reliability would continue to improve over time. Wear-out is a zone on the curve when the failure rate is increasing, it is a fact of life due to fatigue or depletion of materials.

When a system is subjected to repetitive loading, the Load-Capacity interference theory can be used to derive a failure rate. In this theory, infant mortality, constant failure rate and aging are correlated with capacity variability, load variability, and capacity deterioration.

In the following sections, various possible combinations of failure types are used to obtain the failure rate and the reliability in each case. The following assumptions are used to create the failure rate model by using Load-Capacity interference theory.

- Parameter values are $\nu = 1.5$, $\rho_l = 0.15$, $\rho_c = 0.10$, $\alpha = 0.1$, and $\gamma t_0 = 100$.
- The load applications occur randomly at the assumed time interval.
- The load magnitudes are independent and identically distributed with CDF of the load.
- The capacity formula is $c(t) = c_0 - g(t)$ where $g(t)$ is calculated from:

$$g(t) = \alpha.c_0(t/t_0)^m \tag{5.22}$$

5.5.1 Combination of Failure Types

In this section, combination of different failure types are tabulated in terms of presence of each failure mode in each model and density distribution of load and capacity. As Table 5.1 indicates, loads and capacities are modeled as normally distributed and the wear effect (aging) as a power of time. Regarding this table, Lewis and Chen (1994) examined various possible cases by eliminating the failure types, and they were able to plot the bathtub curve when all failure types were present.

Table 5.1: Failure-Type Characterization (Adopted from (Lewis, 1996)).

Failure Type	Capacity, Load or Deterioration	If this failure type is absent	If this failure type is present
I. Infant Mortality (Variable Capacity)	$f_c(c_0)$	$\delta(c_0 - \bar{c}_0)$	$\phi[(c_0 - \bar{c}_0)/\sigma_c]$
II. Poisson Failures (Variable Load)	$f_l(l)$	$\delta(l - \bar{l})$	$\phi[(l - \bar{l})/\sigma_l]$
III. Aging (Deteriorating Capacity)	$g(t)$	0	$\alpha.c_0(t/t_0)^m$

5.5.2 General Formula for Failure Rate Including All Failure Modes

To derive a general formula for the failure rate that includes all three failure modes, we use the failure rate formula in terms of reliability in Eq. 5.13:

$$\lambda(t) = -\frac{1}{R(t)}\frac{d}{dt}R(t) \tag{5.23}$$

General formula for reliability including variable loading and variable capacity was obtained in Eq. 5.21. Substituting R(t) from Eq. 5.21 into Eq. 5.23, we obtain:

$$\begin{aligned}\lambda(t) &= -\frac{\frac{d}{dt}\left\{\int_0^\infty f_c(c_0)\; e^{\left[-\int_0^t dt'\gamma\int_{c(t')}^\infty f_l(l)\; dl\right]}dc_0\right\}}{\int_0^\infty f_c(c_0)\; e^{\left[-\gamma\int_0^t dt'\int_{c(t')}^\infty f_l(l)\; dl\right]}dc_0} \\ &= -\frac{\frac{d}{dt}\left\{\int_0^\infty f_c(c_0)\; e^{\left[-t.\gamma\int_{c(t')}^\infty f_l(l)\; dl\right]}dc_0\right\}}{\int_0^\infty f_c(c_0)\; e^{\left[-\gamma\int_0^t dt'\int_{c(t')}^\infty f_l(l)\; dl\right]}dc_0}\end{aligned} \tag{5.24}$$

We then perform the following mathematical manipulations:

$$\begin{aligned}\lambda(t) &= -\frac{\left\{\int_0^\infty f_c(c_0)\; \frac{d}{dt}e^{\left[-t.\gamma\int_{c(t')}^\infty f_l(l)\; dl\right]}dc_0\right\}}{\int_0^\infty f_c(c_0)\; e^{\left[-\gamma\int_0^t dt'\int_{c(t')}^\infty f_l(l)\; dl\right]}dc_0} \\ &= -\frac{\left\{\int_0^\infty f_c(c_0)\; e^{\left[-t.\gamma\int_{c(t')}^\infty f_l(l)\; dl\right]}\frac{d}{dt}\left[-t.\gamma\int_{c(t')}^\infty f_l(l)\; dl\right]dc_0\right\}}{\int_0^\infty f_c(c_0)\; e^{\left[-\gamma\int_0^t dt'\int_{c(t')}^\infty f_l(l)\; dl\right]}dc_0} \\ &= -\frac{\left\{\int_0^\infty f_c(c_0)\; e^{\left[-\gamma\int_0^t dt'\int_{c(t')}^\infty f_l(l)\; dl\right]}\left[-\gamma\int_{c(t')}^\infty f_l(l)\; dl\right]dc_0\right\}}{\int_0^\infty f_c(c_0)\; e^{\left[-\gamma\int_0^t dt'\int_{c(t')}^\infty f_l(l)\; dl\right]}dc_0} \\ &= \frac{\gamma\int_0^\infty f_c(c_0)\;\int_{c(t')}^\infty f_l(l)\; dl\; e^{\left[-\gamma\int_0^t dt'\int_{c(t')}^\infty f_l(l)\; dl\right]}dc_0}{\int_0^\infty f_c(c_0)\; e^{\left[-\gamma\int_0^t dt'\int_{c(t')}^\infty f_l(l)\; dl\right]}dc_0}\end{aligned} \tag{5.25}$$

Eqs. 5.12, 5.21 and 5.25 constitute a reliability model in which infant mortality, random failures and aging are represented explicitly in terms of capacity variability, loading variability and capacity degradation.

5.5.2.1 Combined Failure Types II & III

In this case, infant mortality (variable capacity) is absent. Figures 5.14 and 5.15 show the scripts which are written using the MAPLE software to generate the graphs shown in Figures 5.16 and 5.17. Furthermore, by using Eqs. 5.26 and 5.27 below, Figures 5.16 and 5.17 are generated for the three aging-exponents, m=1, 2, 4. In these equations, in order to generate Figures 5.16 and 5.17, γ is the homogeneous Poisson process intensity for load application with the assumed value of 0.99956, c_0 is the initial capacity with the assumed value of 10.2, σ_l is the standard deviation of the load with the assumed value of 1.02, α is a constant with the assumed value of 0.1, and l_0 is the initial load with the assumed value 6.8. These values are assumed values selected here to generate characteristic shapes of failure rate and reliability graphs, These values can be changed for the problem at hand.

$$R(t|c_0) = e^{-\int_0^t dt'\gamma \int_{c(t)}^{\infty} f_l(l)dl} \tag{5.26}$$

$$\lambda(t) = \gamma \int_{c(t)}^{\infty} f_l(l)dl \tag{5.27}$$

```
FT := proc( l_0, sigma_l, c_0, alpha, gamma, mn )
  global lambda, m, p :

   for m from 1 by 1 to mn do
    lambda[m] := (int(exp( - ((l-l_0) / sigma_l)^2 * 1 / 2) / (sqrt(2 * Pi)), l = c_0 - ((alpha * c_0)
    * (gamma * t / 100)^m) ..infinity));
    p[m] := plot(lambda[m], t = 0 ..100, y = 0 ..0.01) :
    print (lambda[m]);
   end do:

  plots:-display([p[1]], [p[2]], [p[4]]);
end proc:
```

Figure 5.14: Script Program Used to Generate the Graphs in Figure 5.16.

Figure 5.16 indicates that failure rate is increasing with time. As the value of aging exponent increases, the rate of increase of failure rate becomes steeper. Figure 5.17 shows the time-variant reliability for three different aging exponents. The reliability declines as the time increases. In Figure 5.17 at time 100, reliability values for all

```
RT := proc( l_0, sigma_l, c_0, alpha, gamma, mn )
  global r, m, p :

   for m from 1 by 1 to mn do
    r[m] := exp( - (t * gamma * int(exp( - ((l - l_0) / sigma_l)^2 * 1 / 2) / (sqrt(2 * Pi)), l = c_0
    - ((alpha * c_0) * (gamma * t / 100)^m) ..infinity)));
    p[m] := plot(r[m], t = 0 ..100, y = 0 ..1) :
    print (lambda[m]);
   end do:

  plots:-display([p[1]], [p[2]], [p[4]], axes = boxed);
end proc:
```

Figure 5.15: Script Program Used to Generate the Graphs in Figure 5.17.

values of aging exponent become equal to zero. However, for a given time prior to year 100, the reliability is larger for the larger values of the aging exponent.

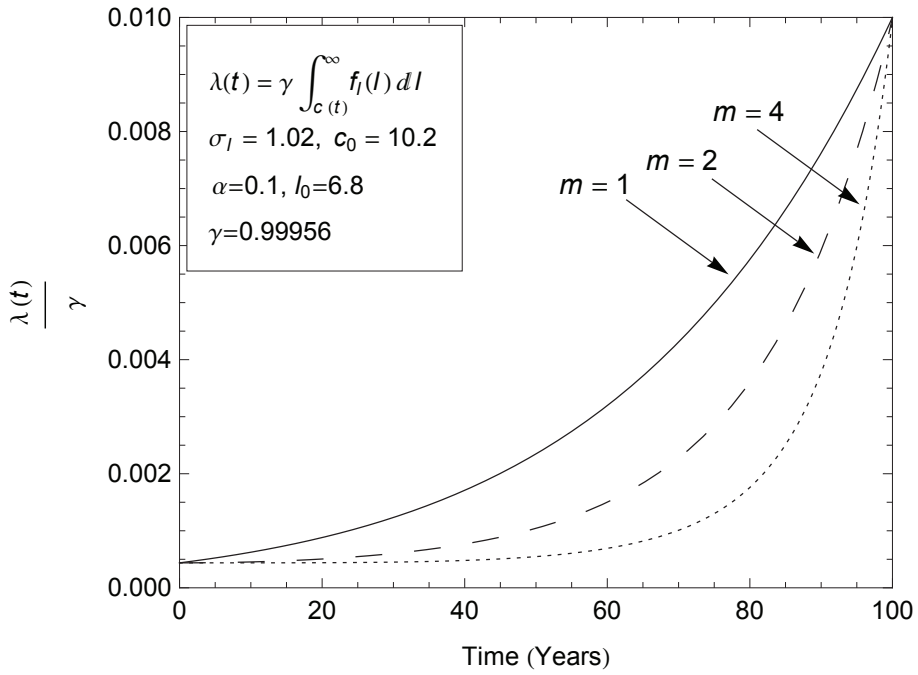

Figure 5.16: Combined Failure Types II and III: Failure Rate vs. Time for Three Aging-Exponents.

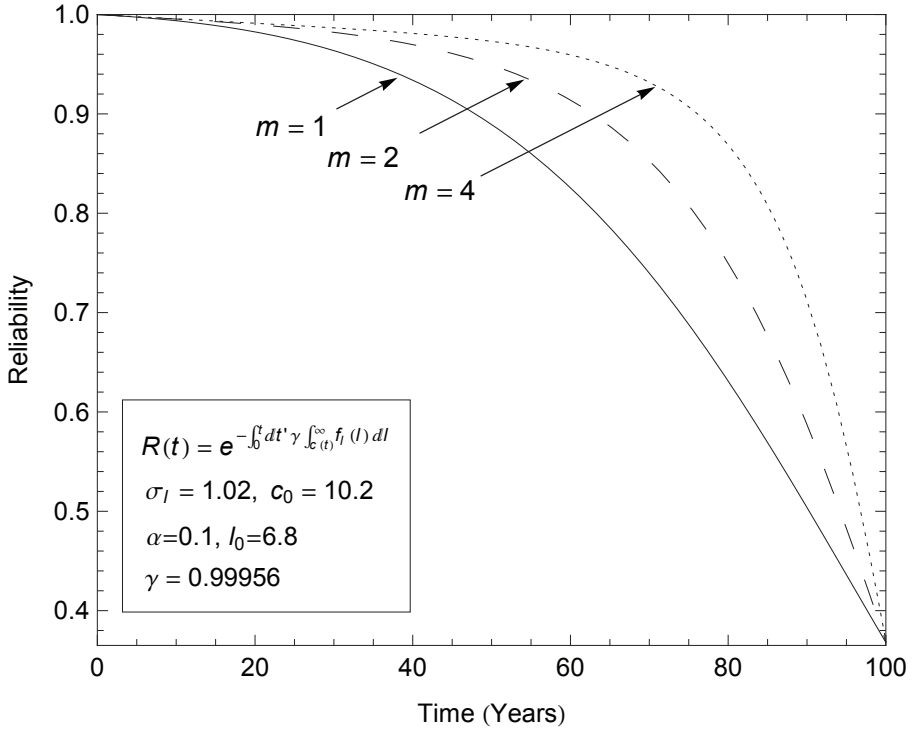

Figure 5.17: Combined Failure Types II and III: Reliability vs. Time for Three Aging-Exponents.

5.5.2.2 Combined Failure Types I & III

In this case, Poisson failure (variable load) is absent. Because of this, we substitute $f_l(l) = \delta(l - \bar{l})$ in Eqs. 5.28 and 5.29 below. After the substitution, we obtain Eqs. 5.30 and 5.31 shown below. By using the produced equations, we were able to generate Figure 5.18. In these equations in order to generate Figure 5.18, where γ is the homogeneous Poisson process intensity for load application with the assumed value of 0.99956, c_0 is the initial capacity with the assumed value of 10.2, σ_l is the standard deviation of the load with the assumed value of 1.02, α is a constant with the assumed value of 0.1, and l_0 is the initial load with the assumed value 6.8.

$$R(t) = \int_0^{\infty} f_{c_0}(c_0) e^{-\int_0^t dt' \gamma \int_{c(t')}^{\infty} f_l(l) dl} dc_0 \tag{5.28}$$

$$\lambda(t) = \frac{\gamma \int_0^{\infty} f_{c_0}(c_0) \left(\int_{c(t')}^{\infty} f_l(l) dl \; e^{-\int_0^t dt' \int_{c(t')}^{\infty} f_l(l) dl} \right) dc_0}{\int_0^{\infty} f_{c_0}(c_0) e^{-\int_0^t dt' \int_{c(t')}^{\infty} f_l(l) dl} dc_0} \tag{5.29}$$

$$\lambda(t) = \frac{\gamma e^{-\gamma t}\left[\int_0^{\bar{l}} f_c(c_0)dc_0 + \int_{\bar{l}}^{\bar{l}+g(t)} e^{\gamma g^{-1}(c_0-\bar{l})} f_c(c_0)dc_0\right]}{1-(1-e^{-\gamma t})\int_0^{\bar{l}} f_c(c_0)dc_0 - \int_{\bar{l}}^{\bar{l}+g(t)}\left\{1-e^{\gamma\left[t-g^{-1}(c_0-\bar{l})\right]}\right\} f_c(c_0)dc_0} \quad (5.30)$$

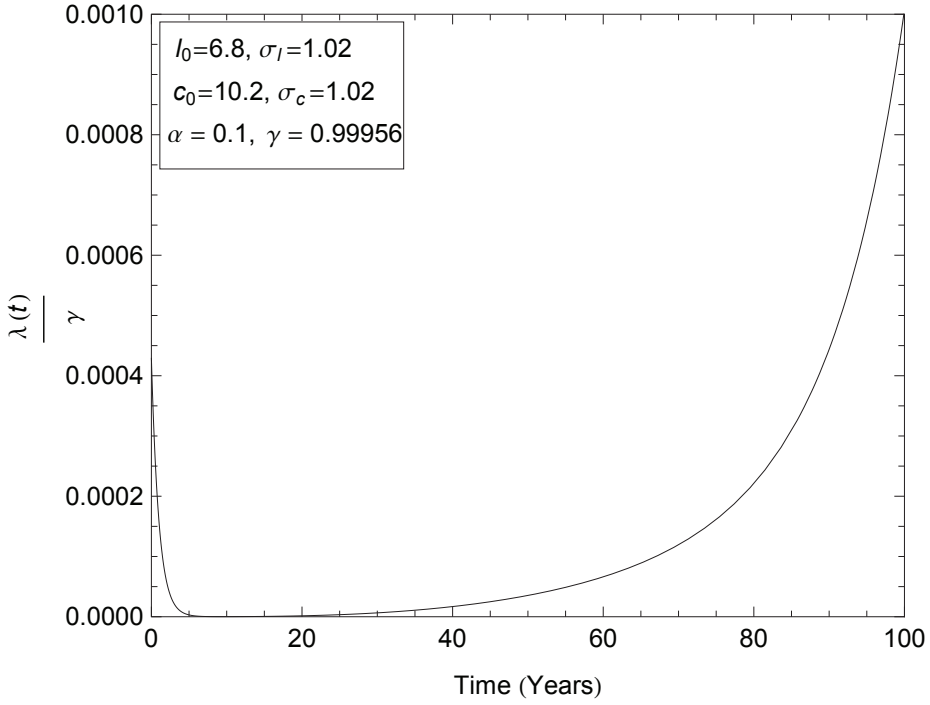

Figure 5.18: Combined Failure Types I and III: Failure Rate vs. Time.

$$R(t) = 1-(1-e^{-\gamma t})\int_0^{\bar{l}} f_c(c_0)dc_0 - \int_{\bar{l}}^{\bar{l}+g(t)}\left\{1-e^{\gamma\left[t-g^{-1}(c_0-\bar{l})\right]}\right\} f_c(c_0)dc_0 \quad (5.31)$$

Figure 5.18 shows a similar behavior encountered frequently in fatigue testing. After the early failure time period (0-5 yrs), fraction of population (for which the initial capacity is less than the load) is removed at the first loading. These are the defective products or components. For human lifetime, they represent infant mortalities. Following this period, in the random failure period the failure rate $\lambda(t)$ is vanishingly small (5-30 yrs) until the effects of aging becomes significant (30-100 yrs) (Lewis & Chen, 1994).

Time variant reliability plotted in Figure 5.19 displays a sudden fall for a short period for reliability at the beginning (0-5 yrs). Afterwards, it declines in a constant rate for a long period (5-50 yrs). As the effects of aging become significant, reliability falls in great magnitude (50-100 yrs). As Figure 5.18 indicates γ is the homogeneous

Poisson process intensity for load application with the assumed value of 0.99956, c_0 is the initial capacity with the assumed value of 10.2, σ_l is the standard deviation of the load with the assumed value of 1.02, α is a constant with the assumed value of 0.1 and l_0 is the initial load with the assumed value 6.8.

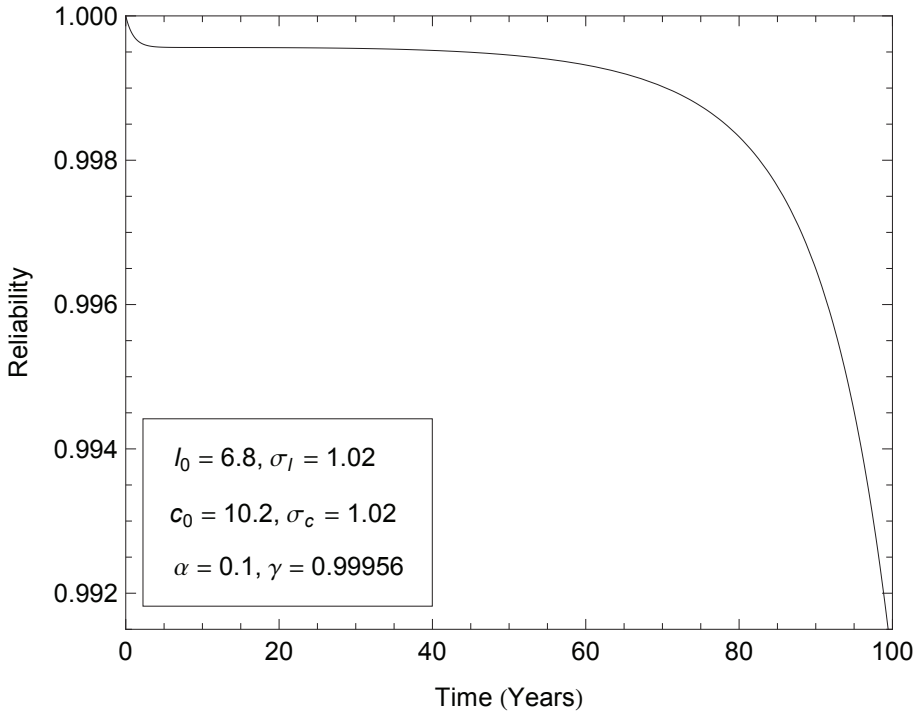

Figure 5.19: Combined Failure Types I and III: Reliability vs. Time.

5.5.2.3 Combined Failure Types I & II

In the absence of aging, infant mortality and Poisson failures occur together. Figure 5.20 shows the script program written using the MAPLE software to generate the graphs in Figure 5.21. By setting $c(t) = c_0$ in Eqs. 5.28 and 5.29, we produce the graphs in Figure 5.21. As the graphs show, failure rates are decreasing with time. The larger the coefficient of variations of capacity, the larger the failure rate becomes. As Figure 5.21 indicates γ is the homogeneous Poisson process intensity for load application with the assumed value of 0.99956, c_0 is the initial capacity with the value of 10.2, σ_l is the standard deviation of the load with the assumed value of 1.02, α is a constant with the assumed value of 0.1 and l_0 is the initial load with the assumed value 6.8.

```
LT := proc( l_0, sigma_l, c_0, sigma_c, alpha, gamma )
    global A, B, t, At, Bt, l, points1, p1 :

    A := A := int(exp( - (c-c_0)^2 / (2 * (sigma_c)^2) ) / sqrt(2 * Pi) * int(exp( - (l-l_0)^2 / (2
      * (sigma_l)^2) ) / sqr
    t(2 * Pi) * exp( - gamma * int(1, td = 0 ..t) * int(exp( - (l-l_0)^2 / (2 * (sigma_l)^2) ) / sqrt(2 * Pi), l
      = c ..inf
    inity) ), l = c ..infinity), c = 0 ..infinity);
    B := int(exp( - (c-c_0)^2 / (2 * (sigma_c)^2) ) / sqrt(2 * Pi) * exp( - gamma * int(1, td = 0 ..t)
      * int(exp( - (l - l
    _0)^2 / (2 * (sigma_l)^2) ) / sqrt(2 * Pi), l = c ..infinity) ), c = 0 ..infinity);

      for t from 0 by 5 to 100 do
        At := evalf (A) : Bt := evalf (B) : l[t] := (At/Bt);
      end do:

    points1 := {seq( [t, l[t]], t = 0 ..100, 5 ) };
    plots:-pointplot(points1, connect = true, view = [0 ..100, 0 ..0.01 ]);
end proc:
```

Figure 5.20: Script Program Used to Generate the Graphs in Figure 5.21.

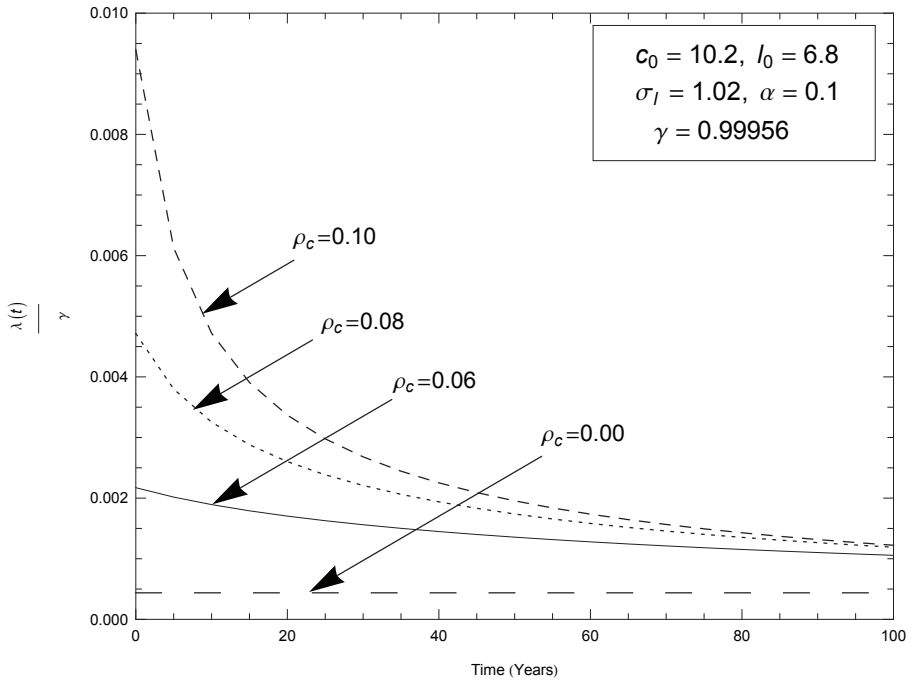

Figure 5.21: Combined Failure Types I and II: Failure Rate vs. Time for Four Separate Coefficients of Variation Values of Capacity.

5.5.2.4 Combined Failure Types I, II and III

This final case represents the most general case for time variant reliability based on repetitive loading and three periods of failure. In this case, all three failure types are

present. The script program shown in Figure 5.22 is written by using Eq. 5.29 and the the MAPLE software to generate the graph in Figure 5.24. The script shown in Figure 5.23 is written by using Eq. 5.28 and the MAPLE software to generate the graph in 5.25. When all failure types are present, we were able to plot the bathtub curve as shown in Figure 5.24. The graphs in Figure 5.26 display curves for various combinations of failure modes. As Figures 5.24 and 5.25 indicate γ is the homogeneous Poisson process intensity for load application with the assumed value of 0.99956, c_0 is the initial capacity with the assumed value of 10.2, σ_l is the standard deviation of the load with the assumed value of 1.02, α is a constant with the assumed value of 0.1 and l_0 is the initial load with the assumed value 6.8.

```
mode := module( )
    option package;
    global f1, f2, f3, f4, At1, Bt1, t, l1, points1, points2, p2, p1 :
    global P1, P2 :
    export lambda;

      lambda := proc(Cobar, sigmaC, lbar, sigmal, gamma)
     f1 := (1/sqrt(2*Pi))*exp(-(Co-Cobar)^2/(2*(sigmaC)^2)) :
     f2 := (1/sqrt(2*Pi))*exp(-(l-lbar)^2/(2*(sigmal)^2)) :
     f3 := exp(-gamma*int(1, td=0..t)*int(f2, l=Co-0.1*Co*(gamma*t/100)^4..infinity)) :
     f4 := int(f2, l=Co-0.1*Co*(gamma*t/100)^4..infinity) :
     P1 := f1*f4*f3 :
     P2 := f1*f3 :

    for t from 0 by 5 to 140 do
     At1[t] := evalf(int(P1, Co=0..infinity)) :
     Bt1[t] := evalf(int(P2, Co=0..infinity)) :
     l1[t] := (At1[t]/Bt1[t]);

    end do:

     points1 := {seq([t, l1[t]], t=0..100, 5)} :
     p1 := pointplot(points1, connect=true, view=[0..100, 0..0.01]) :
     plots:-display([p1], axes=boxed);

    end proc:
end module:
```

Figure 5.22: Script Program Used to Generate the Graph in Figure 5.24.

```
mode := module( )
    option package;
    global f1, f2, f3, Bt1, t, l1, points1, points2, p2, p1 :
    global P2 :
    export R;

      R := proc(Cobar, sigmaC, lbar, sigmal, gamma)
      f1 := (1/sqrt(2*Pi)) * exp(-(Co-Cobar)^2/(2*(sigmaC)^2)) :
      f2 := (1/sqrt(2*Pi)) * exp(-(l-lbar)^2/(2*(sigmal)^2)) :
      f3 := exp(-gamma * int(1, td=0..t) * int(f2, l=Co..infinity)) :
      P2 := f1*f3 :

    for t from 0 by 5 to 100 do
      Bt1[t] := evalf(int(P2, Co=0..infinity)) :
    end do:

      points1 := {seq([t, Bt1[t]], t=0..100, 5)} :

    end proc:
end module:
```

Figure 5.23: Script Program Used to Generate the Graph in Figure 5.25.

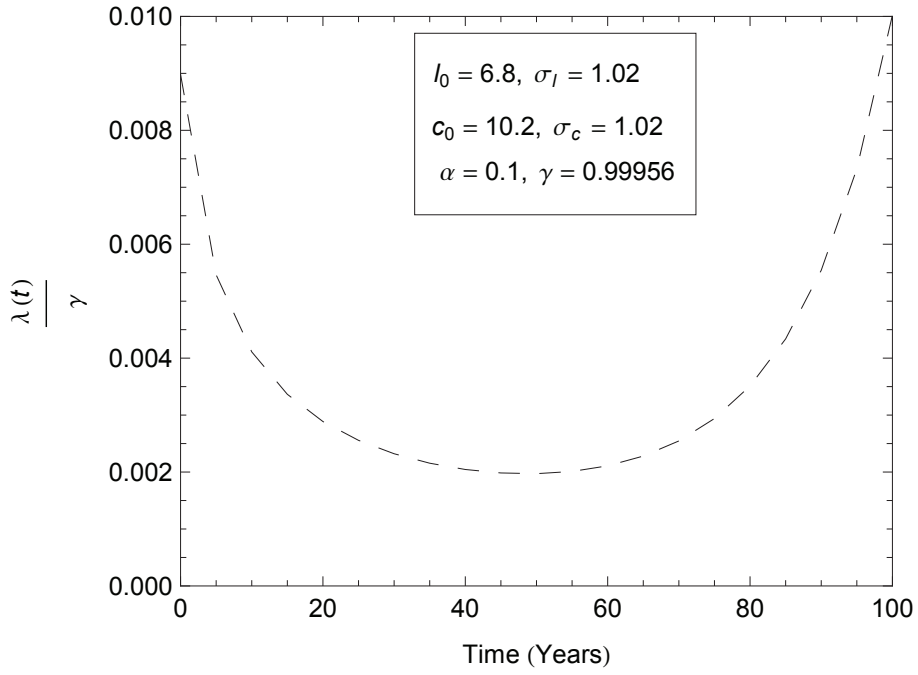

Figure 5.24: Combined Failure Types I, II, III (Bathtub Curve): Failure Rate vs Time.

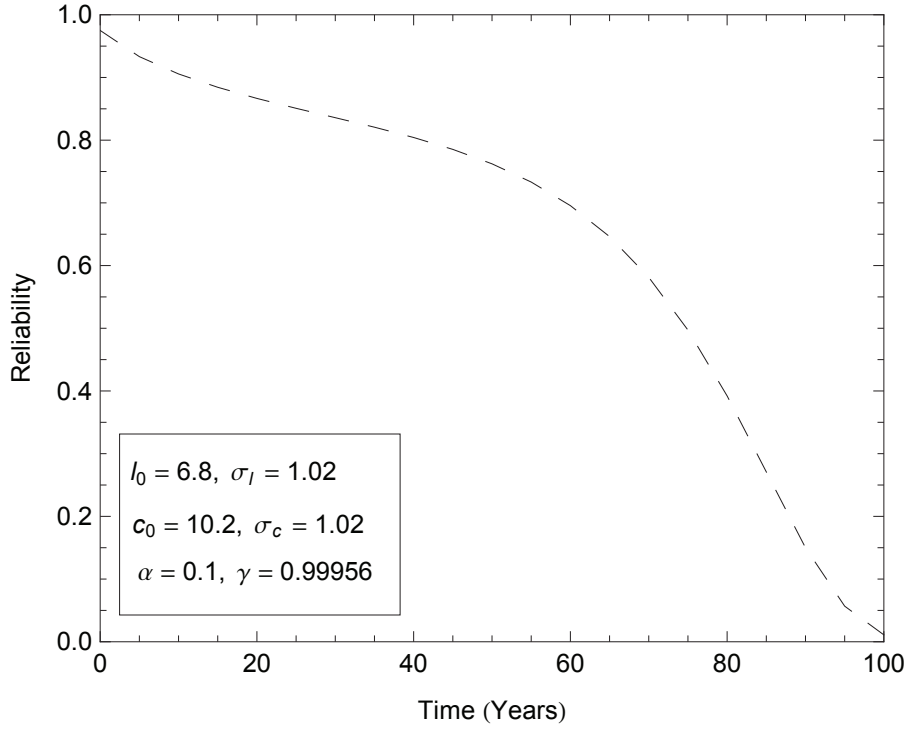

Figure 5.25: Combined Failure Types I, II, III: Reliability vs Time.

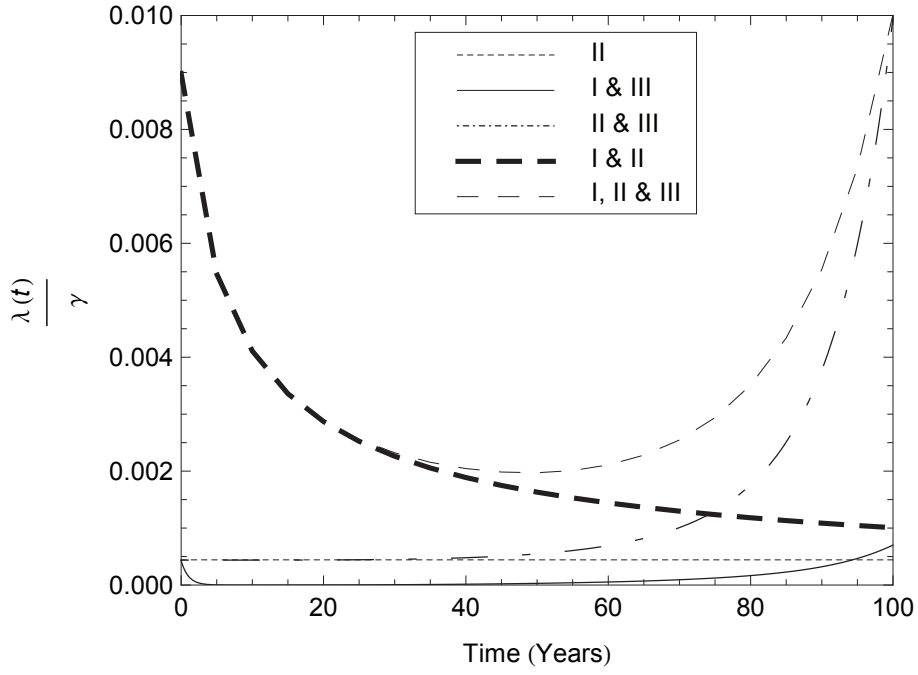

Figure 5.26: Various Combinations of Failure Types and the Bathtub Curve (I, II & III): Failure Rate vs Time.

5.6 Time Dependent Reliability Formulation Based on Stochastic Load model (Two Independent Poisson Load Processes) and Random Strength Degradation Function

In this section, an alternative approach for time dependent reliability formulation is presented based on the woks of Ellingwood and Mori (1993). Resistance of a structural component and the applied load on it vary in time, making structural reliability time dependent. Structural safety under a single load can be calculated as follows (Thoft-Christensen & Baker, 1982):

$$P_s = P(R > S) = \int_0^\infty F_s(r) f_R(r) dr \tag{5.32}$$

where $F_s(r)$ is the CDF of the structural action due to applied load and $f_R(r)$ is the PDF resistance of the structural component. The reliability function is the probability that the structural component survives during a desired time interval (0,t_L):

$$\begin{aligned} R(t_L) &= P(S_1 < r \cap ... \cap S_n < r) \\ &= P(S_1 < r)...(S_n < r) \end{aligned} \tag{5.33}$$

where S_n is the random load intensity. If random load intensities are identically distributed, the equation above can be written as follows:

$$R(t_L) = [F_S(r)]^n \tag{5.34}$$

Strength of the component may deteriorate in time due to environmental stressors. The time dependent resistance (i.e. deterioration) of a bridge component as a function can be modeled as the product of initial resistance and degradation function as follows:

$$r(t) = r_0.g(t) \tag{5.35}$$

where r_0 is the initial resistance, and $g(t)$ is the degradation function. The following

formula can be used for deterioration due to corrosion, sulfate attack and similar environmental effects. However, it does not apply to fatigue. The formulation that follow are adopted from Ellingwood and Mori (1993).

If n events occur within time interval $(0, t_L)$ at deterministic times t_j. $j = 1, ..., n$, we substitute Eq. 5.35 into 5.33:

$$R(t_L) = F_{S_1}(r(t))...F_{S_n}(r(t)) \tag{5.36}$$

thus,

$$R(t_L) = \prod_{j=1}^{n} F_S(r.g_j) \tag{5.37}$$

where $g_j = g(t_j)$ and $t_1 < t_2 < ... < t_n$. In general, loads occur randomly at times $T = T_1, ..., T_n$. These random times can be described by the joint PDF $f_T(t)$. As a result, Eq. 5.36 becomes:

$$R(t_L) = \int_{t_n-1}^{t_L} ... \int_{0}^{t_L} \left[\prod_{j=1}^{n} F_S(r.g_j) \right] f_T(t)dt \tag{5.38}$$

where n is the number of load events occurring within time interval $(0, t_L]$ which is described by the Poisson process. Occurrence times of these load events T are the n order statistic of the random variable $T^* = T_1^*, ..., T_n^*$, which are uniformly distributed.

Since the intensities of the loads are statistically independent and identically distributed, Eq. 5.37 can be written as follows:

$$\prod_{j=1}^{n} F_S \left\{ r.g(T_j) \right\} = \prod_{k=1}^{n} F_S \left\{ r.g(T_k^*) \right\} \tag{5.39}$$

where T_j is the random occurrence times of n events, and T_k^* is the n-order statistics of the random variable T^*.

Joint PDF of T^* given that n events occur within time interval $(0, t_L)$ is:

$$f_{T^*}(t*) = \left(\frac{1}{t_L}\right)^n \tag{5.40}$$

Eq. 5.38 also can be written in terms of T^* as follows:

$$R(t_L) = \int_0^{t_L} ... \int_0^{t_L} \left[\prod_{k=1}^{n} F_S(r.g(T_k^*))\right] f_T^*(t^*)dt^* \tag{5.41}$$

The above equation can be written as follows:

$$R(t_L) = \left[\int_0^{t_L} F_S\left\{r.g(t)\right\} \frac{1}{t_L} dt\right]^n \tag{5.42}$$

The conditioning on the number of load events n within time interval $(0, t_L)$ is removed, this removal is performed by using the Maclaurin Series expansion with the occurrence of load events modeled as Poisson process:

$$R(t_L) = \sum_{n=0}^{\infty} \left[\int_0^{t_L} F_S\left\{r.g(t)\right\} \frac{1}{t_L} dt\right]^n \times \frac{(\lambda t_L)^n e^{-\lambda t_L}}{n!} \tag{5.43}$$

By assuming $p = \int_0^{t_L} F_S\left\{r.g(t)\right\} \frac{1}{t_L} dt$ and $c = (\lambda t_L)^n$, the above equation becomes:

$$\begin{aligned} R(t_L) &= \sum_{n=0}^{\infty} p^n \frac{c^n e^{-c}}{n!} \\ &= e^{-c} \sum_{n=0}^{\infty} \frac{c^n p^n}{n!} \\ &= e^{-c} \sum_{n=0}^{\infty} \frac{(cp)^n}{n!} \end{aligned} \tag{5.44}$$

By using Maclaurin Series:

$$\begin{aligned} e^x &= 1 + \frac{x}{1!} + \frac{x^2}{2!} + ... + x^n n! + ... \\ &= \sum_{n=0}^{\infty} \frac{x^n}{n!} \end{aligned} \tag{5.45}$$

Therefore,

$$e^{cp} = \sum_{n=0}^{\infty} \frac{(cp)^n}{n!} \tag{5.46}$$

By using Eq. 5.46 in Eq. 5.44, the reliability regarding c and p is:

$$\begin{aligned} R(t_L) &= e^{-c} e^{cp} \\ &= e^{-c(1-p)} \end{aligned} \tag{5.47}$$

Therefore, Eq. 5.43 becomes:

$$R(t_L) = e^{-\lambda t_L \left[1 - \frac{1}{t_L} \int_0^{t_L} F_S\{r.g(t)\} dt\right]} \tag{5.48}$$

Moreover, the conditioning on the initial strength is removed in order to take into account the randomness in initial strength as follows:

$$R(t_L) = \int_0^{\infty} e^{-\lambda t_L \left[1 - \frac{1}{t_L} \int_0^{t_L} F_S\{r.g(t)\} dt\right]} \times f_{R_0}(r) dr \tag{5.49}$$

where $f_{R_0}(r)$ is the PDF of the initial strength R_0.

When a component is subjected to two statistically independent load processes S_1 and S_2, only S_1 is time dependent. Then,

$$\begin{aligned} R(t_L) &= P(S_r < r) \\ &= P(S_1 + S_2 < r) \\ &= P(S_1 < r - S_2) \\ &= F_{S_1}(r - S_2) \end{aligned} \tag{5.50}$$

By using the law of total probability, Eq. 5.49 becomes:

$$R(t_L) = \int_0^{\infty} \int_0^{\infty} e^{-\lambda t_L \left[1 - \frac{1}{t_L} \int_0^{t_L} F_{S_1}\{r.g(t) - s_2\} dt\right]} \times f_{S_2}(s_2) f_{R_0}(r) ds_2 dr \tag{5.51}$$

Based on these formulations, the probability of failure and the reliability for various cases are investigated. In all the cases, the following assumptions are used:

- It is assumed that $V_D = 0$, which means that the coefficient of variation for dead load is zero. Therefore, Eq. 5.49 is used, in which $F_S\{r.g(t)\}$ is replaced by $F_L\{r.g(t) - \mu_D\}$.
- Linear degradation model is used ($g(t) = 1 - at$).
- $g(40) = 0.8$ which means that 80 percent of the initial strength remains at 40 year.

Ellingwood and Mori (1993) used a large volume of statistical data to obtain the means, coefficients of variation, and PDFs of the resistance with respect to common design limit states of several concrete structural components found in nuclear power plants. To obtain the resistance statistics, it was assumed that the rate of the applied load to the component is relatively slow, levels of on-site quality control that are typical of those found nuclear plant construction sites coincide with variabilities in material properties and dimensions, and long-term strength deterioration in concrete or steel are ignored.

Coefficient of variation values of resistance based on the statistical data were selected as 0.13, 0.18 and 0.14 for beam or slab flexure, beam shear, short wall shear, and short column compression, respectively. However, they used 0.15 as the initial coefficient of variation of resistance in their study which happens to be the average of these three values. In order to investigate the effect of the variation of resistance on the component reliability, the value of initial V_R was increased by 20% and 60%. Therefore, three different values of coefficient of variation (0.15, 0.18, 0.24) resistance were used in their study.

Based on analysis results of a survey on nuclear power plants, coefficient of variation values of various loads were also obtained by Ellingwood and Mori (1993). These coefficient of variation values are for the dead load (C.O.V = 0.07), equipment load (C.O.V = 0.04), accidental pressure load (C.O.V= 0.20), accidental temperature load (C.O.V=0.08). The other coefficient of variation value for the live load is 0.50. They used 0.50 the initial coefficient of variation of resistance in their study. In order to investigate the effect of the variation of the load on the component reliability, the value of initial V_L was increased by 20% and 60%. Therefore, three different values

of the coefficient of variation (0.5, 0.6, 0.8) for the live load were used in their study.

It is important to consider that there are remarkable uncertainties in these estimates since in some cases they are based on a few responses. Therefore, in this part of thesis, different values for the load occurrence rate, the coefficient of variation of the strength and live load from Ellingwood and Mori (1993)'s investigation are used to investigate the effects of mentioned parameters on the reliability of a component.

Furthermore, a script program is written based on these formulations and using the MAPLE software to generate the upcoming graphs (Figures 5.28 and 5.29).

```
MyModn := module( )
  option package;
  global a, g, j, f1, f2, f21, f3, f4, zx, tl, xc, points1, p1, p, R, Pf, points :
  export c2f;
  c2f := proc(muR, sigmaR, muL, sigmaL, muD, lambda)
  Digits := 14 :
  with(plots) :
  f1 := (1 / (r* sigmaR * sqrt(2 * Pi))) * exp( - (ln(r) - muR)^2 / (2 * sigmaR^2));
  f2 := exp( - (l - muL)^2 / (2 * sigmaL^2)) / (sigmaL * sqrt(2 * Pi));
  f21 := int( f2, l = 0 ..r* (1 - (t - 30) / 200) - muD);
  f3 := int( f21, t = 0 ..tl);
  f4 := exp( - lambda * (tl - f3));
  zx := f1 * f4;

  for tl from 0 by 5 to 100 do xc[tl] := evalf(zx) :
    R[tl] := evalf[18](Int(xc[tl], r = 0 ..infinity, method = _Dexp, epsilon = 10^( - 10))) :
    print(R[tl]);
    Pf[tl] := 1 - R[tl] :
    print("Pf" = Pf[tl]);
  end do;

  points := {seq([tl, Pf[tl]], tl = 0 ..100, 5)} :
  p1 := pointplot(points, connect = true, view = [0 ..100, 0 ..0.018]) :
  display([p1], axes = boxed) :

end proc:end module:
```

Figure 5.27: Script Program Used to Generate the Graph in Section 5.6.

In the first case, the effect of load occurrence rate λ on the probability of failure and reliability is studied. Three different values for load occurrence rate are used where the coefficient of variation for resistance is assumed to be 0.10 ($V_R = 0.10$), and the coefficient of variation for the live load is assumed to be 0.17 ($V_L = 0.17$) which is the average of five different load types of Ellingwood and Mori. The graphs in the Figures 5.28 and 5.29 show the time variant probability of failure and the reliability for three different load occurrence rates. As the graphs in Figure 5.28 show, the highest graph

belongs to the highest value of λ, and the lowest graph belongs to the lowest value of λ. As the graphs in Figure 5.29 show, the highest time variant reliability belongs to the lowest value of λ, and the lowest time variant reliability belongs to the highest value of λ. This means that for the larger value of λ , the probability of failure will be larger and the reliability will be lower.

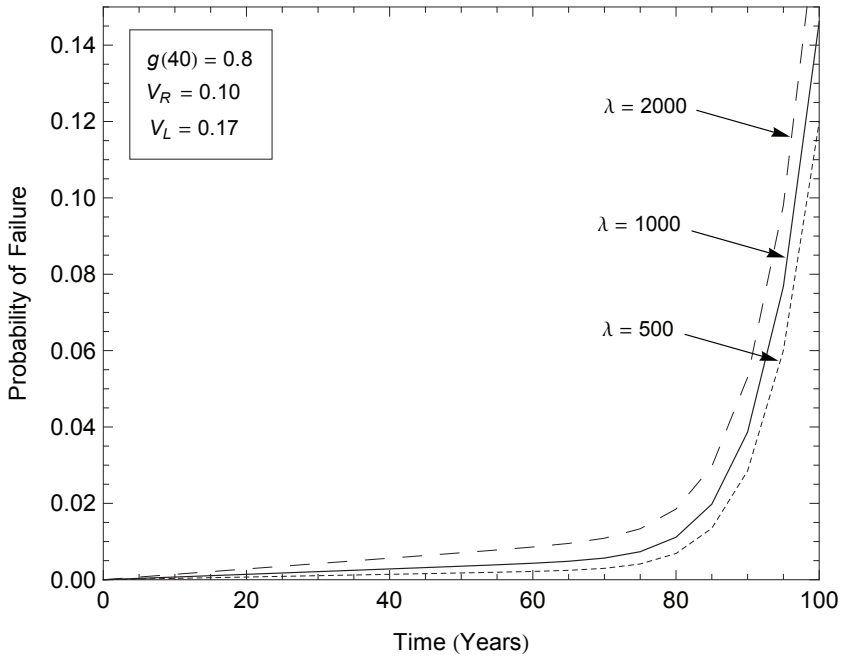

Figure 5.28: Probability of Failure vs. Time for Three Different Values for the Load Occurrence Rate.

In the second case, the effect of the live load V_L on the probability of failure and reliability is studied (Ellingwood & Mori, 1993). To this end, three separate values for the coefficient of variation of live load are used, the coefficient of variation for resistance is assumed to be 0.10 ($V_R = 0.10$), and the load occurrence rate λ is assumed to be 1000. The graphs in the Figures 5.30 and 5.31 show the time variant probability of failure and reliability for three different coefficient of variation values of the live load, respectively. As the graphs in Figure 5.30 show, the highest graph belongs to the highest value of V_L, and the lowest graph belongs to the lowest value of V_L. And as the graphs in Figure 5.31 show, the highest graph belongs to the lowest value of $_L$, and the lowest graph belongs to the highest value of V_L. This means that for the higher values of V_L , the probability of failure will be higher and the reliability will be lower.

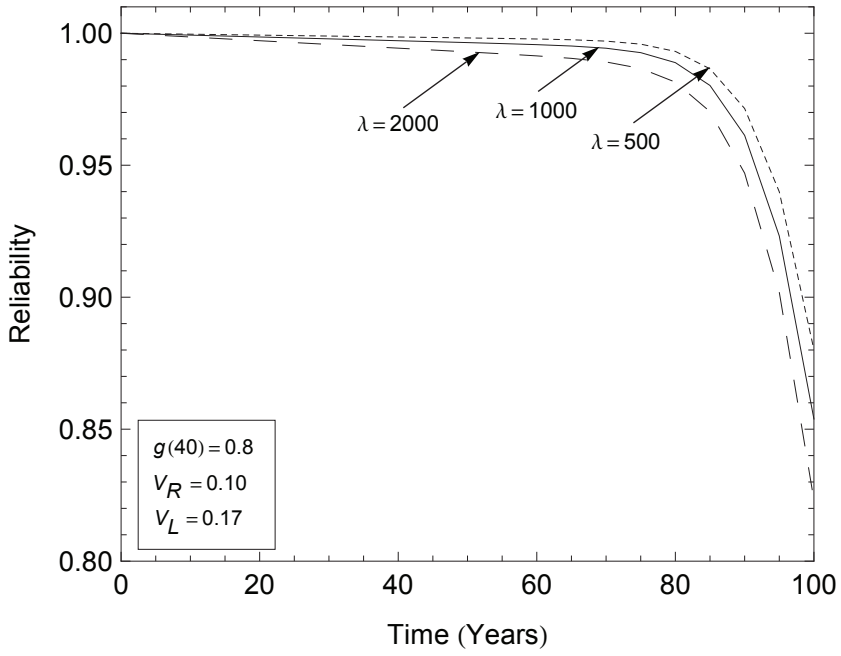

Figure 5.29: Reliability vs. Time for Three Different Values for the Load Occurrence Rate.

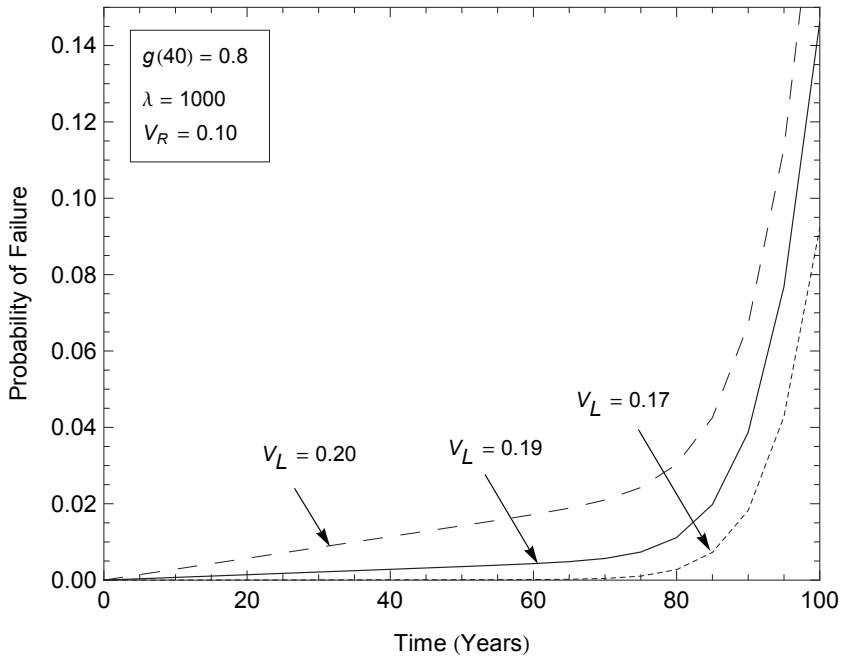

Figure 5.30: Probability of Failure vs. Time for Three Different Values for Coefficient of Variation of the Live Load.

In the third case, the effect of component strength V_R on the probability of failure and reliability is studied (Ellingwood & Mori, 1993). To this end, three different values

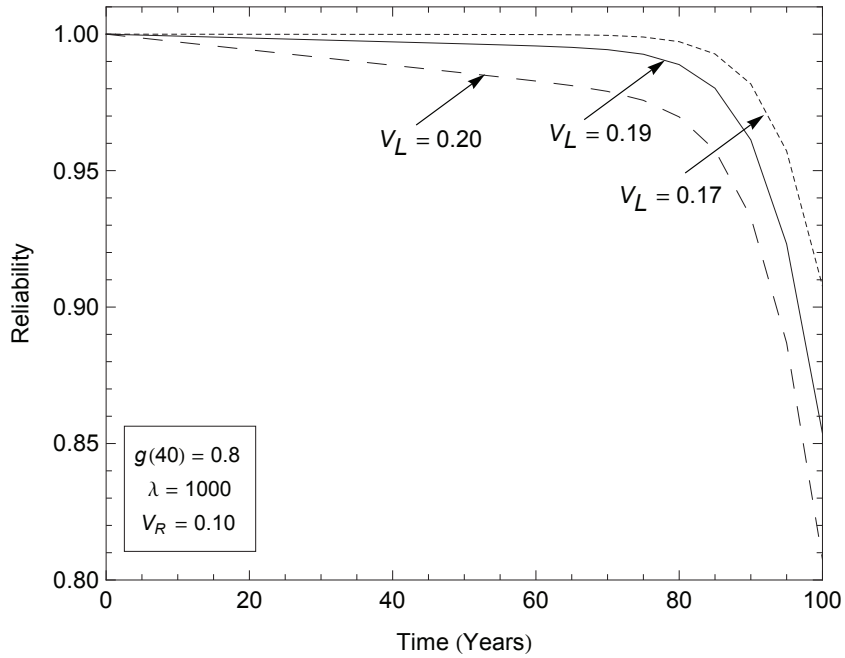

Figure 5.31: Reliability vs. Time for Three Different Values for the Coefficient of Variation of the Live Load.

for the coefficient of variation of the strength are used, the coefficient of variation for the live load is assumed to be 0.17 ($V_L = 0.17$), and the load occurrence rate λ is assumed to be 1000. The graphs in the Figures 5.32 and 5.33 show the time variant probability of failure and reliability for three different coefficient of variation values of strength, respectively. As the graphs in Figure 5.32 show, the highest graph belongs to the highest value of V_R, and the lowest graph belongs to the lowest value of V_R. Similarly, as the graphs in Figure 5.33 show, the highest graph belongs to the lowest value of V_R, and the lowest graph belongs to the highest value of V_R. This means that for the higher value of V_R , the probability of failure will be higher and the reliability will be lower.

In the last case, the effect of degradation time t_0 is studied (Ellingwood & Mori, 1993). A linear strength degradation model by taking into account t_0 is used as follows:

$$g(t, t_0) = 1 - a(t - t_0) \tag{5.52}$$

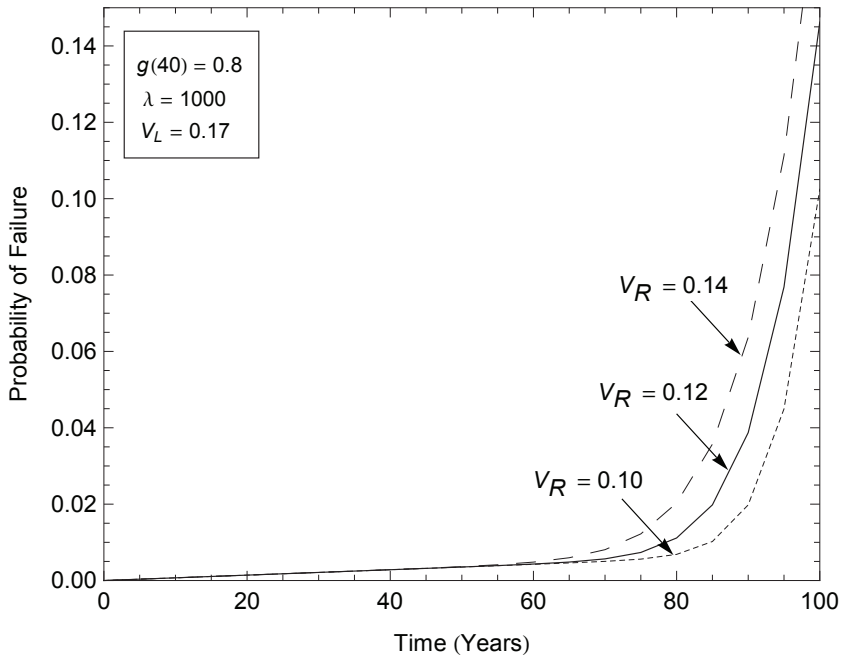

Figure 5.32: Probability of Failure vs. Time for Three Different Values for the Coefficient of Variation of Strength.

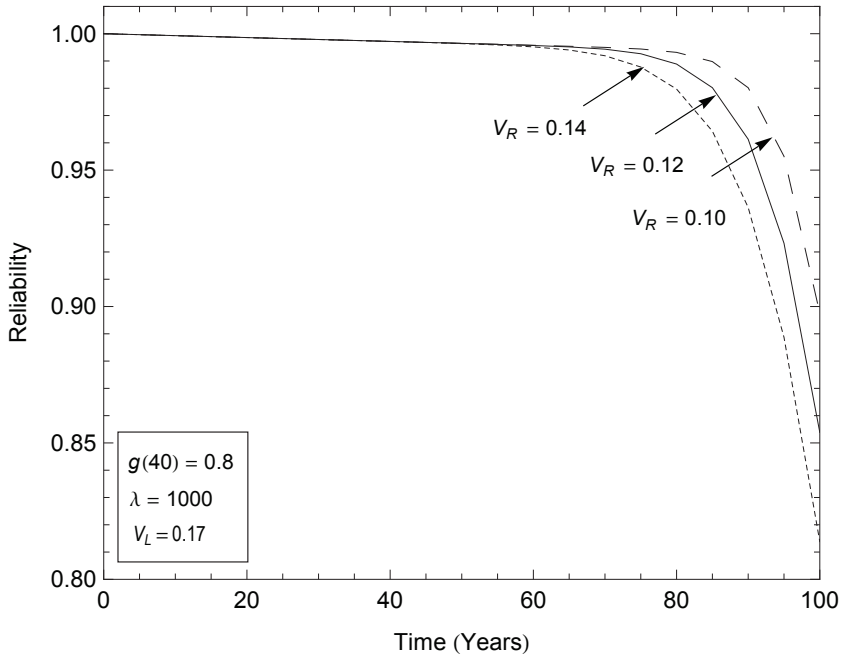

Figure 5.33: Reliability vs. Time for Three Different Values for the Coefficient of Variation of Strength.

To this end, four different values for degradation time t_0 are used, the coefficient of variation for resistance is assumed to be 0.10 ($V_R = 0.10$), and the coefficient of

variation for the live load is assumed to be 0.17 ($V_L = 0.17$). The graphs in the Figures 5.34 and 5.35 show the time variant probability of failure and reliability for four different degradation times respectively. As the graphs in Figure 5.34 show, the highest graph belongs to the lowest value of t_0, and the lowest graph belongs to the highest value of t_0. Similarly, as the graphs in Figure 5.35 show, the highest graph belongs to the highest value of t_0, and the lowest graph belongs to the lowest value of t_0. This means that for the higher values of t_0, the time variant probability of failure will be lower and the reliability will be higher.

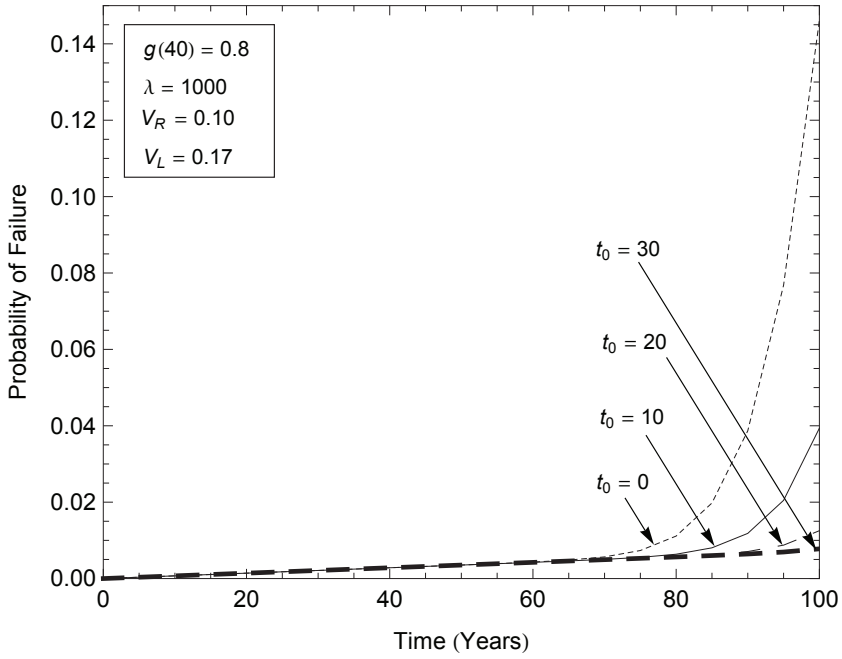

Figure 5.34: Probability of Failure vs. Time for Four Different Values of Degradation Time.

5.7 Formulation Based on Load and Capacity

In addition to different approaches of time variant formulations for reliability presented in sections 5.2 through 5.6, time variant reliability can also be obtained in a discretized way based on the FORM technique. If we assume that the load and capacity of a structural component are normally distributed, capacity may be assumed to be changing by time based on a relationship such as the one given below:

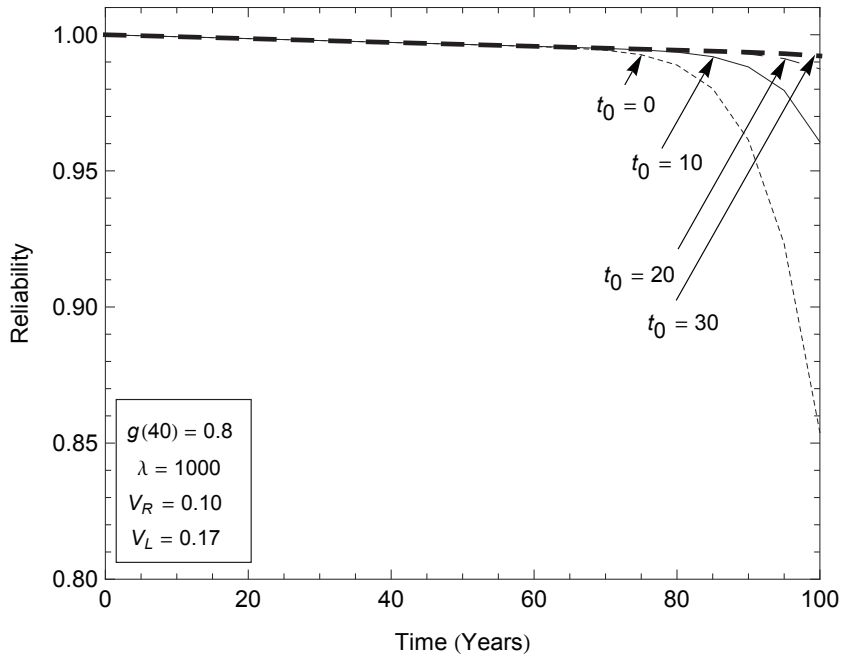

Figure 5.35: Reliability vs. Time for Three Various Values of Degradation Time.

$$c(t) = c_0(1 - 0.0018t - 0.00001t^2) \tag{5.53}$$

With this assumption, time variant reliability can be calculated by using a computer algorithm developed in this study, The flowchart of time variant reliability calculation using the convolution integral presented in Section 4.2 (Eq. 4.13) is shown in Figure 5.36, where the values for reliability are obtained for time interval between 0 and 100 years. As the time variant reliability graph in Figure 5.37 shows, aging of the structure is associated with deterioration of capacity. In Figure 5.37, the convolution integral and the traffic spray damage deterioration model are used to calculate the time variant reliability, where μ_c with the assumed value of 5 is the mean value of capacity, σc with the assumed value of 0.5 is the standard deviation of the capacity, μ_l with the assumed value of 3 is the mean value of the load, and σ_l with the assumed value of 0.3 is the standard deviation of the load.

Also in Figure 5.38, normal distribution of capacity and load for assumed mean values are plotted vertically showing the capacity deterioration and the mean load at ten year intervals.

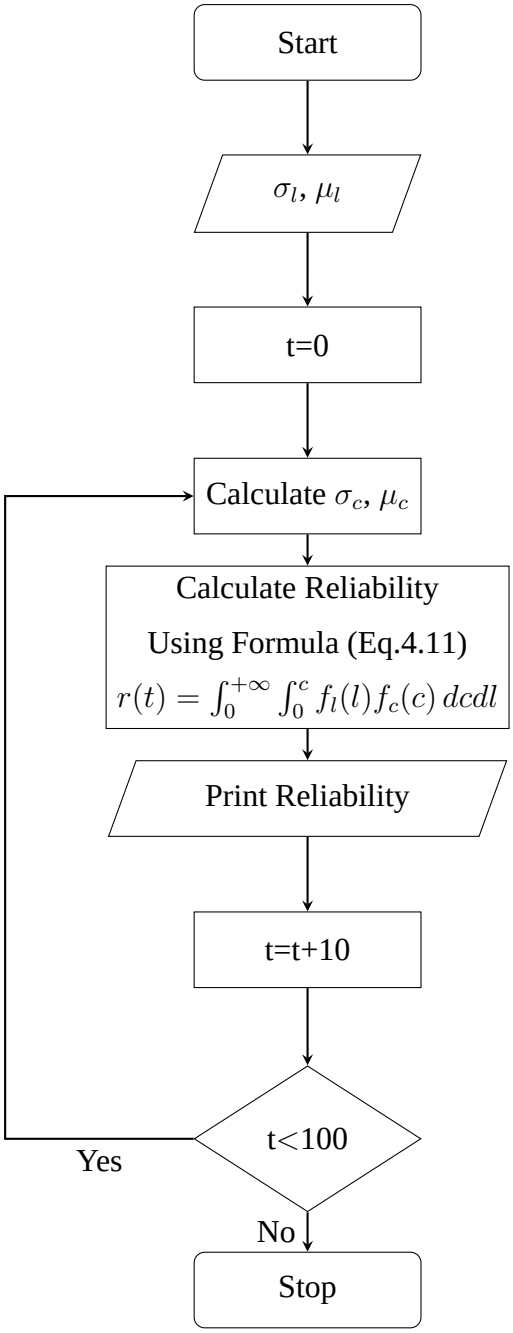

Figure 5.36: Flowchart for Calculating the Time Variant Reliability Using the Convolution Integral.

5.8 Condition Deterioration Models

In order to obtain realistic results from a time variant reliability analysis, the analysis must be based on a so-called condition deterioration model. Bridges deteriorate due to the effects of aging, live loads, corrosion, environmental factors, fatigue, among

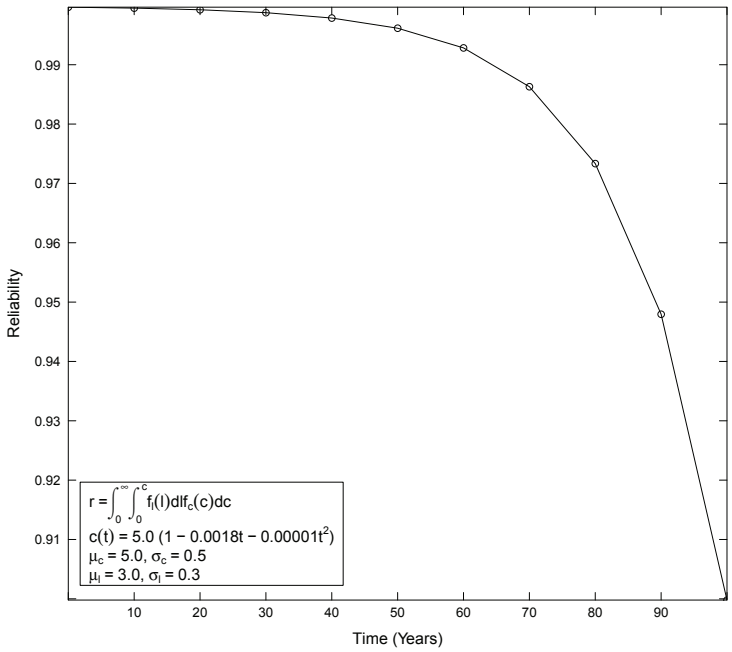

Figure 5.37: Reliability vs. Time by Using the Convolution Integral.

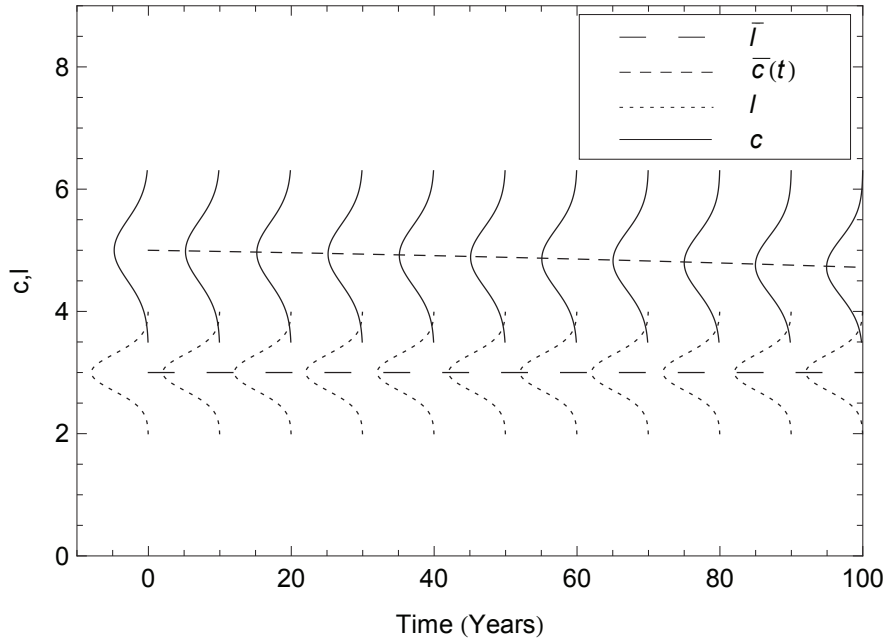

Figure 5.38: Capacity and Load Distributions vs Time Displaying Time Variant Capacity Deterioration.

many other causes. To study these phenomena, there have been various studies in the past to obtain deterioration models since 1965. These research studies can be classified into different groups based on the methods used.

Barkiw et al. (1965), Golabi et al. (1992), Hawk (1995), Ng and Moses (1999), Hearn (2000), Bruhwiler et al. (2001), and Frangopol and Liu (2005) used Markov chain or semi-Markov process in their models. Markov chain is used in Barkiw et al's model because it gives the opportunity of describing the complete system in case there is an approximately exponential failure law. Moreover, it can be considered the stochastic as past history has no predictive value, a property which is regarded a liability. Semi-Markov process is also defined in this model to represent the transitions between states that take place only at certain times. Similarly, Hawk used Markov chain to model bridge element deterioration in BRIDGIT (a bridge management system used in the U.S.) and obtained the following Markovian transition probability matrix relationship:

$$\frac{NEWQUAN}{TOTQUAN} = [P]^Y [\frac{QUAN}{TOTQUAN} \tag{5.54}$$

where NEWQUAN is the quantity of elements in state i in Y years, TOTQUAN is the total quantity of an element, QUAN is the quantity of the elements in state i ($1 \leq i \leq 5$) at the beginning of the year of the analysis, and P_{ii} is the probability that a quantity in state i will still remain in that state one year later.

Ng and Moses (1999) also proposed the application of a semi-Markov model in which transitions from one state i to another state j are controlled by the transition probabilities P_{ij} while the duration in state i prior to the transition is controlled by the holding time distribution h_{ij}.

Another feature in using Markov chain introduced by Frangopol and Liu (2005) is that it can be used to model bridge deterioration continuously and/or mechanistically. That is to say, a limited number of previous states are considered in the model and the immediately preceding state is only considered in the one step Markov model. There is consistency in the essential transition matrix prescribing the probabilities of changing from one state to another state throughout the specified time horizon in stationary models. Monte Carlo simulation can be also used to obtain statistical time varying performance profiles of deteriorating structures under maintenance, assuming that there is sufficient available data. Likewise, Hearn (2000) used Markov chain to explain the transition probability P of an element moving to the next condition state

as a function of the time spent in the current state $t_{Resistence}$ as:

$$P = 1 - \frac{1}{t_{Resistence}} \tag{5.55}$$

$$t_{Resistence} = t_{State} + t_{Trans} \tag{5.56}$$

where, t_{State} is the prior time in current state (year), and t_{Trans} is the time left before the transition (year).

Additionally , Golabi et al. (1992), in the Pontis Technical Manual, explained two condition state prediction models. When two consecutive biennial inspection reports are absent, they used the prior model in which probability P_{ij} of transiting from state i to state j in two years is:

$$P_{ij} = 1 - 0.5^{2/T_1} \tag{5.57}$$

where T_1 is the engineer's estimate. When there is statistical data from at least two consecutive inspection reports, they use the posterior model to determine the transition probabilities in the Markov chain by linear regression.

Moreover, Bruhwiler et al. (2001) interpreted the Markovian transition probability matrix based on the Bayesian theorem in two different ways: (1) the percentage of a segment changed from condition state i to condition state j and (2) the probability of a unit quantity of a segment to pass from condition state i to condition state j.

Other methods to obtain a deterioration model are suggested for NBI bridges by Busa et al (1985) and the Pennsylvania Department of Transportation (PennDOT) (1987). In Busa et al.'s model, condition states of the bridge deck, superstructure, and substructure are formulated as a function of bridge age, and traffic value as follows:

$$Deck = 9 - 0.119(AGE) - 2.158 \times 10^{-6}(ADT \times AGE) \tag{5.58}$$

$$Super = 9 - 0.103(AGE) - 1.982 \times 10^{-6}(ADT) \tag{5.59}$$

$$Sub = 9 - 0.105(AGE) - 2.051 \times 10^{-6}(ADT) \tag{5.60}$$

where AGE is the age of the bridge (years), and ADT is the average daily traffic.

Pennsylvania Department of Transportation (PennDOT) model is based on bridge condition ratings (CNR). CNR at equivalent age is:

$$CNR = 9\left(1 - \frac{EQA}{ESL}\right)^{0.7} \tag{5.61}$$

where EQA is the equivalent age of bridge element (years), and ESL=estimated life of bridge element (years).

Miyamaoto (2001) also proposed a model for reinforced-concrete bridges, where bridge age shows up on the abscissa and the mean soundness scores of load-carrying capacity and durability are displayed on the ordinate. In this model, load carrying capacity is defined as:

$$S_L(t) = f_0(t) = b_L - a_L t^4 \tag{5.62}$$

where a_L and b_L are emprical constants, t is the bridge age (years), and $f_0(t)$ is the deterioration function from the beginning of service until the first inspection. Similarly, durability is defined as:

$$S_D(t) = g_0(t) = b_D - a_D t^3 \tag{5.63}$$

where a_D and b_D are emprical constants, t is the bridge age (years), and $g_0(t)$ is the deterioration function from the beginning of service until the first inspection time.

In similar manner, Ellingwood (1998) presented a function for concrete deterioration including the depth of penetration or section loss:

$$X(t) = C(t - t_i)^{\alpha} \tag{5.64}$$

where C is the rate parameter (random variable), α is the time-order parameter, and t_i=induction or initiation period for deterioration process (random variable). C and α are determined by regression analysis of experimental data. Possible values for α's are $\frac{1}{2}$ and 1. For diffusion-controlled processes, such as alkali-aggregate reaction, α's value is $\frac{1}{2}$ and for reaction- controlled one, such as corrosion and sulfate attacks, α's value is 1. In this thesis, Ellingwood's model will be used in Section 5.9.

In order to estimate the lifetime reliability of a short bridge concrete slab when it is subjected to chloride attacks, Thoft-Christensen (1998) introduced a sensitivity factor and determined whether stochastic or deterministic analysis can be used in the modeling. Initially, the physical properties of the structure and the dynamic factors are critical. Considering the estimation of the deterioration in reinforced-concrete decks, Fitch et al. (1995) state that this is a typical combination of a phenomenological model with statistical data obtained from inspection, rehabilitation history, anti-icing needs, and average daily traffic (ADT) in order to estimate the time to rehabilitation (TTR). The formula for the resulting model is as follows:

$$y' = -10.2 + 14.0x - 11.4x^{1.05} \tag{5.65}$$

where y' is the fitted time to rehabilitate decks based on applicable standards, and x is the percentage of deck delaminated, spalled, or patched.

In the snowbelt (a region in the U.S.) the function is modified as follows:

$$y' = -11.2 + 5.34x - 3.41x^{1.1} \tag{5.66}$$

where x is the percentage of the worst traffic lane delaminated, spalled, or patched. The last deterioration model is developed for the reinforced-concrete suggested by Madanat and Lin (2000) in which the authors used a Bayesian method (Yanev, 2007).

5.9 Time Variant Evaluation of Reliability for a Structural Component Based on the FORM Technique

In this thesis, a FORTRAN 95 shell algorithm is developed to calculate the time variant reliability of a component and/or a system by using a core FORM program developed by Estes, A.C. and Frangopol, D.M. (1997). Figures 5.39 and 5.40 show the flowchart of the generated algorithm. The following information explains the variables used in the flowchart.

- t_h = Time horizon
- t_Δ = Time increment
- LNCONV (LogNormal CONVersion) = A subroutine which calculates the parameters of lognormal distribution whenever the resistance is lognormally distributed
- μ_R = Mean value of the resistance
- σ_R = Standard deviation of the resistance
- μ_L = Mean value of the live load
- σ_L = Standard deviation of the live load

Due to variations in resistance and live load, reliability is time variant. The difference between the time variant reliability algorithm developed in this thesis and the one developed by Enright and Frangopol (1998) (i.e. RELTSYS) is that; for a realistic analysis of reliability, in this program five different deterioration models and two different live load models are defined. The user is able to choose which deterioration and live load models to use.

The resistance of a structure deteriorates due to distress mechanism and aging. This time dependent deterioration can be modeled by the use of the resistance degradation function. This can be performed by multiplication of initial resistance by resistance degradation function as follows:

$$R(t) = R_0.g(t) \tag{5.67}$$

In this study, four different degradation functions are used for modeling deterioration. Each degradation function represents a specific degradation mechanism (Norris et al., 1994) as follows:

Eq.5.68 is used to model corrosion mechanism, where a_L is a coefficient that may vary due to the degradation rate.

$$g(t) = 1 - a_L t \tag{5.68}$$

Eq. 5.69 is used to model Sulfate attack mechanism, where a_P is a coefficient that may vary due to the degradation rate.

$$g(t) = 1 - a_P t^2 \tag{5.69}$$

Eq. 5.70 is used to model diffusion controlled degradation mechanism, where a_S is a coefficient that may vary due to the degradation rate.

$$g(t) = 1 - a_S \sqrt{t} \tag{5.70}$$

Eq. 5.71 is used to model traffic spray damage mechanism, where k_1 and k_2 are random variables.

$$g(t) = 1 - k_1 t + k_2 t^2 \tag{5.71}$$

Another deterioration model which is implemented in the developed program is based on the load-carrying capability. This model is as follows:

$$R(t) = R_0 - a_M t^4 \tag{5.72}$$

where R_0 is the initial resistance, and a_M is a constant.

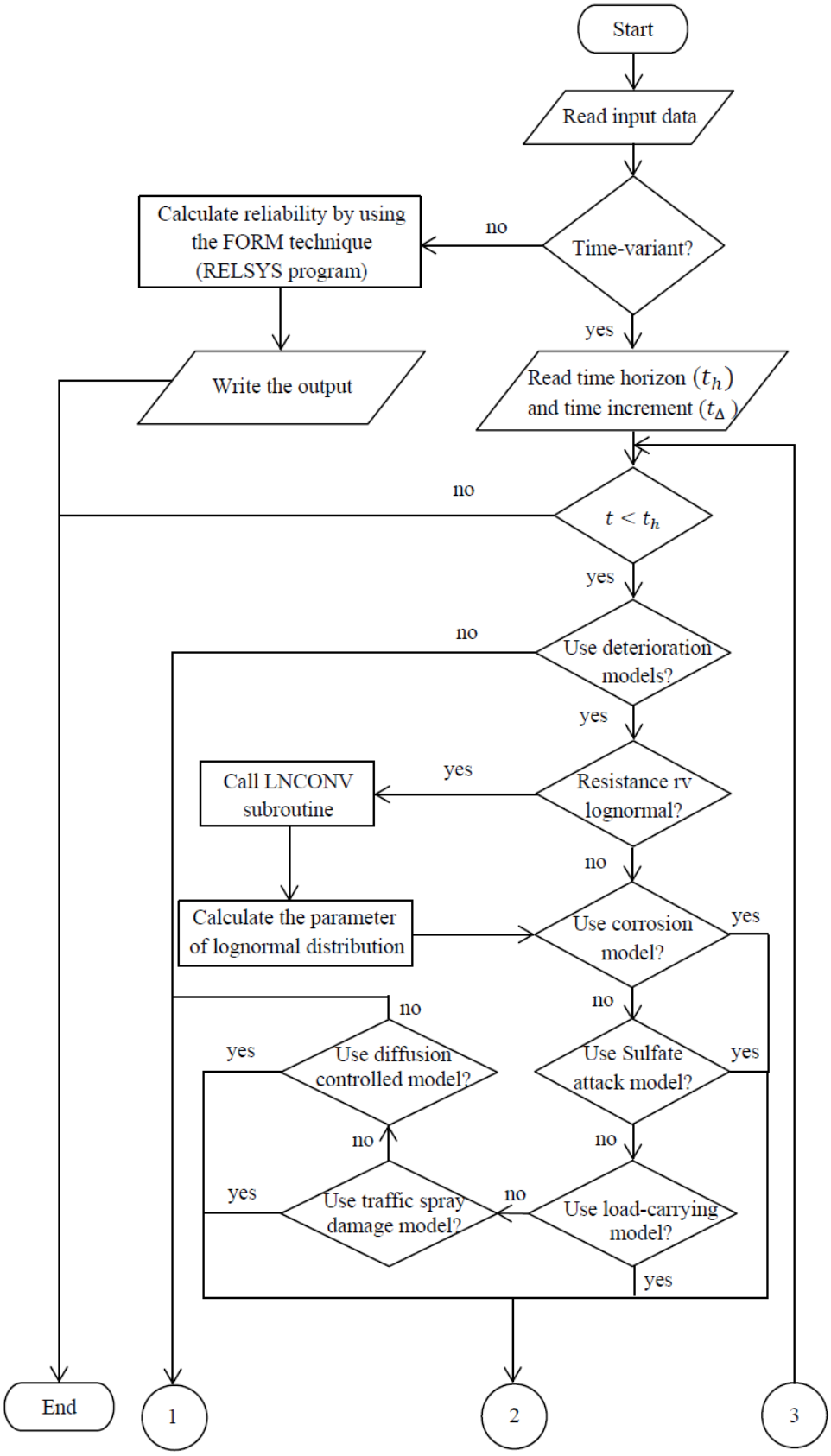

Figure 5.39: Flowchart for Time Variant Reliability Shell Program Using the Core Program RELSYS Based on the FORM Technique (Continued).

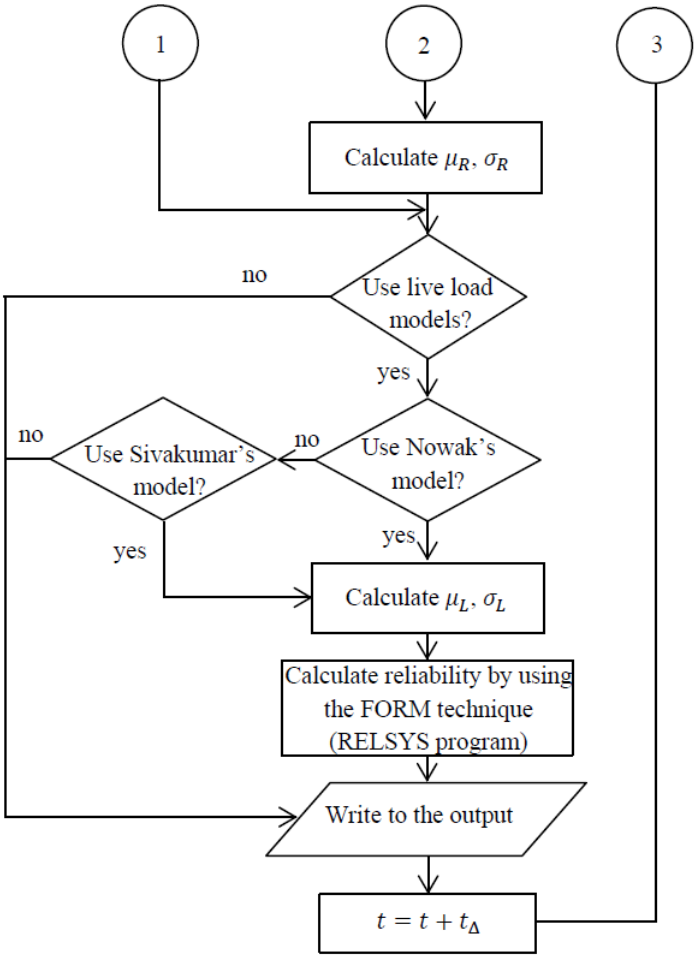

Figure 5.40: Flowchart for Time Variant Reliability Shell Program Using the Core Program RELSYS Based on the FORM Technique.

Figure 5.41 shows the graphs of five different deterioration functions explained above when initial resistance is 1000 for a period of 75 years. In this figure, the deterioration is considered with reference to an assumed residual strength value at 60^{th} year. In other words, $g(60) = 0.85$, refers to 85% of the initial strength remaining at 60 years.

In addition to resistance degradation modeling, the live load effects on the bridge must also be modeled in order to perform a realistic time variant reliability analysis for bridges. Therefore, it is crucial to calculate the maximum number of trucks for a given period of time in order to develop a live load model since such a model is also in direct correlation with the safety of a bridge. To achieve this goal, Nowak's (A. Nowak, 1993) and Sivakumar's (Sivakumar, Ghosn, & Moses, 2008) live load models are used in this thesis.

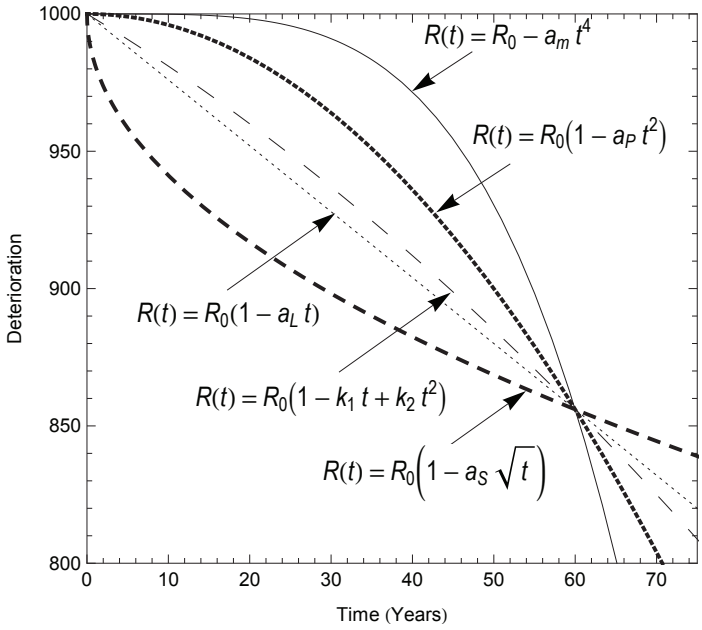

Figure 5.41: Five Different Degradation Functions (Deterioration Models) for Resistance.

In Nowak's model, the CDFs and extrapolation is used in order to project maximum moments and shears for the assigned time periods. To establish the initial lognormal distribution of maximum moment value, A. Nowak (1993) used the obtained mean value and standard deviation due to the fact that the presence of a single truck on the bridge at the initial time is the determining factor. Consequently, the future mean value of the maximum moment is calculated according to the number of actual trucks for a future time. Nowak considered a sample size $n = 300000$ for a year. In this analysis, not only the maximum moment but also the maximum value of the sample size are random variables; therefore, each has its own probability distribution. If the initial distribution is normal or lognormal, when the sample size n is selected as a large number, the initial distribution converges to Gumbel distribution over time. Mean and standard deviation values of the Gumbel distribution in terms of the values of descriptors of the initial distribution are as follows:

$$\mu_t = \mu_0 + \left(u_n + \frac{\gamma}{\alpha_n}\right)\sigma_0 \tag{5.73}$$

$$\mu_t = \left(\frac{\pi}{\sqrt{6}\alpha_n}\right)\sigma_0 \tag{5.74}$$

where $\gamma = 0.5772166$, $\mu_0 =$ initial mean value, $\sigma_0 =$ initial standard deviation, and u_n and α_n are the location and scale parameters. These parameters for an initial normal or lognormal variate can be obtained from the following formulas:

$$u_n = \alpha_n - \frac{1}{2\alpha_n}\left(\ln\left[\ln(n)\right] + \ln(4\pi)\right) \tag{5.75}$$

$$\alpha_n = \sqrt{2\ln(n)} \tag{5.76}$$

In comparison to Nowak's live load model, Sivakumar et al. (2008) proposed a new formulation to analyze the same live load process. In this model, the formulations are more analytic, and they are given as follows:

$$\mu_t = \mu_0 + \sigma_0\sqrt{2\ln(n)} - \frac{\sigma_0\left(\ln(\ln(n)) + \ln(4\pi)\right)}{\sqrt{2\ln(n)}} \tag{5.77}$$

$$\sigma_t = \frac{\sigma_0}{\sqrt{2\ln(n)}} \tag{5.78}$$

In this thesis, first, the traffic spray damage deterioration model and Nowak's live load model are used to calculate the time variant reliability. This is illustrated in Examples 1 through 5. Finally, Example 3 is used to compare the time variant reliability for five different deterioration models and two different live load models.

5.9.1 Example 1: Uncorrelated Normally Distributed Resistance and Load

Let us suppose that the resistance R of a structural component is normally distributed. Likewise, the applied load Q is also assumed to be normal. Then, the limit state function can be written as:

$$g(X) = R - Q \tag{5.79}$$

For this problem, it is assumed that the resistance deteriorates in time and the applied load is changing with respect to the number of trucks in a year. The graphs in Figures

5.42, 5.43, and 5.44 show the time variant reliability index, probability of failure and the reliability, respectively. In Figure 5.42 R and Q are normally distributed with the assumed mean values of 1000 for R and 480 for Q, the assumed standard deviation values of 100 for R and 48 for Q, and m is the number of trucks passing over the bridge per year, which is assumed as 1000. As the graph in Figure 5.42 shows, the value for the reliability index at time $t = 0$ is 4.6879. When t=0, the live load model is not applied yet. After applying the live load model, the reliability index drops drastically within the first year and reaches to 3.5692, whereas after this sudden drop, the reliability index decreases gradually.

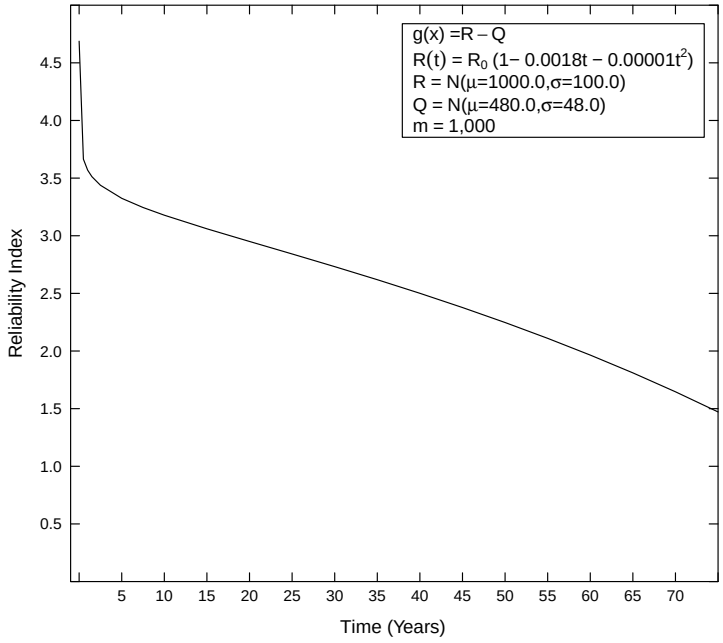

Figure 5.42: Reliability Index vs. Time for the Uncorrelated Normally Distributed Resistance and Load.

5.9.2 Example 2: Uncorrelated Lognormally Distributed Resistance and Load

The problem presented in Example 1 is solved here again. However, this time, the resistance (structural strength) R and the applied load Q are lognormally distributed. The parameters of the lognormal distribution (λ, ν) are calculated using Eqs. 5.80 and 5.81 below.

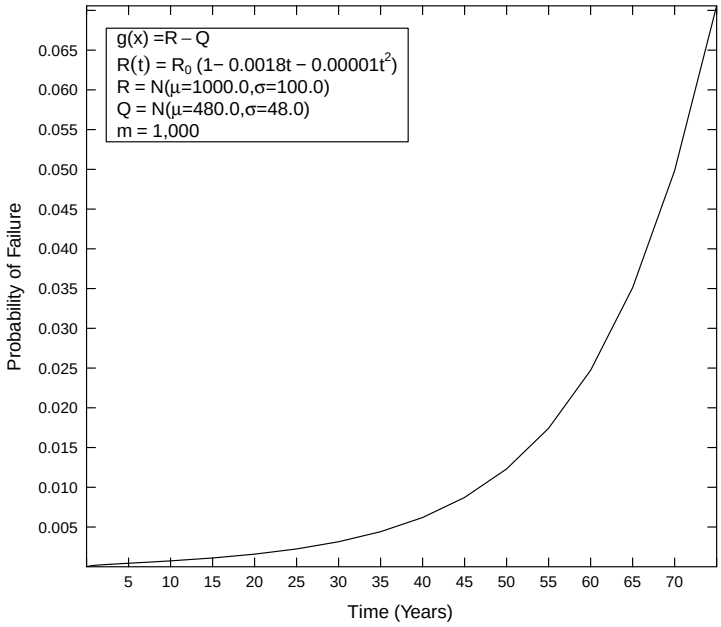

Figure 5.43: Probability of Failure vs. Time for the Uncorrelated Normally Distributed Resistance and Load.

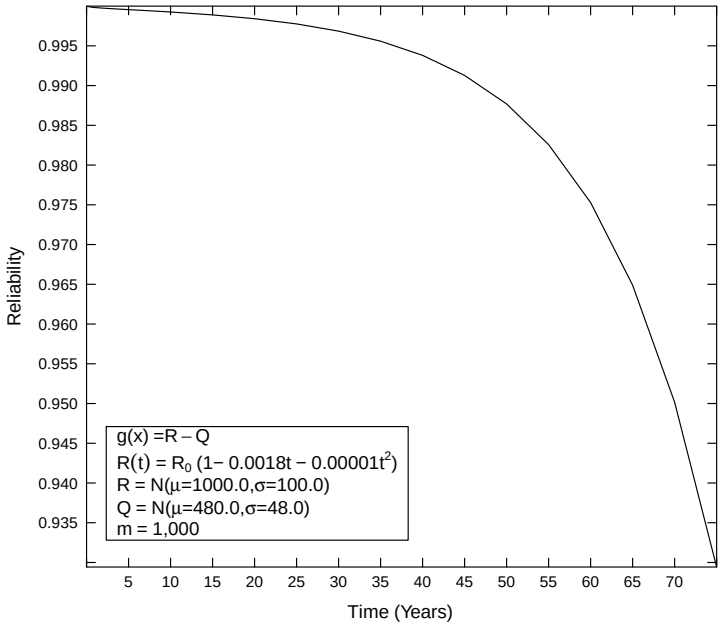

Figure 5.44: Reliability vs. Time for the Uncorrelated Normally Distributed Resistance and Load.

$$\lambda = \ln \mu - \frac{\nu^2}{2} \tag{5.80}$$

$$\nu = \sqrt{\ln\left(1 + \left(\frac{\sigma}{\mu}\right)^2\right)} \tag{5.81}$$

The same resistance deterioration model and live load model as in Example 1 are used. The graphs in Figures 5.45, 5.46, and 5.47 show the time variant reliability index, probability of failure and reliability plots, respectively. In Figure 5.45 R and Q are lognormally distributed with the assumed mean values of 1000 for R and 480 for Q, the assumed standard deviation values of 100 for R and 48 for Q, and the number of trucks passing over the bridge per year, is assumed as 1000. As shown in Figure 5.45, the value for the reliability index at time $t = 0$ is 4.6355. When $t = 0$, the live load model is not applied yet. After applying the live load model, the reliability index drops drastically within the first year and reaches to a value of 3.0871, whereas after this sudden drop, the reliability index decreases gradually.

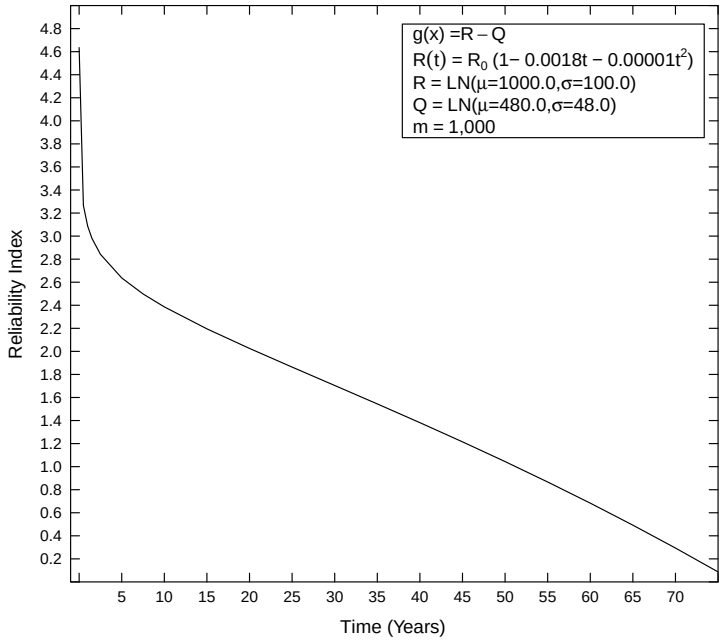

Figure 5.45: Reliability Index vs. Time for the Uncorrelated Lognormally Distributed Resistance and Load.

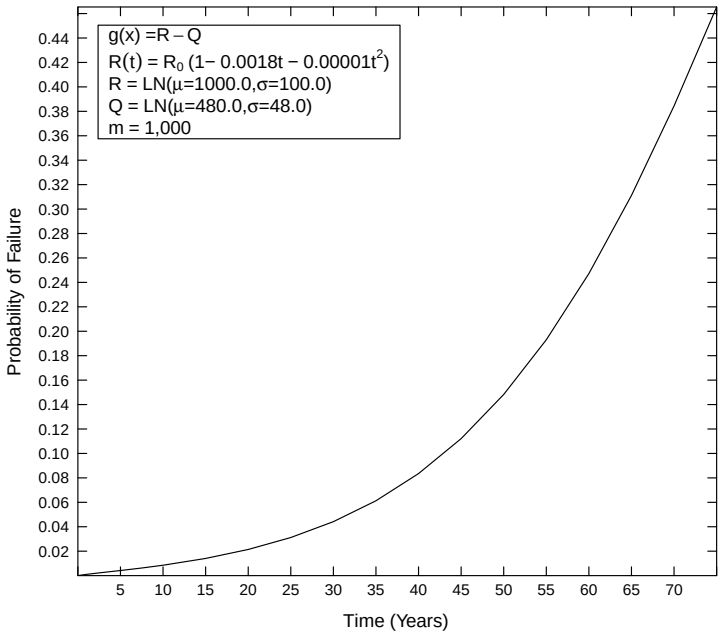

Figure 5.46: Probability of Failure vs. Time for the Uncorrelated Lognormally Distributed Resistance and Load.

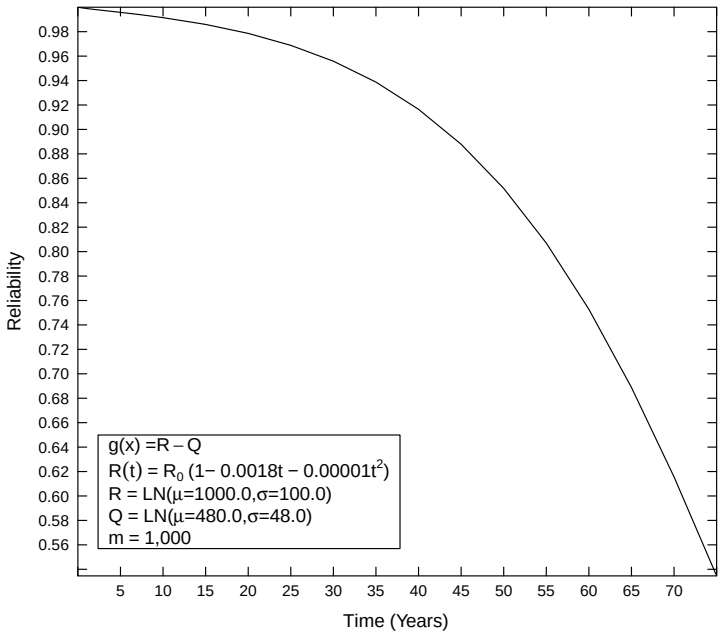

Figure 5.47: Reliability vs. Time for the Uncorrelated Lognormally Distributed Resistance and Load.

5.9.3 Example 3: Uncorrelated Normally Distributed Resistance, Live Load and Dead Load

Suppose that the resistance R of a structural component is normally distributed. Let us now separate the applied load Q into two parts, i.e. a live load component L and a dead load component D. Let us assume that, the live load L and the dead load D are also normal. Then, the new limit state function for this problem can be written as:

$$g(X) = R - L - D \tag{5.82}$$

The same resistance deterioration model and the live load model as in Example 1 are used agian. The graphs in Figures 5.48, 5.49, and 5.50 show the time variant reliability index, probability of failure and reliability plots, respectively. In Figure 5.48 R, L and D are normally distributed with the assumed mean values of 5348.88 for R, and 1407 for L and 1889.4 for D. In addition, the assumed standard deviation values are 588.376 for R, 351.9 for L and 188.974 for D, and m, the number of trucks passing over the bridge per year, is assumed as 300,000. As shown in Figure 5.48, the value for the reliability index at time $t = 0$ is 2.8853. When $t = 0$, the live load model is not applied yet. After applying the live load model, the reliability index drops drastically within the first year and reaches to a value of 1.7001, whereas after this sudden drop, the reliability index decreases gradually.

5.9.4 Example 4: Uncorrelated Non-Normally Distributed Resistance, Live Load and Dead Load

The problem presented in Example 3 is solved here again, however, this time, the resistance (structural strength) R is lognormal, the live load is normal, and the dead load is Type-I largest value. The parameters of the lognormal distribution (λ, ν) are calculated using Eqs. 5.80 and 5.81 mentioned in Section 5.9.3 and the parameters of the Type-I largest value distribution are calculated using Eqs. 5.83 and 5.84 shown below.

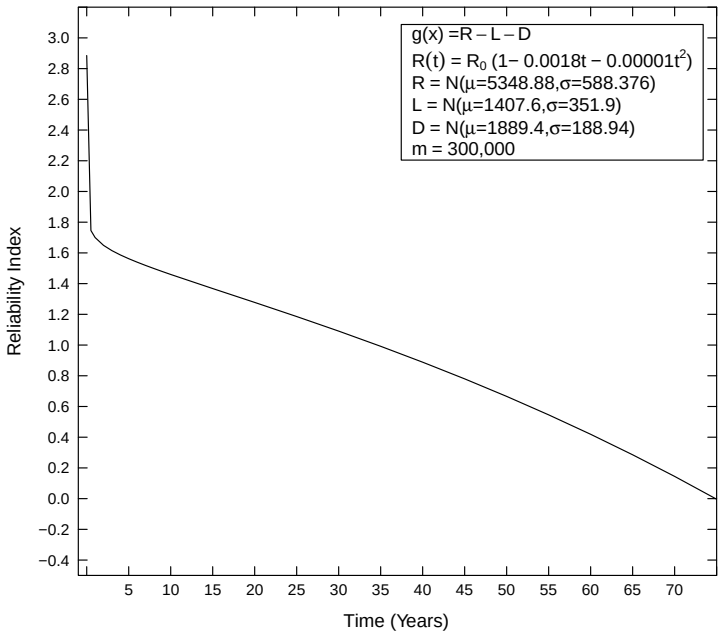

Figure 5.48: Reliability Index vs. Time for the Uncorrelated Normally Distributed Resistance, Live Load and Dead Load.

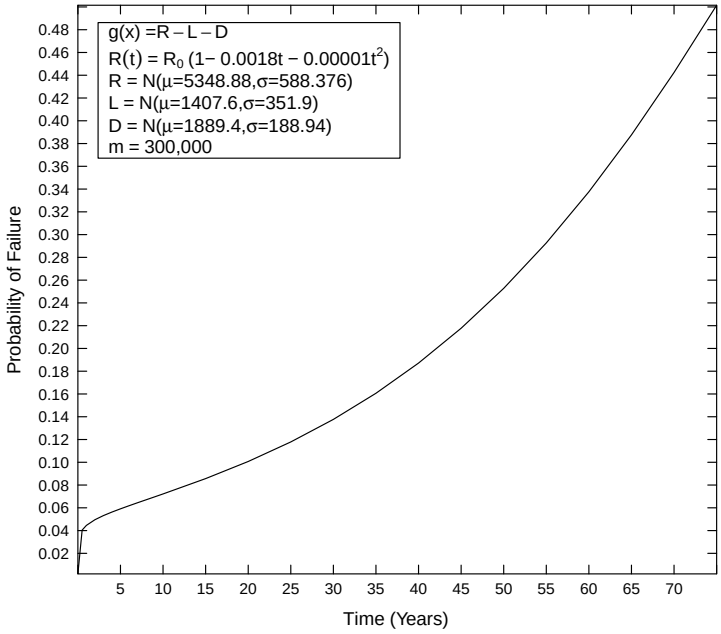

Figure 5.49: Probability of Failure vs. Time for the Uncorrelated Normally Distributed Resistance, Live Load and Dead Load.

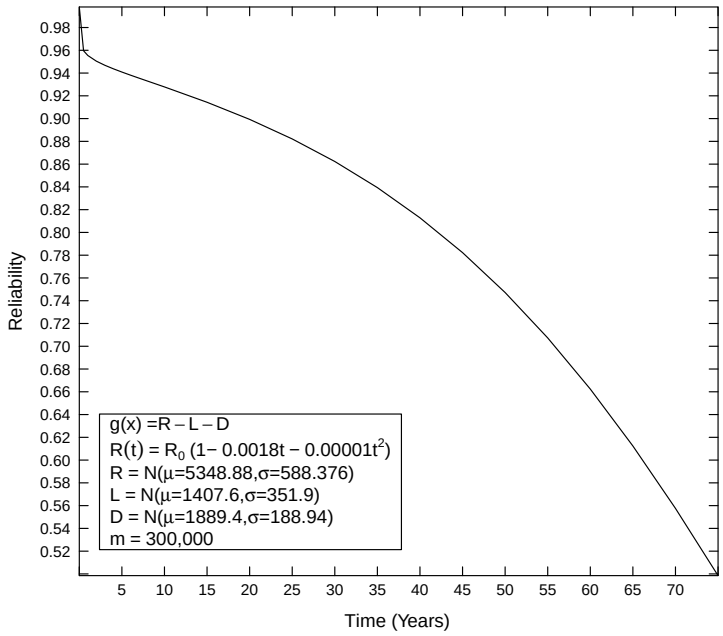

Figure 5.50: Reliability vs. Time for the Uncorrelated Normally Distributed Resistance, Live Load and Dead Load.

$$\alpha = \frac{\pi}{\sqrt{6}}\frac{1}{\sigma} \tag{5.83}$$

$$u = \mu - \frac{0.577}{\alpha} \tag{5.84}$$

The same resistance deterioration model and live load model as in Example 1 are used. The graphs in Figures 5.51, 5.52, and 5.53 show the time variant reliability index, probability of failure and reliability plots, respectively. In Figure 5.51 R is lognormally distributed, L is normally distributed and D is Type-I largest value with the assumed mean values of 5348.88 for R, and 1407 for L and 1889.4 for D. In addition, the assumed standard deviation values are 588.376 for R, 351.9 for L and 188.974 for D, and m, the number of trucks passing a bridge per year, is assumed as 300,000. As shown in Figure 5.51, the value for the reliability index at time $t = 0$ is 2.8253. When $t = 0$, the live load model is not applied yet. After applying the live load model, the reliability index drops drastically within the first year and reaches to a value of 1.7779, whereas after this sudden drop, the reliability index decreases

gradually.

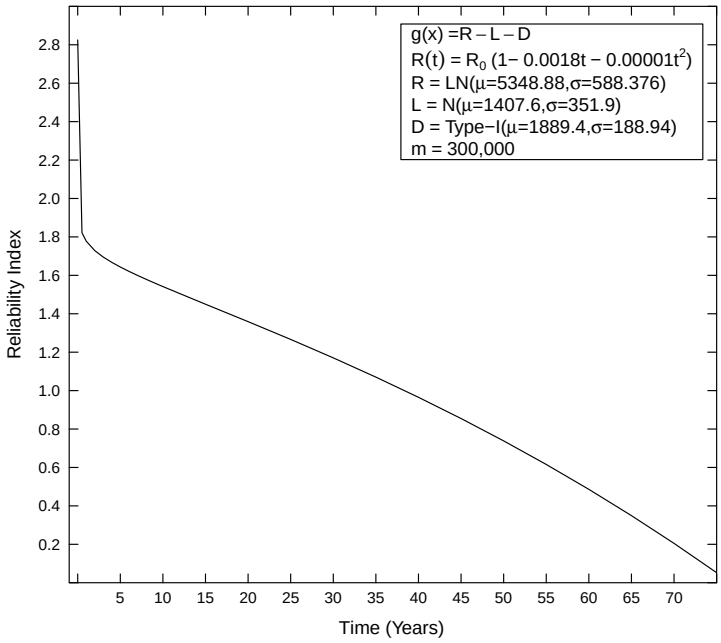

Figure 5.51: Reliability Index vs. Time for the Uncorrelated Non-Normally Distributed Resistance, Live Load and Dead Load.

5.9.5 Example 5: Correlated Normally Distributed Resistance, Live Load and Dead Load

The problem presented in Example 3 is solved here again, but this time including correlation among some of the random variables. R is normally distributed. Likewise, the live load L and the dead load D are also assumed to be normal. Resistance and dead load are assumed to be positively correlated. Similarly, dead load and live load are also partially correlated. Variables are correlated as follows:

$$\rho_{R,D} = 0.80$$

$$\rho_{R,L} = 0$$

$$\rho_{D,L} = 0.30$$

The same resistance deterioration model and live load model as in Example 1 are used. The graphs in Figures 5.54, 5.55, and 5.56 show the time variant reliability

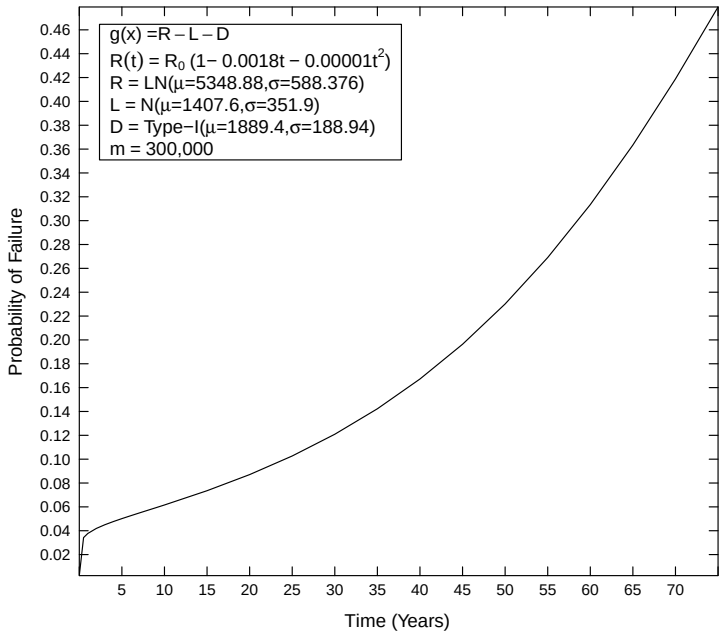

Figure 5.52: Probability of Failure vs. Time for the Uncorrelated Non-Normally Distributed Resistance, Live Load and Dead Load.

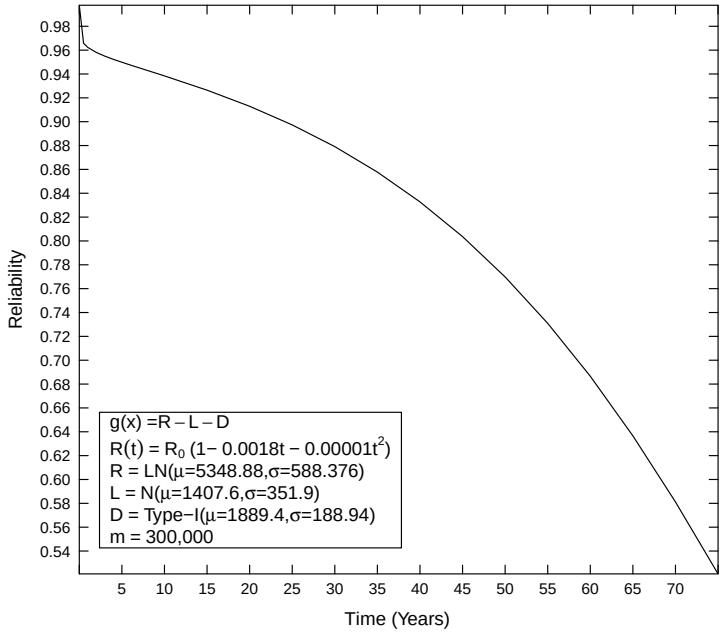

Figure 5.53: Reliability vs. Time for the Uncorrelated Non-Normally Distributed Resistance, Live Load and Dead Load.

index, probability of failure and reliability plots, respectively. In Figure 5.54 R, L and D are normally distributed with the assumed mean values of 5348.88 for R, and 1407 for L and 1889.4 for D. In addition, the assumed standard deviation values are 588.376 for R, 351.9 for L and 188.974 for D, and m, the number of trucks passing over the bridge per year, is assumed as 300,000. As shown in Figure 5.54, the value for the reliability index at time $t = 0$ is 3.3836. When $t = 0$ the live load model is not applied yet. However, after applying the live load model, the reliability index drops drastically within the first year and reaches to a value of 1.8168. However, after this sudden drop, the reliability index decreases gradually.

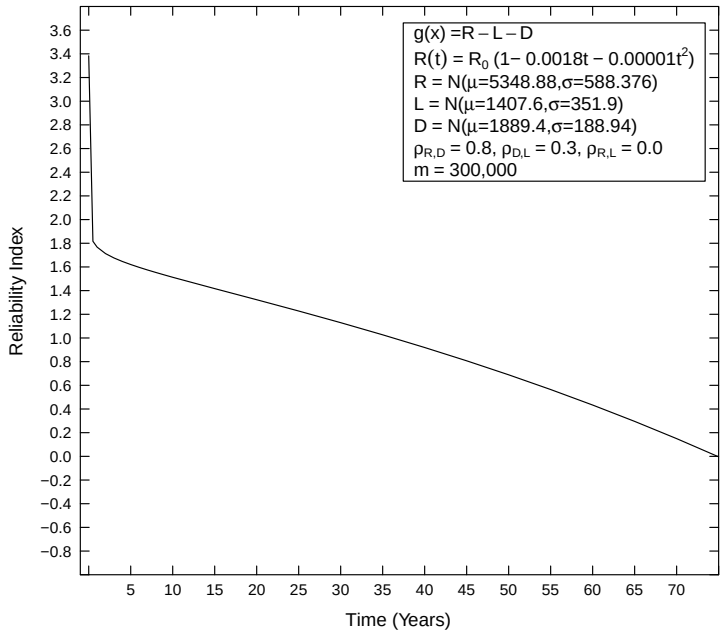

Figure 5.54: Reliability Index vs. Time for the Correlated Normally Distributed Resistance, Live Load and Dead Load.

5.9.6 Time Variant Reliability Analysis Based on Different Deterioration and Live Load Models

The problem presented in Example 3 is solved here, but this time comparing five different deterioration models and two live load models. The analyses of this problem resulted in four different figures. The graphs in Figures 5.57 and 5.59 show the time variant reliability index, and Figures 5.58 and 5.60 show the time variant reliability

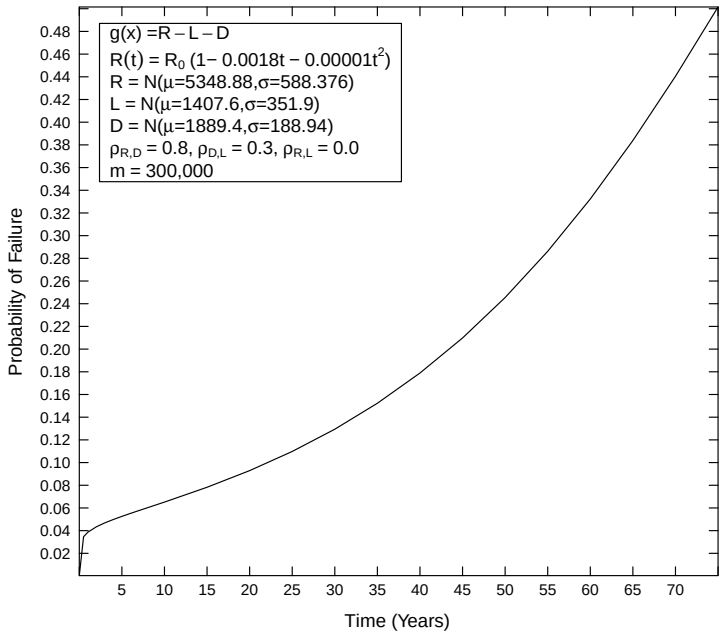

Figure 5.55: Probability of Failure vs. Time for the Correlated Normally Distributed Resistance, Live Load and Dead Load.

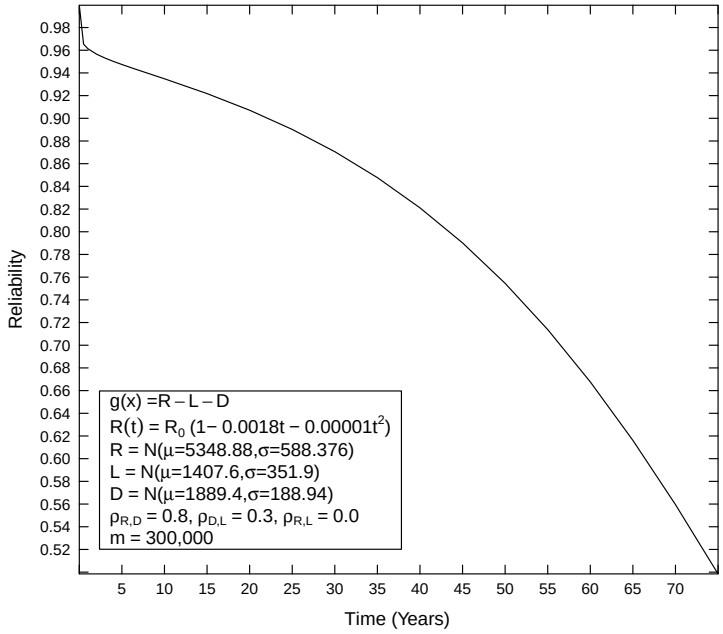

Figure 5.56: Reliability vs. Time for the Correlated Normally Distributed Resistance, Live Load and Dead Load.

plots. As shown in Figure 5.57, there is a dramatic fall for all the reliability index in the first year. Up to the 60^{th} year, the highest graph belongs to the reliability index with load-carrying capability deterioration model, and the second highest one belongs to the Sulfate attack for the same time interval. Respectively, the lowest graph belongs to diffusion controller degradation model, and corrosion and the traffic spray damage cause a similar behavior. Interestingly, these behaviors change completely after the 60^{th} year. That is to say, the highest reliability index belongs to diffusion controller degradation model while the lowest belongs to load-carrying capability deterioration model.

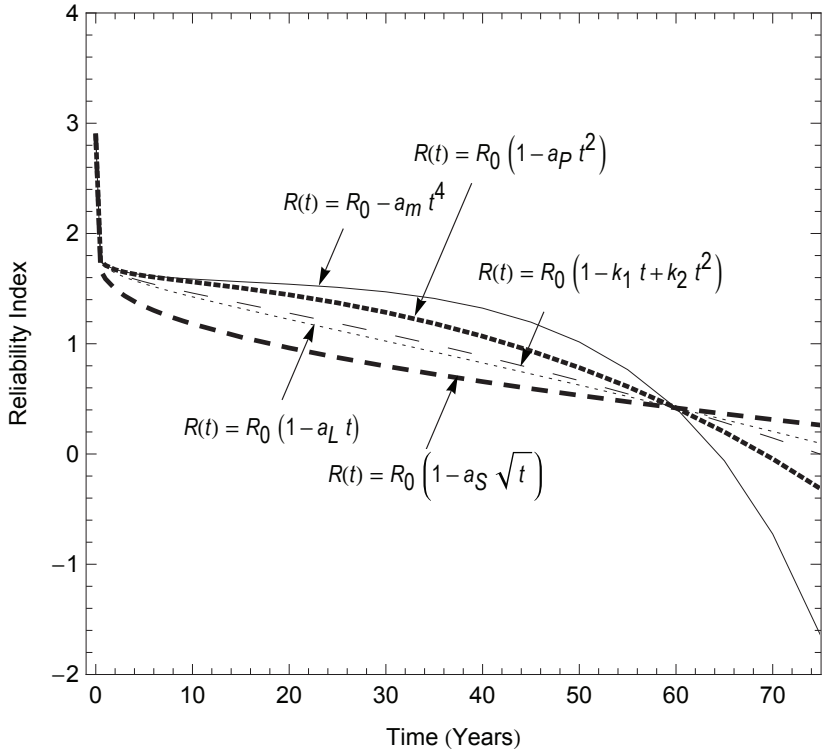

Figure 5.57: Time Variant Reliability Index for Five Different Deterioration Models and Nowak's Live Load Model for a Period of 75 Years.

In order to obtain the time variant reliability profiles shown in Figure 5.58, the reliability index is used, and consequently, the results have the same trend as in Figure 5.57.

To compare two different live load models by A. Nowak (1993) and Sivakumar et al. (2008), sulfate attack model is used in Figure 5.59 and 5.60. Considering Figure 5.59,

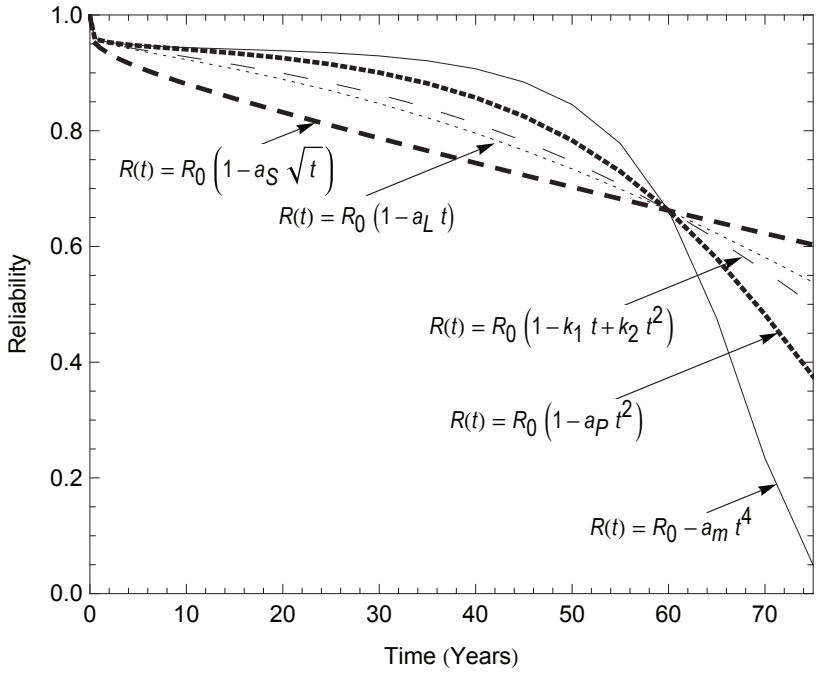

Figure 5.58: Time Variant Reliability for Five Different Deterioration Models and Nowak's Live Load Model for a Period of 75 Years.

it is evident that the reliability index in Sivakumar's model is moderately higher that that in Nowak's model. Therefore, the trend for both models in Figure 5.60 is also similar in terms of the reliability profile.

5.10 Summary

To have a complete analysis of time variant reliability, theory of which was explained in Chapter 4 for the time invariant case, this chapter discussed time variant reliability and developed formulations based on time to calculate the reliability profile.

First, repetitive loading and three periods of failure was discussed. In this section, it was assumed that the load occurred at random time intervals considering three separate cases: (1) when there is no loading variability, (2) when there is no loading and capacity variability but there is capacity deterioration, and (3) when there is no capacity variability but there is constant capacity and loading variability.

Based on the presented cases, the related time variant failure rate and time variant

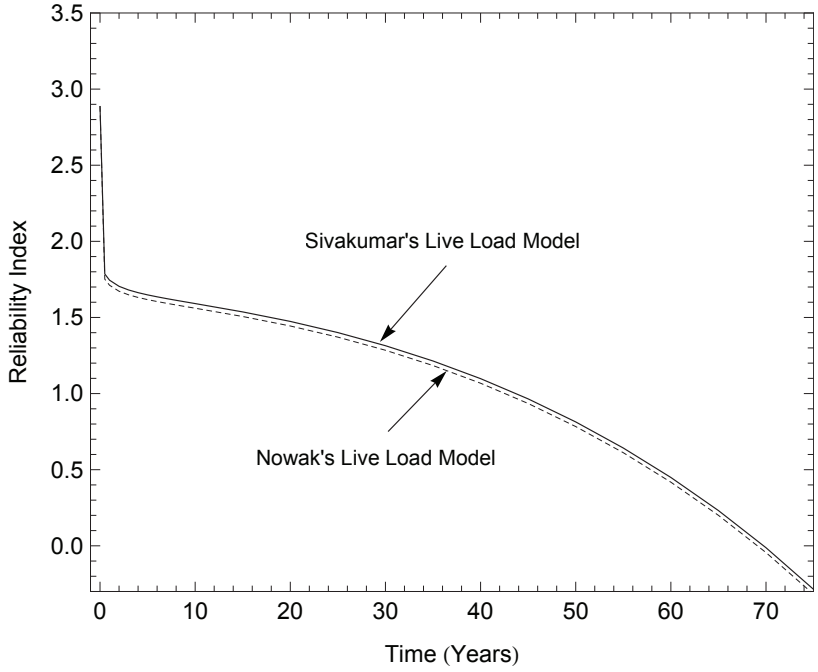

Figure 5.59: Time Variant Reliability Index for Sulfate Attack Deterioration Model and Nowak's and Sivakumar's Live Load Models for a Period of 75 Years.

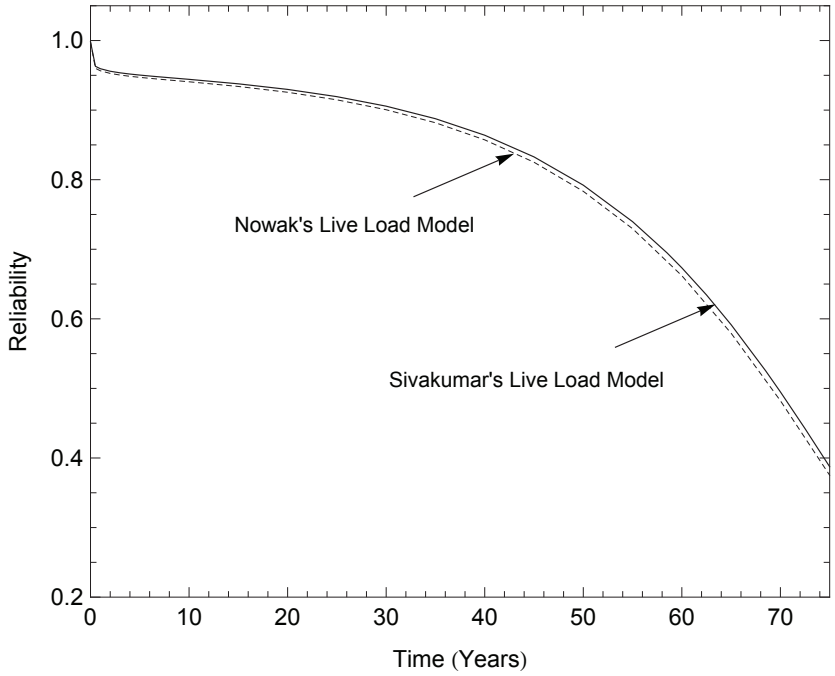

Figure 5.60: Time Reliability for Sulfate Attack Deterioration Model and Nowak's and Sivakumar's Live Load Models for a Period of 75 Years.

reliability graphs were plotted for the three separate cases. In case one, the component does not fail because capacity is always more than load, so reliability is 1. In case two,

the component starts to fail at a specific time because of the deterioration of capacity. Reliability remains 1 up to the time to failure, and after that reliability decreases. In case three, reliability decreases starting from the initial time.

Another model to which the formulations were based was the bathtub curve model, which is used to study the failure of a system made up of many components or units. A system may fail in three different periods,i.e. in early failure, useful life, and wear-out failure periods. For each case, the formulations were obtained to calculate the time variant reliability.

As an alternative approach, time dependent reliability formulation based on a stochastic load model and random strength degradation function was also discussed. Based on this formulation, the effects of load occurrence rate, live load, component strength, and degradation time on reliability were investigated.

Finally, convolution integral and deterioration function were used to obtain a formulation to calculate time variant reliability.

In the last section, a computer algorithm was developed to calculate the time variant reliability based on the FORM technique, and incorporating different deterioration and live model models. Various cases of random variables such as normally distributed, non-normally distributed, correlated or uncorrelated, were examined including the effects of the traffic spray damage deterioration model and Nowak's live load models. For the problem of normally distributed and uncorrelated random variables, comparisons were made among five different deterioration models and two live load models.

CHAPTER 6

CONCLUSIONS

This thesis started with an investigation of the previous studies carried out on time invariant and time variant reliability of bridges. Previously, engineers concentrated on time invariant reliability studies since they did not have the computational technology to compute time variant reliability. Therefore, most of the developments were in analytical and theoretical nature. As of today, the development of computer technology enabled the fast computation of time variant reliability possible. After this investigation, the thesis sought to devise a time variant reliability algorithm with reference to the studies both on time invariant and time variant reliability. In chapter 4, a detailed analysis and evaluation of load and capacity reliability problems is presented by using the First-Order Reliability Method (FORM) which is implemented in the RELSYS program. First, the reliability of the RELSYS was verified by solving numerous examples involving both components and systems. Then, the conducted analyses and evaluations provided the basis for devising a time variant reliability algorithm. For the verification, RELSYS program was examined for various random variables with normal and non-normal distributions, and for the cases of both correlation and no correlation among these random variables.

During the last decades, engineers attempted to devise different formulations in order to evaluate time variant reliability. Some of these formulations are derived in this thesis and are presented in Chapter 5. These approaches which are closely examined in this thesis can be summarized as listed below.

1. **Repetitive Loading, Capacity Variability and Capacity Deterioration.** In this approach, due to the occurrence of repetitive loading at random time inter-

vals, failure of a component or a system is investigated in three different cases. The first case is when there is no variability in loading and capacity. Since capacity does not deteriorate, there will be no failure; therefore, the reliability will always be equal to 1. The second case is when there is no variability in loading and capacity, but there is deterioration in capacity. Because of the deterioration, the capacity will cross the mean load (i.e. it will become less than the mean load) at the time to failure. The reliability will remain equal to 1 until this instance. However, there will be a rapid exponential decay in reliability after this time to failure. The third case is when there is no capacity variability, there is constant capacity deterioration, and there is variability in loading. In this case, exponential decay in reliability occurs starting from the initial time. All these cases described above are generated in Chapter 5.4. The differences between each case and it formulations are closely examined.

2. **Generation of Bathtub Curve.** A system may fail in the early years of its operation, during its normal life, or at the end of normal life (wear-out period). Therefore, it is necessary to study the failure rate for various possible combinations of failure types. In order to do this, it is necessary to derive the formulations for the combinations of these failure types, and for the time variant failure rate and reliability for each combination accordingly. The first case is when variable load (Poisson failures) and deteriorating capacity (aging) are present (Chapter 5.5.2.1). In this combination, there is no sudden drop in the failure rate, which starts almost from 0 and increases gradually due to the absence of variable capacity. The second case is when variable capacity (infant mortality) and deteriorating capacity (aging) are present (Chapter 5.5.2.2). In this combination, there is a drastic drop in the failure rate in the early years due to the presence of variable capacity. However, there is a short constant failure rate during the normal life time of the system because of the absence of variable load. In fact, the failure rate will rise gradually after its drastic drop due to deterioration capacity. The third case is when variable capacity (infant mortality) and variable load (Poisson failures) are present (Chapter 5.5.2.3). In this case, the failure rate drops because of the presence of variable capacity and continues in a constant rate due to variable load. As the deterioration capacity is absent,

the failure rate is not increasing. The last case is when variable capacity (infant mortality), variable load (Poisson failures), and deteriorating capacity (aging) are present (Chapter 5.5.2.4). In this case, all failure types are present; therefore, the failure rate drops drastically in the early years. Afterwards, it shows a constant behavior. Consequently, it will increase gradually. The reliability of this case is more realistic than the other three cases due to the presence of all the three failure modes. Formulations for each of the possible combinations of failure modes described above are individually derived and then script programs are developed using the MAPLE software to generate the graphs of the time variant reliability and failure rate. It has been observed that the graphs obtained verified the behavior of each case described above.

3. **Stochastic Load Model and Random Strength Degradation Function.** In this approach, the effects of load occurrence rate, live load, strength of component and degradation time are formulated. The less the load occurrence rate on a component is, the more reliable the component will be for the desired time interval. It has been observed that for the same mean value of live load with different coefficient of variation, the component with greater coefficient of variation will fail earlier in comparison to the less coefficient of variation. Similarly, for the same mean value of strength with different coefficient of variation, the component with greater coefficient of variation will fail earlier in comparison to the less coefficient of variation. However, for different degradation life times, the two cases show the same behavior until year 70. After that time, the reliability becomes less and less for the smaller degradation lifetime case, a behavior which eventually results in failure.

4. **Load and Capacity.** The convolution integral, which is obtained in Chapter 4, and the traffic spray damage deterioration model are used to generate a computer program. The flowchart of the developed program is presented in Chapter 5.7. Moreover, new values of mean and standard deviation for each time increment are obtained by the use of traffic spray damage deterioration model. In each step, the new mean and standard deviation values are used in the convolution integral to obtain the reliability. It is observed that the reliability of the structural component decrease by time as expected.

After examining the results of derived formulations, analyses and evaluations described above, a computer program was developed to evaluate the time variant reliability of a structural component or system. This program uses RELSYS program (based on the FORM technique) as the core module, and available deterioration and live load models in the literature. Using the developed program, calculation of the time variant reliability is achieved by analyzing the traffic spray damage deterioration model and Nowak's live load model. The analyses results are illustrated in Examples 1 through 5, which are categorized according to two different limit state functions. The first group includes Example 1 with resistance and load that are uncorrelated and normally distributed. Example 2 includes resistance and load that are uncorrelated and lognormally distributed. Comparing these two examples at the initial time, it is observed that the value of reliability at $t = 0$ is slightly larger if random variables are normally distributed. However, with the passage of time, at year 75, in both cases the value of reliability decreases although this decrease is very evident when lognormally distributed random variables are used.

The second group includes Example 3 with resistance, live load, and dead load which are uncorrelated and normally distributed, Example 4 with resistance, live load, and dead load which are uncorrelated and non-normally distributed, and Example 5 with resistance, live load, and dead load which are correlated and normally distributed. Among these examples, the highest reliability belongs to the correlated and normally distributed random variables at time $t = 0$, and the lowest reliability belongs to the uncorrelated and non-normally distributed random variables. However, with the passage of time, the highest reliability belongs to uncorrelated and non-normally distributed random variables at time $t = 75$, and the lowest reliability belongs to correlated and normally distributed random variables. The latter values are faintly lower than the values obtained from uncorrelated and normally distributed random variables.

From the five examples investigated, Example 3 is selected as a sample problem to be used in the developed program in order to compare the effects of various deterioration models on reliability when Nowak's live load model is used. For all of the reliabilities calculated, a drastic fall in the first year is observed. The reliability obtained using the load-carrying capability deterioration model has the highest reliability up to the 60th year. The second highest reliability for the same period belongs to the sulfate attack

model. Within the same interval, the lowest reliability observed is for the diffusion controlled degradation model, while corrosion and the traffic spray damage models are observed to display a similar behavior. However, there is a complete reversal in these trends after the 60th year. This means that the highest reliability is obtained for the diffusion controlled degradation model, and the lowest reliability is produced when using the load-carrying capability deterioration model. Furthermore, while Example 3 is still used as a sample problem, this time, live load models of Nowak's and Sivakumar's are compared. Accordingly, it is observed that the Sivakumar's model produces slightly higher reliability values than that Nowak's model.

In conclusion, as a result of the studies presented in this thesis, a computer program is developed for examining time variant reliability for bridges. The contribution of the developed program to the reliability theory is that it has the capability to read from the input data. If the reliability is time variant or time invariant based, and if it is time invariant, it only calculates the reliability of the given data; otherwise, it starts the time steps assigned to analyze the input data for time variant case. The most important advantage of the developed algorithm is that the user has the option of defining which deterioration and live load model to use for the problem at hand for a given time horizon. Finally, there is also an option of defining specific input data, for instance if resistance deterioration, live load model and/or both cases are only needed to be calculated. By using the developed program, effects of different deterioration models and different live load models on the time variant reliability of a bridge component or system are observed and evaluated. This study showed that, because of highly uncertain nature of time variant reliability, the selection of a degradation model and a live load model to be used for a given analysis may have an important effect on time variant reliability computation. Furthermore, implementation and testing of available or newly developed deterioration and load models into time variant bridge reliability programs is an area that requires further study.

BIBLIOGRAPHY

Akgul, F. (2002). *Lifetime system reliability prediction for multiple structure types in a bridge network,* (Ph.D Dissertation). Department of Civil, Environmental and Architectural Engineering, University of Colorado at Boulder, Colorado, USA.

Ang, A. H.-S., & Tang, W. H. (1975). *Probability concepts in engineering planning and design, Vol. 2: Decision, risk, and reliability*. Wiley.

Bin, D., Zhao, R., & Xiang, T. (2010). Lifetime reliability analysis of flexural cracking for existing prestressed concrete bridge under corrosion attack. *ICCTP*, 3810-3818.

CBS Minnesota. (2013). *Years Later, Minn. Disposing Of I-35W Bridge Steel*. Retrieved from: http://minnesota.cbslocal.com/2013/07/31/years-later-minn-disposing-of-i-35w-bridge-steel/.

Choi, H.-H., Lee, S.-Y., Choi, I.-Y., Cho, H.-N., & Mahadevan, S. (2006). Reliability-based failure cause assessment of collapsed bridge during construction. *Reliability Engineering and System Safety*, *91*(6), 674–688.

Conor Quinn. (2010). *Consider six factors before selecting your led power supply.* Retrieved from: http://electronicdesign.com/energy/consider-six-factors-selecting-your-led-power-supply.

Coppola, A. (1984). Reliability engineering of electronic equipment: A historical perspective. *IEEE Transactions On Reliability*, *R-33*(1), 29-35.

Czarneckia, A. A., & Nowak, A. S. (2008). Time-variant reliability profiles for steel girder bridges. *Journal of Structural Safety*, *30*(1), 49-64.

Davis-McDaniel, C., Chowdhury, M., Pang, W., & Dey, K. (2013). Fault-tree model for risk assessment of bridge failure: Case study for segmental box girder bridges. *Journal of Infrastructure Systems, American Society of Civil Engineers, 19*(3), 326-334.

Dennis J. Wilkins. (2002). *The bathtub curve and product failure behavior. Part*

One - The bathtub curve, infant mortality and burn-in. Retrieved from: http://www.weibull.com/hotwire/issue21/hottopics21.htm.

Ellingwood, B. R., & Mori, Y. (1993). Probabilistic methods for condition assessment and life prediction of concrete structures in nuclear power plants. *Nuclear Engineering and Design*, *142*, 155-166.

Enevoldsen, I., & Sørensen, J. (1993). Reliability based optimization of series systems of parallel systems. *Journal of Structural Engineering*, *119*(4), 1069–1084.

Enright, M. P., & Frangopol, D. M. (1998). Service-life prediction of deteriorating concrete bridges. *Journal of Structural Engineering*, *124*(3), 309-317.

Enright, M. P., & Frangopol, D. M. (2000). RELTSYS: A computer program for life prediction of deteriorating systems. *Structural Engineering and Mechanics*, *9*(6), 557-568.

Estes, A. C. (1997). *A system reliability approach to the lifetime optimization of inspection and repair of highway* (Ph.D Dissertation). Department of Civil, Environmental and Architectural Engineering, University of Colorado at Boulder, Colorado, USA.

Estes, A.C. and Frangopol, D.M. (1997). *Relsys: Reliability of systems. User's Manual*. Department of Civil, Environmental, and Architectural Engineering, University of Colorado at Boulder, Colorado, USA.

Frangopol, D., Lin, K., & Estes, A. (1997). Reliability of reinforced concrete girders under corrosion attack. *Structural Engineering*, *123*(3), 286–297.

Ghosn, M. (2010). Reliability based structural system performance indicators for highway bridges. *Structures Congress*, 2781-2792.

González, J., Andrade, C., Alonso, C., & Feliu, S. (1995). Comparison of rates of general corrosion and maximum pitting penetration on concrete embedded steel reinforcement. *Cement and Concrete Research*, *25*(2), 257–264.

Huang, X., & Chen, J. (2015). Time-dependent reliability model of deteriorating structures based on stochastic processes and bayesian inference methods. *Journal of Engineering Mechanics*, *141*(3).

Kand, W.-H., Song, J., & Gardoni, P. (2008). Matrix-based system reliability method and applications to bridge networks. *Reliability Engineering and System Safety*, *93*(11), 1584-1593.

Kayser, J. R., & Nowak, A. S. (1989). Reliability of corroded steel girder bridges. *Journal of Structural Safety*, *6*(1), 53-63.

Kuschel, N., & Rackwitz, R. (2000). Optimal design under time-variant reliability constraints. *Structural Safety*, *22*(2), 113-127.

Lebeau, K., & Wadia-Fascetti, S. (2000). A fault tree model of bridge deterioration. *8th ASCE Specialty Conference on Probabilistic Mechanics and Structural Reliability, Notre Dame, Indiana, USA*.

Leira, B., & Lindgard, J. (2000). Statistics analysis of laboratory test data for service life prediction of concrete subjected to chloride ingress. *International Conference on Applications of Statistics and Probability, Sydney, Rotterdam: Balkema*, 291-295.

Lewis, E. E. (1996). *Introduction to reliability engineering.* Second Ed., John Wiley Sons, U.S.A.

Lewis, E. E., & Chen, H.-C. (1994). Load-capacity interference and the bathtub curve. *IEEE Transactions On Reliability*, *43*(3), 470-475.

Ling, Y. (2013). *Uncertainty quantification in time-dependent reliability analysis*, (Ph.D Dissertation). Department of Civil Engineering, Vanderbilt University at Nashville, Tennessee, USA.

Lopez, R., Miguel, L., Belo, I., & Cursi, J. S. (2014). Advantages of employing a full characterization method over FORM in the reliability analysis of laminated composite plates. *Composite Structures*, *107*, 635–642.

Mahadevan, S., & Dey, A. (1997). Adaptive Monte Carlo simulation for time-variant reliability analysis of brittle structures. *AIAA journal*, *35*(2), 321-326.

Melchers, R. E. (1999). *Structural reliability analysis and prediction*. John Wiley.

Mishra, R. C. (2006). *Reliability and maintenance engineering*. New Age International.

Misra, K. B. (2008). *Handbook of performability engineering*. Springer Science Business Media.

Norris, W., Graves, H. I., Naus, D., Oland, C., & Ellingwood, W., B.R.; Nuclear Regulatory Commission. (1994). Aging management of containment structures in nuclear power plants. *(Technical Report) Oak Ridge, Tenn. : Oak Ridge National Laboratory. ; Oak Ridge, Tenn. : Distributed by the Office of Scientific and Technical Information, U.S. Dept. of Energy*.

Nowak, A. (1993). Live load model for highway bridges. *Journal of Structural Safety, 13*, 53-66.

Nowak, A., & Hong, Y. (1991). Bridge live load models. *Journal of Structural Engineering, 117*(9), 2757–2767.

Nowak, A. S. (2004). System reliability models for bridge structures. *Technical Sciences, 52*(4), 321-328.

Nowak, A. S., & Zhou, J. (1990). System reliability models for bridges. *Structural Safety, 7*, 247-254.

Olsen, A. I. (2006). *Time-variant reliability of dynamic systems by importance sampling and probabilistic analysis of ice loads*, (Ph.D Dissertation). Department of Structural Engineering, Norwegian University of Science and Technology at Trondheim, Norway.

Papadakis, V., Roumeliotis, A., Fardis, M., & Vagenas, C. (1996). Mathematical modeling of chloride effect on concrete durability and protection measures. *in Dhir R. & Jones M. Concrete repair, rehabilitation and protection. London, EF Spon*, 165-174.

Patev, R., Schaaf, D., & James, R. (2000). Time-dependent reliability for structures subjected to alkali-aggregate reaction. *in Proceedings of 9th United Engineering Foundation Conference California Reston: ASCE*, 152-163.

Rao, S. S. (2015). *Reliability engineering*. Pearson.

Rausand, M., & Hoyland, A. (2004). *System reliability theory: Models, statistical methods, and applications*. A John Wiley and Sons.

Rendell, F., Jauberthie, R., & Grantham, M. (2002). *Deteriorated concrete: Inspection and physicochemical analysis*. London, Thomas Telford.

Saleh, J., & Marais, K. (2006). Highlights from the early (and pre-) history of reliability engineering. *Reliability Engineering and System Safety, 91*(2), 249-256.

Sianipar, P., & Adams, T. (1997). Fault-tree model of bridge element deterioration due to interaction. *Journal of Infrastructure Systems, 3*(3), 103–110.

Sivakumar, B., Ghosn, M., & Moses, F. (2008). Protocols for Collecting and Using Traffic Data in Bridge Design: NCHRP. *(Technical Report) Washington, D.C., TRB, Transportation Research Board*.

Stewart, M. G., & Rosowsky, D. V. (1998). Time-dependent reliability of deteri-

orating reinforced concrete bridge decks. *Journal of Structural Safety, 20*(1), 91-109.

Straub, D. (2009). Stochastic modeling of deterioration processes through dynamic bayesian networks. *Journal of Engineering Mechanics, 135*(10), 1089–1099.

Tabsh, S., & Nowak, A. (1991). Reliability of highway girder bridges. *J. Struct. Eng., 117*(8), 2372-2388.

Thoft-Christensen, P., & Baker, M. J. (1982). *Structural reliability theory and its applications*. Berlin: Springer-Verlag.

Val, D. V., & Melchers, R. E. (1997). Reliability of deteriorating RC slab bridges. *Journal of Structural Engineering, 123*(12), 1638-1644.

Val, D. V., Stewart, M. G., & Melchers, R. E. (1998). Effect of reinforcement corrosion on reliability of highway bridges. *Engineering Structures, 20*(11), 1010–1019.

van Noortwijk, J., van der Weide, J., Kallen, M., & Pandey, M. (2007). Gamma processes and peaks-over-threshold distributions for time-dependent reliability. *Reliability Engineering and System Safety, 92*(12), 1651-1658.

Vu, K. A. T., & Stewart, M. G. (2000). Structural reliability of concrete bridges including improved chloride-induced corrosion models. *Structural Safety, 22*(4), 313-333.

Wikipedia. (2015). *List of bridge failures*. Retrieved from: https://en.wikipedia.org/wiki/List_of_bridge_failures.

Yanev, B. (2007). *Bridge management*. Hoboken, N.J: Wiley.

Zhang, Z., Sun, X., & Wang, X. (2003). Determination of bridge deterioration matrices with state national bridge inventory data. *9th International Bridge Management Conference*. (Orlando, Florida Transportation Research Board.)

Zhu, W. (2008). *An investigation into reliability based methods to include risk of failure in life cycle cost analysis of reinforced concrete bridge,* (Master Dissertation). School of Civil, Environmental and Chemical Engineering Science, Engineering and Technology Portfolio, RMIT University at Melbourne, Victoria, Australia.